

SECOND CHAPTER:

“EFFECTS OF XENOBIOTICS ON

THE SUICIDAL DEATH OF ERYTHROCYTES”

8. ABBREVIATIONS

ABCG2: ATP-binding cassette sub-family G member 2

ANOVA: analysis of variance

AP-1: activator protein 1

ATP: adenosine triphosphate

Band 3: anion transport protein

BasoE: basophilic erythroblasts

Bax: Bcl-2-associated X protein, pro-apoptotic Bcl-2 protein

BCL-2: B-cell lymphoma 2

Bcl-xL: anti-apoptotic Bcl-2 protein

BCRP: breast cancer resistance protein

BFU-E: burst-forming unit erythroid

Bid: BH3 interacting-domain death agonist

Bik: pro-apoptotic protein, BCL-2 family member

Bok: pro-apoptotic Bcl-2 protein identified in the ovary

BSA: bovine serum albumin

CA4: combretastatin A4

CA4P: combretastatin A4 phosphate

CD163: cluster of differentiation 163

CD36: cluster of differentiation 36

CD47: Cluster of differentiation 47

CD91: alpha 2-macroglobulin receptor; low density lipoprotein-related protein

CDK4: cyclin-dependent kinase 4

CFU-E: colony-forming unit erythroid

CFU-GEMM: colony-forming unit granulocyte erythroid monocyte and megakaryocyte

Chk1: checkpoint kinase 1

Chk2: checkpoint kinase 2

CK1: casein kinase 1

CK1: casein kinase 1

CKD: chronic kidney disease

c-kit: stem cell factor receptor

CMF: 5-chloromethylfluorescein

CMFDA: 5-chloromethylfluorescein diacetate

c-myc: oncogenic transcription factor

Cox: cyclooxygenase

CXCL16: chemokine (C-X-C motif) ligand 16

CYP3A; cytochrome P-450 3A4: cytochrome P450, family 3, subfamily A

[Ca²⁺]_i: intracellular calcium activity

D4476: 4-(4-(2,3-Dihydrobenzo[1,4]dioxin-6-yl)-5-pyridin-2-yl-1H-imidazol-2-yl)benzamide

DCF: 2',7'-dichlorodihydrofluorescein

DCFDA: 2',7'-dichlorodihydrofluorescein diacetate

DMSO: dimethylsulfoxide

EGTA: glycol-bis(2-aminoethylether)-N,N,N',N'-tetraacetic acid

EMA: european medicine agency

EPO: erythropoietin

FACS: fluorescence-activated cell sorting

Fas: Fas cell surface death receptor

FDA: food and drug administration

FITC: fluorescein isothiocyanate

FL-1: fluorescence channel 1

Fluo-3 AM: Fluo-3 acetoxymethyl ester

Fpn: ferroportin

FSC: forward scatter

GPA: glycophorin A

GPC: glycophorin C

G6PD: glucose-6-phosphate dehydrogenase

Glut1: glucose transporter 1

GSH: glutathione

H3: histone 3

Hb-C: hemoglobin C

HO-1: heme oxygenase-1

HUS: hemolytic uremic syndrome

ICAM-4: intercellular adhesion molecule 4

IgG: immunoglobulin G

IgM: immunoglobulin

JAK1: Janus kinase 1

JAK1: Janus kinase 1

LAMP1: lysosomal-associated membrane protein 1

LW: antigen of adult and infant erythrocytes

MAPK: p38 mitogen-activated protein kinase

mTOR: mammalian target of rapamycin

NF-Kb: nuclear factor kappa-light-chain-enhancer of activated B cells

NO: nitric oxide

NSC: non selective cation channel

OrthoE: orthochromatic erythroblasts

P21^{WAF1}: cyclin-dependent kinase inhibitor 1

p53: tumor protein p53

PAF: platelet-Activating Factor

PBS: phosphate-buffered saline

PC: phosphatidylcholine

PCBP family: cytoplasmic chaperones of the poly(rC) binding protein family

PE: phosphatidylethanolamine

PGE2: prostaglandin E2

P-gp/ABCB1: efflux transporters P-glycoprotein-1; ATP binding cassette subfamily B member 1

PI: phosphatidylinositol

PKC: protein kinase C

PolyE: polychromatophilic erythroblasts

ProE: proerythroblasts

PS: phosphatidylserine

RBCs: red blood cells

(R)-DRF053: (2R)-2-[[9-(1-Methylethyl)-6-[[3-(2-pyridinyl)phenyl]amino]-9H-purin-2-yl]amino]-1-butanol dihydrochloride

Rh: rhesus factor

Retic: reticulocyte stage

ROS: reactive oxygen species

RPA32: replication factor A protein 2

RPM: revolutions per minute

SB203580: 4-(4-Fluorophenyl)-2-(4-methylsulfinylphenyl)-5-(4-pyridyl)-1H-imidazole

Scr: scramblase

SEM: standard error of mean

SM: sphingomyelin

SR-PSOX: scavenger receptor for phosphatidylserine and oxidized Low Density Lipoprotein

SSC: side scatter

STAT3: signal transducer and activator of transcription 3

STAT3: signal Transducer and Activator of Transcription 3

TNF- α : tumor necrosis factor- α

TRPC6: transient receptor potential cation channel, subfamily C, member 6

TSP: thrombospondin-1

VDA: vascular disrupting agent

VEGF: vascular endothelial growth factor

VEGF-1: vascular endothelial growth factor 1

VEGF-2: vascular endothelial growth factor 2

VEGF-3: vascular endothelial growth factor 3

VEGFR1: vascular endothelial growth factor receptor 1

zVAD-FMK: benzyloxycarbonyl-Val-Ala-Asp(OMe)-fluoromethylketone

10. ABSTRACT

Erythrocytes may enter eryptosis, the suicidal death of erythrocytes characterized by cell shrinkage, membrane blebbing and cell membrane scrambling [96, 97]. This study was conducted in order to investigate prospective antitumoral products which are used against tumor growth in humans, in particular CA4P or Pazopanib, or compounds used *in vitro*, such as Nocodazole, Terfenadine, Piceatannol, Ceranib-2 and Sclareol, in order to unveil the effects on erythrocytes survival and to clarify the mechanisms and signalling involved in their action [98-104]. Human erythrocytes drawn from healthy individual were incubated *in vitro* at a hematocrit of 0.4% in Ringer solution. Where indicated, RBCs were exposed for 48 hours to the drugs at the indicated concentrations. The main hallmarks of eryptosis were investigated by flow cytometry. Phosphatidylserine exposure at the cell surface was estimated from annexin-V-binding, cell volume from forward scatter, $[Ca^{2+}]_i$ from Fluo3-fluorescence, reactive oxygen species (ROS) formation from DCF-dependent fluorescence, GSH levels by CMF-dependent fluorescence and ceramide abundance utilizing specific antibodies. Hemoglobin concentration in the supernatant was taken as measure of hemolysis. ATP levels following CA4P treatment were measured using luciferin-luciferase assay kit. For studying the effect of Nocodazole on tubulin in human erythrocytes, TubulinTracker™ Green reagent was used. A 48 hours exposure of human erythrocytes to CA4P treatment ($\geq 50 \mu\text{M}$) increased the percentage of annexin-V-binding cells and decreased forward scatter. $100 \mu\text{M}$ CA4P significantly increased Fluo3-fluorescence. The effect of CA4P ($100 \mu\text{M}$) on annexin-V-binding was significantly blunted, but not abolished, by removal of extracellular calcium. CA4P ($\geq 50 \mu\text{M}$) significantly decreased GSH abundance and ATP levels. A 48 hours exposure of human erythrocytes to Pazopanib significantly increased the percentage of annexin-V-binding ($\geq 25 \mu\text{g/ml}$) and of shrunken erythrocytes ($\geq 50 \mu\text{g/ml}$). Pazopanib further resulted in significant hemolysis ($\geq 25 \mu\text{g/ml}$). The effect of Pazopanib on annexin-V-binding was significantly blunted but not abolished by removal of extracellular Ca^{2+} . Pazopanib significantly increased DCF-fluorescence ($50 \mu\text{g/ml}$) and ceramide abundance ($50 \mu\text{g/ml}$). A 48 hours exposure of human erythrocytes to Nocodazole treatment ($\geq 30 \mu\text{g/ml}$) significantly increased the percentage of annexin-V-binding cells, increased Fluo3-fluorescence, increased DCF-fluorescence and significantly increased ceramide surface abundance. The effect of Nocodazole on annexin-V-binding was significantly blunted, but not abolished by removal of extracellular Ca^{2+} and was not modified in the presence of caspase-3 inhibitor zVAD ($1 \mu\text{M}$). Nocodazole treatment reduced total tubulin abundance. A 48 hours exposure of human erythrocytes to Terfenadine ($\geq 5 \mu\text{M}$) significantly increased the percentage of annexin-V-binding cells and increased the percentage of hemolytic erythrocytes. The effect of Terfenadine on annexin-V-binding was significantly blunted but not abolished by removal of extracellular Ca^{2+} . Exposure of erythrocytes to Ca^{2+} ionophore

ionomycin (1 μM , 15 min) significantly triggered annexin-V-binding, an effect significantly augmented by Terfenadine pretreatment (10 μM , 48 hours). Terfenadine (7.5 μM) significantly increased Fluo3-fluorescence. A 48 hours exposure of human erythrocytes to Piceatannol (10 - 20 μM) significantly increased the percentage of annexin-V-binding cells, decreased forward scatter, increased DCF-fluorescence, increased ceramide abundance. Removal of extracellular Ca^{2+} slightly blunted but did not abolish the effect of Piceatannol on annexin-V-binding and forward scatter. Piceatannol (20 μM) significantly augmented the increase of annexin-V-binding, but significantly blunted the decrease of forward scatter following treatment with ionomycin. A 48 hours exposure of human erythrocytes to Ceranib-2 treatment significantly increased the percentage of annexin-V-binding cells ($\geq 50 \mu\text{M}$) and the percentage of hemolytic cells ($\geq 10 \mu\text{M}$) but did not modify forward scatter. Ceranib-2 significantly increased Fluo3-fluorescence, DCF-fluorescence and ceramide abundance. The effect of Ceranib-2 on annexin-V-binding was not significantly blunted by removal of extracellular calcium. A 48 hours exposure of human erythrocytes to Sclareol ($\geq 50 \mu\text{M}$) significantly increased the percentage of annexin-V-binding cells. Sclareol ($\geq 50 \mu\text{M}$) further triggered hemolysis. Sclareol (100 μM) significantly increased Fluo3-fluorescence, but the effect of Sclareol on annexin-V-binding was not significantly blunted by removal of extracellular Ca^{2+} . Instead, the effect of Sclareol on annexin-V-binding was significantly blunted in the presence of p38 kinase inhibitor skepinone (2 μM) and in the presence of casein kinase 1 α inhibitor D4476 (10 μM). To conclude, these xenobiotics trigger eryptosis through different mechanisms [98-104].

Keywords: eryptosis, antitumoral products, flow cytometry, phosphatidylserine

11. ERYPTOSIS INTRODUCTION

11.1 Erythrocytes

Red blood cells (“RBCs”) are also known as “erythrocytes” (from Greek *erythros* for "red" and *kytos* for "hollow vessel"). Morphologically, human erythrocytes have the shape of biconcave disk with thickness at the thickest point of 2-2.5 μm and a minimum thickness in the centre of 0.8-1 μm and a diameter of 6-8 μm . They are the most common type of blood cell and the vertebrate organism's principal means of delivering oxygen (O_2) to the body tissues through the circulatory system. RBCs lack organelles like mitochondria and nucleus, in order to accommodate the maximum space for hemoglobin. The cells develop in the bone marrow and circulate for about 100-120 days in the body before their components are recycled by macrophages [105]. Erythrocytes are produced by a complex regulated process of erythropoiesis and they are continuously produced in the red bone marrow of large bones. Their production can be stimulated by the hormone erythropoietin (EPO), synthesised by the kidney [106]. Erythropoiesis passes from pluripotent stem cell through the multipotent progenitor CFU-GEMM (colony-forming unit granulocyte erythroid monocyte and megakaryocyte), and then BFU-E (burst-forming unit erythroid) and CFU-E (colony forming unit erythroid), to the first recognizable erythrocyte precursor in the bone marrow, the pronormoblast (Fig. 23) [106, 107]. This cell gives rise to a series of progressively smaller normoblasts with increasing content of hemoglobin. The nucleus is finally extruded from the late normoblast leading to mature red blood cell through the reticulocyte stage. Erythropoiesis ends with the mature circulating red cell, which is a non-nucleated biconcave disc, performing its function of oxygen delivery. In this process, the glycoprotein hormone erythropoietin has been known as the major humoral regulator of red cell production [107].

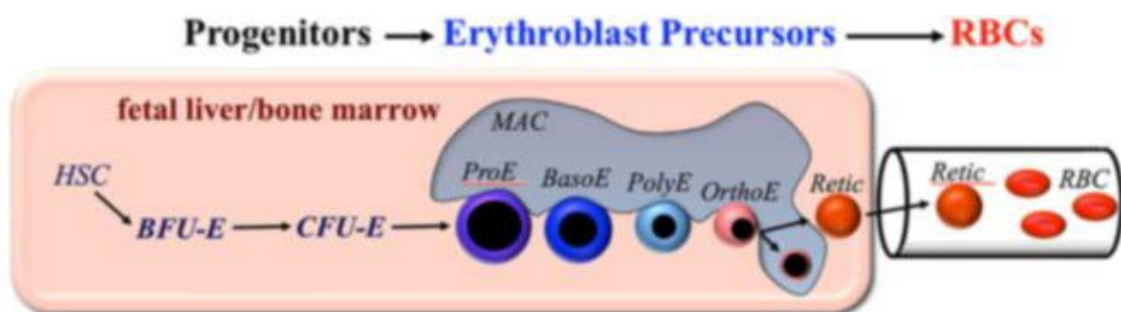


Fig. 23: Erythropoiesis in mammals [106]. Definitive erythropoiesis in the adult organism is derived from HSC (hematopoietic stem cells). Erythroid progenitors (BFU-E and CFU-E) are defined by their capability to form colonies of maturing erythroid cells *in vitro*. Erythroid precursors are classified morphologically as ProE (proerythroblasts), BasoE (basophilic erythroblasts), PolyE (polychromatophilic erythroblasts) and OrthoE

(orthochromatic erythroblasts). The nucleus is finally extruded from the late normoblast leading to mature red blood cell (RBC) through the reticulocyte stage (Retic).

11.2 Erythrocytes membrane composition

The structural organization of the human red cell membrane provides properties essential for physiological cell function, such as deformability and stability while traversing the circulatory system and specifically the capillary network [108]. The red blood cell membrane consists of three basic components: the glycocalyx on the exterior (rich in carbohydrates), the lipid bilayer (contains many transmembrane proteins and its lipidic main constituents) and the membrane skeleton located on the inner surface of the lipid bilayer (structural network of proteins) (shown in Fig. 24) [108].

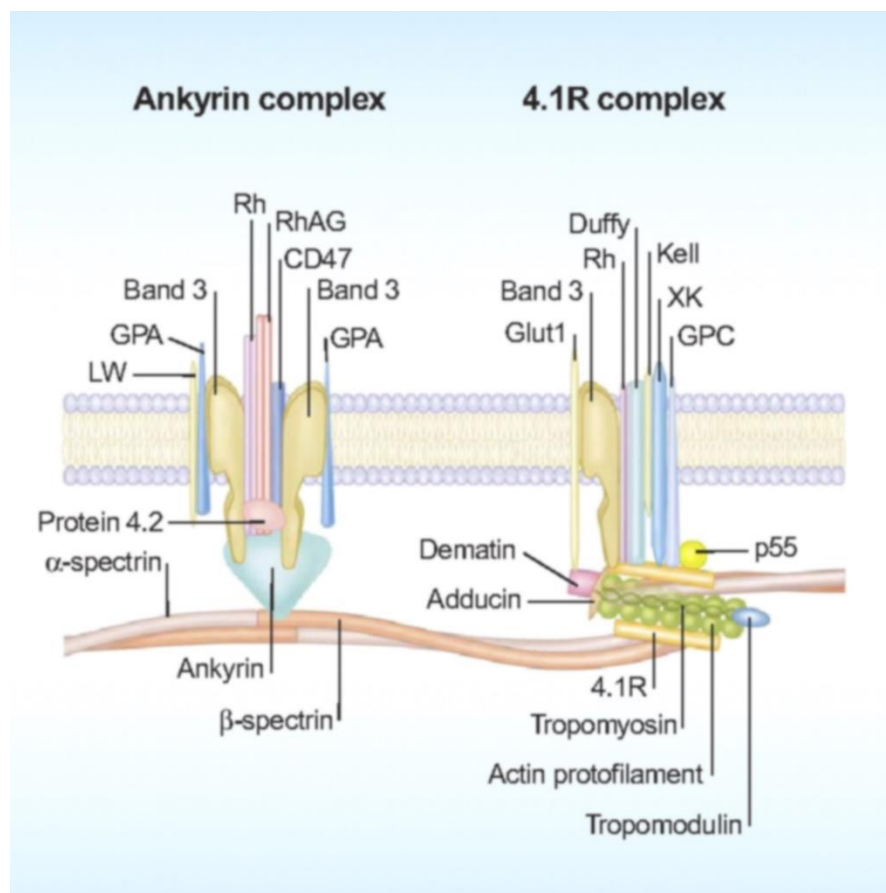


Fig. 24: Structural organization of the human red cell membrane [108]. The membrane of red blood cells is composed of a lipid bilayer penetrated by integral proteins and surrounding the cytoskeleton.

The dense glycocalyx is composed by the polysaccharide chains of glycolipids and glycoproteins carbohydrates capped by sialic acid, which can provide a negative charge to erythrocytes surface [109]. The lipid composition is important as it defines many physical properties such as membrane permeability and fluidity. The relative amounts of cholesterol and phospholipids are responsible for the fluid properties of the erythrocyte membrane. Alterations in the membrane cholesterol-phospholipid ratio result in morphologically abnormal erythrocytes with decreased life span [110]. Unlike cholesterol, which is evenly distributed between the inner and outer monolayer, the 5 major phospholipids are asymmetrically distributed. Phosphatidylcholine (PC) and sphingomyelin (SM) are present in the outer monolayer, whereas the inner monolayer is characterized by phosphatidylethanolamine (PE) and phosphatidylserine (PS) [111]. This asymmetric phospholipid distribution is the result of the activity of several phospholipid transport proteins [108]. Proteins called “flippases” move phospholipids from the outer to the inner monolayer, whereas “floppases” do the opposite operation, against a concentration gradient and in an energy dependent manner. Additionally, there are “scramblases” that move phospholipids in both directions at the same time down their concentration gradients. Since phosphatidylserine-exposing erythrocytes are subsequently recognized and degraded by macrophages [23], the maintenance of an asymmetric phospholipid distribution in the bilayer is crucial for the cell integrity and function. Membrane proteins with transport function include band 3 (anion transporter), aquaporin 1 (water transporter), Glut1 (glucose and L-dehydroascorbic acid transporter), Na⁺-K⁺-ATPase, Ca²⁺ ATPase, Na⁺-K⁺-2Cl⁻ cotransporter, Na⁺-Cl⁻ cotransporter, Na⁺-K⁺ cotransporter, K⁺-Cl⁻ cotransporter and Gardos Channel. Membrane proteins with adhesive function include ICAM-4, which interacts with integrins and Lu, the laminin-binding protein [108]. The erythrocyte cytoskeleton consists of several proteins that form a structural network under the lipid bilayer. The network is composed of spectrin, ankyrin, actin, protein 4.1, band 4.2, dematin, adducin, tropomyosin and tropomodulin [112]. Cytoskeletal proteins interact with integral proteins and lipids of the bilayer to maintain membrane integrity [112, 113].

11.3 Iron transporters and eryptosis

DMT1 is a key player in iron transport and absorption and is also expressed in immature erythroid cells [23]. Mutations that reduce its activity are associated with a severe defect in erythroid iron utilization and are correlated with hypochromic microcytic anemia both in human patients and rodent models (Belgrade rats) [6]. It has been shown that DMT1 knockout animals (Slc11a2^{-/-}) die in the first week of life due to iron deficient erythropoiesis [114]. DMT1 deficiency leads to an

impaired erythroid differentiation hallmarked by accumulation of immature forms of erythroblast, accelerated death of erythroid precursors and a decrease survival in the erythroid progenitors [114]. DMT1 deficiency in reticulocytes could correlate to reduced rate of heme synthesis. Iron deficiency, thalassemia and sickle cell disease are associated with shortened life span of erythrocytes. Iron deficiency may limit the synthesis of heme that in turn limits the synthesis of haemoglobin and decreases the production of red blood cells in the bone marrow, resulting in anemia. The accelerated clearance of RBCs during anaemia can be attributed to an increase in membrane stiffness and a decrease in deformability. The decrease in deformability and increase in membrane stiffness of RBCs can be attributed to oxidative stress [115]. Oxidative stress may increase haemoglobin autoxidation and subsequent generation of ROS can account for the shorter RBC lifespan and other pathological changes associated with iron-deficiency anaemia [115]. However, the accelerated clearance of erythrocytes can be attributed to excessive hemolysis or induction of programmed cell death of erythrocytes, called eryptosis [114]. In contrast to nucleated cells, however, erythrocytes lack nuclei and mitochondria which actively participate in the machinery underlying apoptosis [97]. Thus, eryptosis lacks several hallmarks of apoptosis, such as mitochondrial depolarization and condensation of nuclei. Eryptosis is fostered by an increase in cytosolic calcium; iron deficient erythrocytes when exposed to stress conditions have been demonstrated to activate Ca^{2+} -permeable cation channels allowing Ca^{2+} entry (Fig. 25) [96]. Ca^{2+} entry through these channels lead to activation of a scramblase with subsequent phosphatidylserine exposure, and to activation of the Gardos channels leading to KCl loss and cell shrinkage [116].

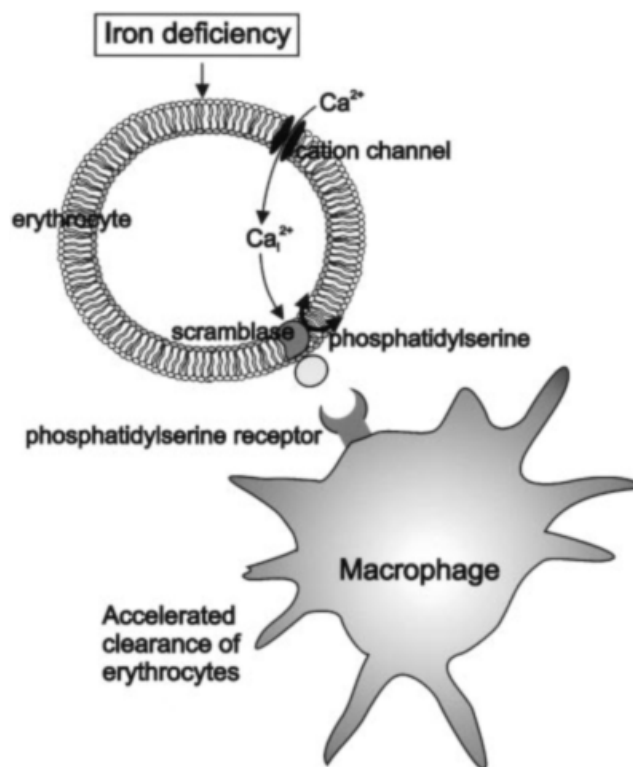


Fig. 25: Iron deficiency and the induction of eryptosis [96]. Iron deficient erythrocytes when exposed to stress conditions have been demonstrated to activate Ca^{2+} -permeable cation channels leading to Ca^{2+} entry.

Eryptosis is characterized by cell shrinkage, membrane blebbing and cell membrane scrambling apparent from phosphatidylserine translocation to the cell surface [96, 97]. Phosphatidylserine-exposing erythrocytes are subsequently recognized and degraded by macrophages (Fig. 26) [23, 96]. Approximately 80% of the iron comes from the breakdown of hemoglobin following macrophage phagocytosis of senescent erythrocytes. It has been shown that both NRAMP1 and NRAMP2 (DMT1) proteins play an important role in macrophage iron recycling. During the maturation process of the phagosome, NRAMP1 is recruited to the phagosomal membrane after bacterial engulfment and colocalizes with the lysosomal-associated membrane protein (LAMP1). Iron released from erythrocytes degradation is transported out of the phagosome by DMT1 [23]. Export of Fe^{2+} from the macrophage may be a function of the plasma membrane expression of ferroportin (Fig. 26) [117]. NRAMP1 may contribute to macrophage antimicrobial function by extruding from the phagolysosome (via H^+ /metal ion cotransport) divalent metal ions (such as Mn^{2+} and Fe^{2+}) that are essential cofactors for bacteria-derived enzymes (in particular superoxide dismutase) or are required for bacterial growth [117, 118].

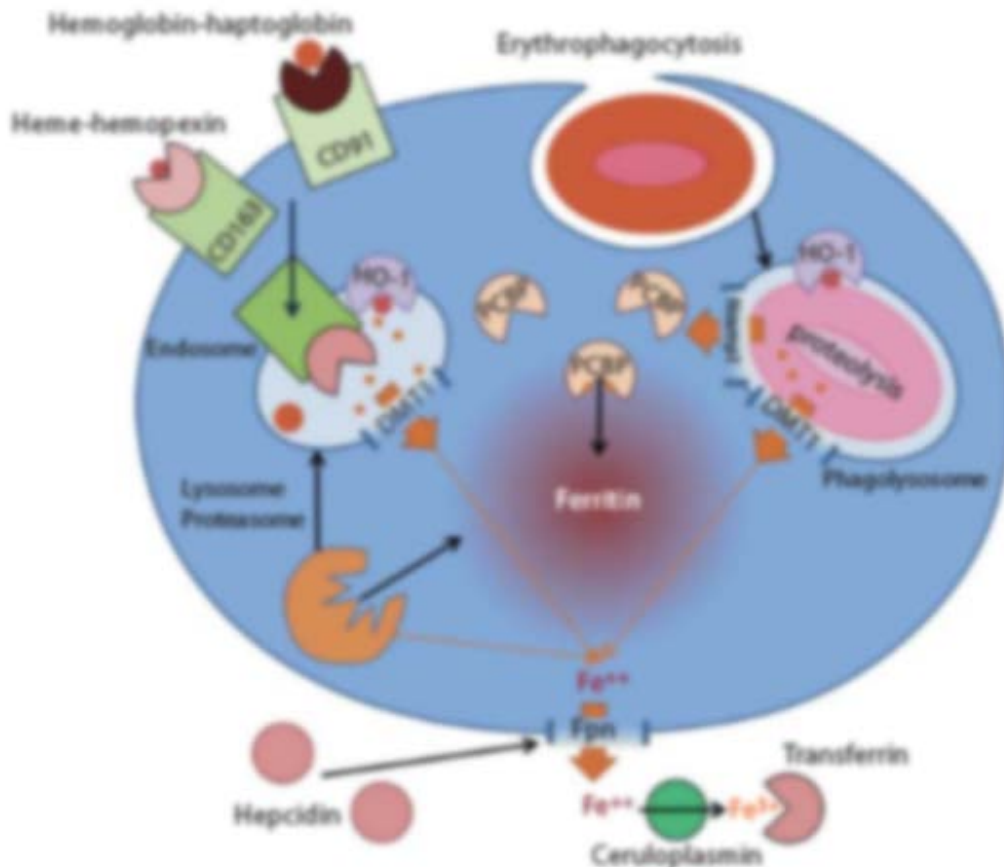


Fig. 26: Macrophages iron transporters (NRAMP1 and DMT1) [117]. Iron is taken up by macrophages through erythrophagocytosis of damaged or senescent erythrocytes. Macrophages can also collect heme and hemoglobin (hemopexin and haptoglobin, respectively) through receptor-mediated endocytosis (CD163 and CD91 receptor, respectively). Furthermore, hemoglobin undergoes proteolysis in order to release heme. Heme is degraded by Heme Oxygenase-1 (HO-1) to release iron, which is transported to the cytoplasm by DMT1 and NRAMP1. Cytoplasmic chaperones of the poly(rC) binding protein (PCBP) family may deliver iron for storage in ferritin. In addition, iron from endosomes or phagolysosomes may be delivered by a carrier to ferroportin (Fpn) for export.

11.4 Mechanism and pathophysiological significance of eryptosis

Similar to apoptosis of nucleated cells, erythrocytes may enter eryptosis, the suicidal death of erythrocytes characterized by phosphatidylserine translocation to the cell surface [96, 97]. Eryptosis lacks several hallmarks of apoptosis, such as mitochondrial depolarization and condensation of nuclei. Eryptotic cells are removed and thus prevented from undergoing hemolysis. Eryptosis is triggered by Ca²⁺ entry, ceramide formation, oxidative stress induced by ROS, energy depletion, activated caspases, and activation of some kinases, such as PKC and p38 kinase [97]. Eryptosis is induced by an increase in cytosolic calcium; erythrocytes when exposed to

stress conditions have been demonstrate to activate NSC channels (non-selective cation channels) allowing Ca^{2+} entry. In eryptosis, an increase of $[\text{Ca}^{2+}]_i$ may activate Ca^{2+} -sensitive K^+ channels (such as Gardos Channels) with subsequent activation of scramblases and leading to K^+ exit, cell membrane hyperpolarization, Cl^- exit and cellular loss of KCl with water leading to erythrocytes shrinkage [116, 119]. An increase of $[\text{Ca}^{2+}]_i$ further triggers cell membrane scrambling with translocation of phosphatidylserine from the inner monolayer of the cell membrane to the cell surface [116, 119]. Ca^{2+} entry may also activates calpain, a protein belonging to the family of calcium-dependent cysteine proteases, which in turn may degrade skeletal proteins and may foster cell membrane scrambling [97]. The Ca^{2+} sensitivity of cell membrane scrambling is enhanced by ceramide [97, 120]. Erythrocytes express PAF receptors, and PAF (Platelets-Associated Factor) stimulates the activation of sphingomyelinase which in turn can lead to ceramide formation [120]. Eryptosis could be stimulated by genetic or pharmacological knockout of AMPK, cGMP-dependent protein kinase, and sorafenib/sunitinib sensitive kinases. Eryptosis is stimulated by a variety of xenobiotics [121]. Eryptosis is also triggered by stress conditions, such as hyperosmolarity, oxidative stress and energy depletion. Erythrocytes express p38 kinase which is activated during hyperosmotic shock [97, 122]. The p38 kinase inhibitors SB203580 and Skepinone blunt the eryptosis following osmotic shock [122]. Erythrocytes further express casein kinase 1 (CK1). The CK1 inhibitors D4476 and (R)-DRF053 may blunt eryptosis following energy depletion or oxidative stress [97, 123]. RBCs contain considerable amounts of caspase-3 and -8, whereas essential components of the mitochondrial apoptotic cascade were missing [124, 125]. zVAD is a cell-permeable pancaspase inhibitor that irreversibly binds to the catalytic site of caspase proteases [101, 125]. Eryptosis is inhibited by nitric oxide, catecholamines and a variety of further small molecules [105]. Erythropoietin counteracts eryptosis in part by inhibiting the Ca^{2+} -permeable cation channels [121]. Eryptosis is fostered in several clinical conditions, such as iron deficiency, renal insufficiency, sepsis, haemolytic uremic syndrome (HUS), mycoplasma infection, malaria, sickle-cell anemia, and beta-thalassemia (Fig. 27) [105, 121, 126].

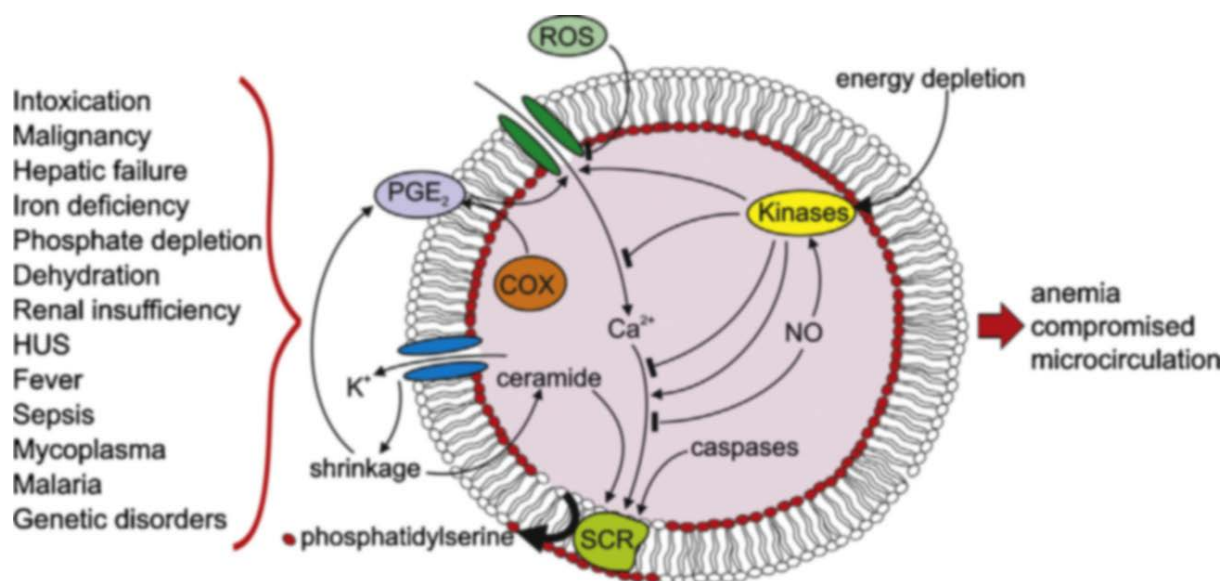


Fig. 27: Mechanism of eryptosis [105]. Eryptosis is fostered in several clinical conditions, for example intoxication, malignancy and iron deficiency. Erythrocytes when exposed to stress conditions may activate non-selective cation channels allowing calcium entry. In eryptosis, an increase of $[Ca^{2+}]_i$ may activate Ca^{2+} -sensitive K^+ channels with subsequent activation of scramblases and leading to K^+ exit, cell membrane hyperpolarization, Cl^- exit and cellular loss of KCl with water, leading to erythrocytes shrinkage. An increase of intracellular calcium may further trigger cell membrane scrambling with translocation of phosphatidylserine to the outer membrane.

11.5 Importance of eryptosis

As phosphatidylserine exposing erythrocytes are rapidly cleared from circulating blood, excessive eryptosis may result in anemia, which could develop whether the generation of new erythrocytes fails to replenish the loss of erythrocytes by eryptosis [105, 121]. Anemia may result from blood loss, impaired erythropoiesis caused by inadequate production of erythropoietin, decreased availability of iron or from decreased lifespan of erythrocytes [127]. Phosphatidylserine exposure to the erythrocytes surface fosters adherence to endothelial cells of the vascular wall and that binding of eryptotic cells to endothelial cells is mediated by the transmembrane CXCL16 (CXC chemokine ligand 16) [128]. Furthermore, phosphatidylserine may bind to other molecular partners, such as to the endothelial or subendothelial thrombospondin-1 (TSP) or to the endothelial CXCL16/SR-PSOX. Externalised phosphatidylserine on outer leaflet of eryptotic erythrocytes could also bind to platelets expressing CXCL16 and CD36 [129-131]. The adherence of phosphatidylserine-exposing erythrocytes to the vascular wall may impede microcirculation. Phosphatidylserine-exposing erythrocytes could further stimulate blood clotting. Thus, excessive eryptosis may foster

thrombosis [132, 133]. Eryptosis is a physiological mechanism which allow the clearance of defective erythrocytes from circulating blood prior to hemolysis [105]. Hemolysis is important in order to prevent lysis with subsequent release of hemoglobin into the blood flow [121]. Hemolysis is the rupturing of red blood cells, resulting in the release of their cytoplasm into blood vessels or extravascularly. Haemolysis may cause major harmful outcomes that could eventually progress to renal dysfunction, vascular disease, or chronic inflammation. Furthermore hemolysis of defective erythrocytes leads to release of hemoglobin, which passes the renal glomerular filter, precipitates in the acidic lumen of renal tubules, occludes nephrons and may thus trigger renal failure [134]. Eryptosis could overcome haemolysis, allowing the elimination of cells prior to the rupture of erythrocytes and providing beneficial effects. Hemolytic disorders could be paralleled by excessive eryptosis. Eryptosis is fostered following invasion of the malaria pathogen *Plasmodium*. Following entry into the erythrocyte, the pathogen induces the so-called new permeability pathways (NPP) [135] and also a subsequent oxidative stress, which in turn activates the Ca^{2+} -permeable cation channels and thus triggers eryptosis. The suicidal death is followed by the clearance of infected erythrocyte together with the pathogen, in order to counteract parasitemia [135]. Enhanced eryptosis is observed in newly formed erythrocytes of healthy individuals returning from high altitudes or space flight, a phenomenon called “neocytolysis” [121].

11.6 Xenobiotics tested

As has already been said, eryptosis is triggered also by many xenobiotics. This study was conducted in order to investigate prospective antitumoral products which are used against tumor growth in humans, in particular CA4P or Pazopanib, or compounds used *in vitro*, such as Nocodazole, Terfenadine, Piceatannol, Ceranib-2 and Sclareol, in order to unveil the effects on erythrocytes survival and to clarify the mechanisms and signalling involved in their action. CA4P and Pazopanib are used for the treatment of malignancies in humans and they may lead to apoptosis *in vitro*. Nocodazole, Terfenadine, Piceatannol, Ceranib-2 and Sclareol are drugs used *in vitro* and they may induce apoptosis through different mechanisms in cancer cell lines. So the present study explored whether these drugs stimulate eryptosis, the suicidal erythrocyte death characterized by cell shrinkage and phospholipid scrambling of the cell membrane with phosphatidylserine translocation to the cell surface.

11.6.1 CA4P

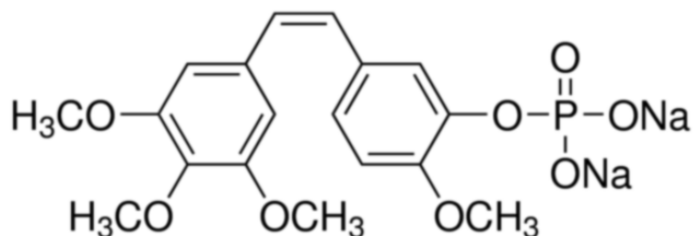


Fig. 28: Structure of CA4P [136].

Combretastatin A4 phosphate disodium (CA4P) (Fig. 28) is an antiangiogenic drug effective against several malignancies [137-141]. Vascular disrupting agents (VDAs) represent a new important therapeutic strategy to target the tumour neovasculature acutely to deprive tumours of blood supply [142-145]. CA4P is a drug of VDAs family and is a phosphate prodrug of combretastatin A4 which is isolated from *Combretum caffrum* (South African tree) and is a tubulin-binding microtubule depolymerizing agent that acts as a VDA [139]. Tubulin-binding agents, like vincristine or vinblastine, are potent anticancer drugs and colchicine was the first tubulin-binding agent discovered to have antivasular effects [140]. The mechanism of action of CA4P is thought to involve the binding of CA4 to tubulin leading to cytoskeletal and morphological changes in endothelial cells that lead to an increase of vascular permeability and disrupt tumor blood flow [146]. The active drug CA4 can induce also autophagy [147, 148], can counteract tumor cell migration [149], and trigger apoptosis [148]. This compound triggers eryptosis [98].

11.6.2 PAZOPANIB

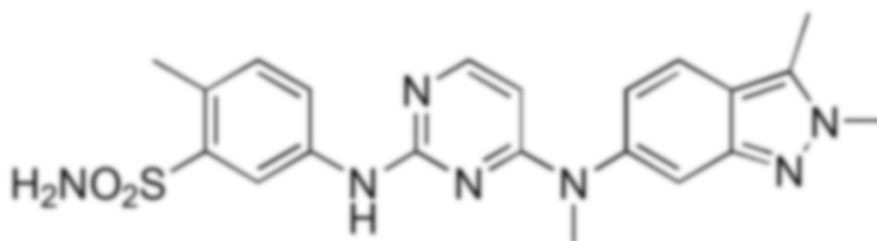


Fig. 29: Structure of Pazopanib [150].

Pazopanib (also known as “Votrient”) (Fig. 29) is an oral multi-target tyrosine kinase inhibitor targeting receptors of vascular endothelial growth factor (VEGF-1, -2 and -3), platelet derived growth factor (α and β) and stem cell factor (c-kit) [151]. Pazopanib exhibits *in vivo* and *in vitro* activity against tumor growth and in early clinical trials is well tolerated with few side effects, such as hypertension, fatigue and gastrointestinal disorders [152]. This drug is approved by FDA and EMA, and is used for the treatment of advanced renal cell carcinoma [153] and advanced soft tissue sarcoma [151]. Pazopanib is also used to counteract epithelial ovarian cancer [154], gastroenteropancreatic neuroendocrine tumours [155], malignant glioma [156], urothelial cancer [157, 158], breast cancer [159], non small cell lung carcinoma [160] and medulloblastoma [161]. Pazopanib has been shown to stimulate eryptosis [104], apoptosis [162] but may inhibit necroptosis [163]. Metabolism of Pazopanib involves cytochrome P-450 3A4 (CYP3A) [151]. This compound is also a substrate with a moderate affinity for the drug efflux transporters P-glycoprotein-1 (P-gp/ABCB1) and with a high affinity for breast cancer resistance protein (BCRP/ABCG2) [151].

11.6.3 NOCODAZOLE

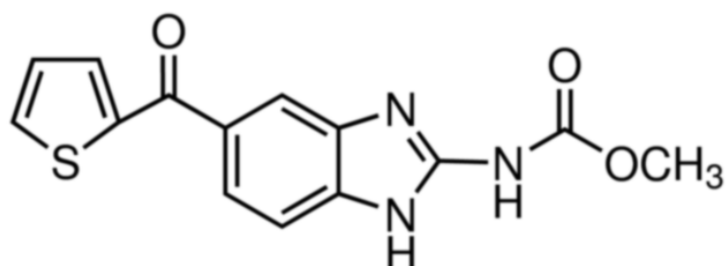


Fig. 30: Structure of Nocodazole [164].

Microtubule active drugs are used in the treatment of malignancies and they may produce mitotic arrest followed by apoptosis [165]. Several drugs including vincristine and colchicine are similar to Nocodazole (Fig. 30) in that they interfere with microtubule polymerization. Microtubules are a component of the cytoskeleton, and the dynamic microtubule network has several important roles in the cell, such as vesicular transport, forming the mitotic spindle and in cytokinesis. Nocodazole interferes with mitosis due to formation of multipolar spindles [166] and leading to cell cycle arrest in G₂/M [167, 168]. By interacting with microtubule function, Nocodazole or related substances trigger caspase-independent mitotic death [169] or caspase dependent apoptosis [165, 167, 170-174]. The triggering of apoptosis involves downregulation of mTOR [175], inactivation of the

antiapoptotic Bcl-2 [165, 176] and mitochondrial depolarization [173]. Nocodazole is thus effective against malignancy [166, 167, 170, 177, 178]. On the other hand, Nocodazole counteracts TNF- α -induced activation of the mitogen-activated protein kinase p38 [179].

11.6.4 TERFENADINE

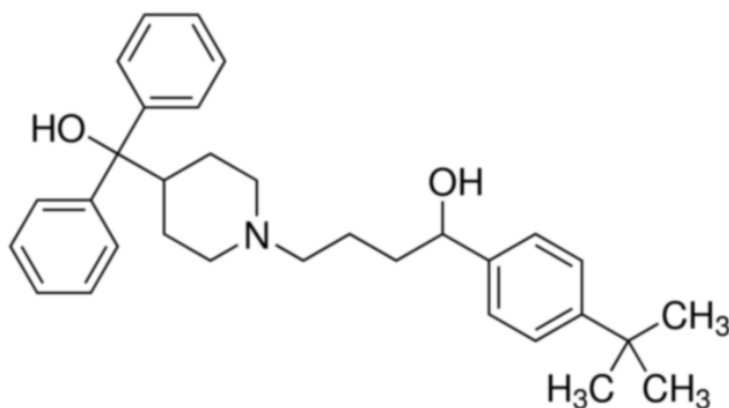


Fig. 31: Structure of Terfenadine [180].

Terfenadine (Fig. 31) is a selective H₁-histamine receptor antagonist [99, 181, 182]. This compound is a prodrug, generally completely metabolized to the active form fexofenadine in the liver by the enzyme cytochrome P-450 3A4. Due to its near complete metabolism by the liver immediately after leaving the gut, Terfenadine normally is not measurable in the plasma. Has been shown that Terfenadine induces a DNA damage response involving the activation of caspase-2 and activation of Chk1 and Chk2 kinases, phosphorylation of RPA32 and acetylation of Histone H3; these processes are correlated to severe mitochondrial dysfunction and the activation of caspase cascades [183-185]. Intracellular Ca²⁺ is commonly involved in cell death signal transduction. An unregulated increase in cytosolic Ca²⁺ levels is often cytotoxic and could induce cell death in most of the cells [184, 186]. Terfenadine can induce a cytosolic Ca²⁺ increase induced in a dose-dependent manner [184]. In addition to its anti-histaminic activity, this compound has been shown to block voltage-dependent ion channels and to reverse drug resistance in a variety of cell types via its interaction with P-glycoprotein [184, 187]. Terfenadine is also clinically used for the treatment of allergic disorders such as hay fever, allergic rhinitis and other histamine-mediated disorders [188-191].

11.6.5 PICEATANNOL

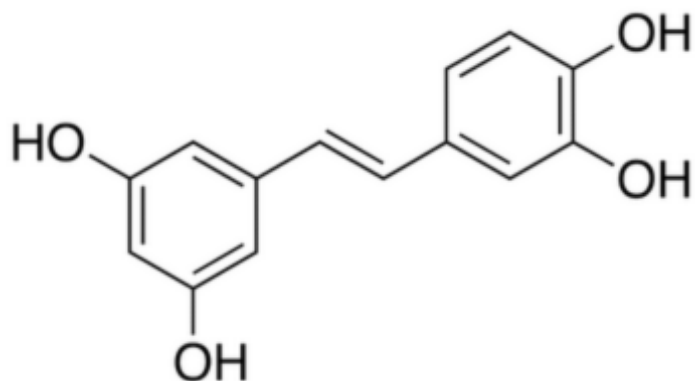


Fig. 32: Structure of Piceatannol [192].

Piceatannol (3, 3', 4, 5'-*trans*-trihydroxystilbene) (Fig. 32), a naturally occurring hydroxylated analogue of resveratrol found in diverse plants including red wine, grapes, white tea and passion fruit [193-195]. This compound is also found in mycorrhizal and non-mycorrhizal roots of Norway spruces (*Picea abies*) [196] and first isolated from the seeds of *Euphorbia lagascae* [197]. Piceatannol is effective against diverse disorders including hypercholesterolemia, arrhythmia, atherosclerosis and malignancy [193-195]. Piceatannol may foster vasodilation, counteracts angiogenesis as well as oxidative stress [194] and displays anti-inflammatory as well as anti-microbial activities [193]. Cellular mechanisms triggered by Piceatannol include inhibition of cyclooxygenase activity [194], cell-cycle arrest [193], upregulation of Bid, Bax, Bik, Bok, Fas as well as P21^{WAF1} [193], down-regulation of Bcl-xL as well as BCL-2 [193], mitochondrial depolarization [193], cytochrome c release [193], and caspase activation [193]. Piceatannol modifies gene expression by downregulation of transcription factor NF- κ B [193] and Janus kinase JAK1 [193]. Depending on the cell type, Piceatannol may either stimulate [193, 198] or inhibit [193] apoptosis. This compound has been reported to be a protein-tyrosine kinase inhibitor with immunosuppressive activity and it could play an important role in preventing graft rejection [199, 200]. Furthermore, Piceatannol possesses anti-inflammatory properties, suppressing the activation of the nuclear transcription factor nuclear factor κ B (NF- κ B) through the inhibition of the inhibitor of NF- κ B kinase and p65 phosphorylation [201, 202]. This compound may prevent interferon- α -induced inhibition of signal transducer and activator of transcription 3 (STAT3) and STAT3 phosphorylation in B and T lymphocytes [203, 204]. These results indicate that Piceatannol abrogates proinflammatory responses by modifying multiple cellular targets [205].

11.6.6 CERANIB-2

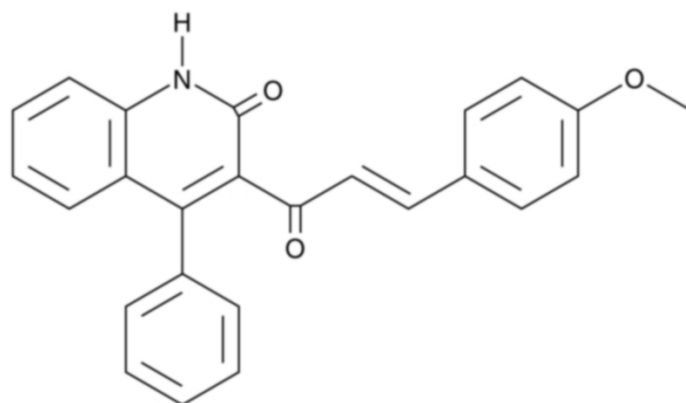


Fig. 33: Structure of Ceranib-2 [206].

The sphingolipid ceramide has been shown to trigger apoptosis in a wide variety of cells [207-213]. Ceramidase catalyzes the hydrolysis of the N-acyl linkage between the fatty acid and sphingosine base in ceramide to produce sphingosine and a free fatty acid. It plays a critical role in regulating cell fate and its inhibition in both malignant and non-cancerous cells leads to apoptosis [214]. Ceranib-2 (Fig. 33) is a non-lipid inhibitor of cellular ceramidase activity [206]. Ceramide induced cell death may involve mitochondria [215-218]. Even though lacking mitochondria, erythrocytes may similarly undergo suicidal death or eryptosis following exposure to ceramide [116]. In addition, it has been demonstrated that tumor cells can escape apoptosis by rapidly removing ceramide with ceramidases [219]. Ceramidases could be interesting targets for anticancer drug development because inhibiting their activity leads to an accumulation of ceramide and tumor cell death [220, 221]. In addition, it is also well known that ceramide may enhance apoptosis in response to paclitaxel, etoposide and gemcitabine [206]. Therefore, inhibition of ceramidase activity could also increase tumor chemosensitivity [206].

11.6.7 SCLAREOL

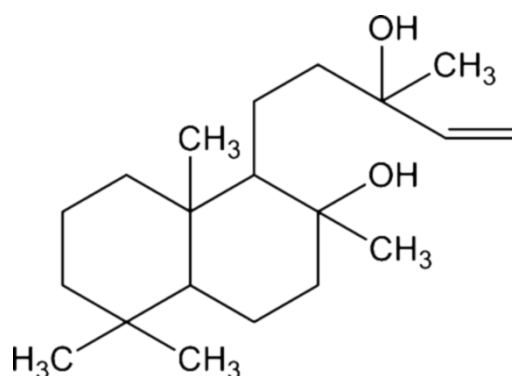


Fig. 34: Structure of Sclareol [222].

A large number of the phytochemicals, diterpenoids, abundantly occur in nature. The ditertiary alcohol, labd-14-ene-8,13-diol (Sclareol) (Fig. 34), which was first isolated from the plant *Salvia sclarea* [223], is abundant in nature, and is used as a fragrance in cosmetics, flavoring additive in food and beverage industry and folk medicine. Plant-derived terpenoids [224] such as the diterpene alcohol Sclareol [225] are effective against cancer [224, 226-236], inflammation [224, 237, 238], and infection [239-241]. Sclareol further influences brain function [242-248]. The effect of Sclareol against cancer is partially due to stimulation of tumor cell apoptosis [226-228, 230, 235, 236, 249]. Sclareol may lead to apoptosis in human leukemia cell lines, through an interesting mechanism that down-regulates *c-myc* without affecting the expression of the anti-apoptotic protein, Bcl-2 [250], and in cells derived from solid tumors by a mechanism that appears to be independent on p53-expression [251]. Sclareol is incorporated into phospholipid model membranes [252] and has been shown to suppress the formation of nitric oxide [238] and prostaglandin E2 (PGE2) [238].

12. AIM OF STUDY

This study investigate the mechanism of eryptosis due to xenobiotics in order to clarify the mechanisms involved in their action. In the experiments performed the erythrocytes were taken from healthy individual. Specimens from same individual were also used for controls. Experimental conditions and every experiment where done with erythrocytes from numerous individuals. In order to investigate the effects of xenobiotics on the suicidal death of erythrocytes, *in vitro* experiments were performed following 48 hours treatment of erythrocytes with various concentrations of the indicated drugs. The main hallmarks of eryptosis, such as phosphatidylserine exposure at the outer membrane of erythrocytes, FSC, increase of intracellular Ca^{2+} , ROS formation, GSH levels, ceramide formation, ATP measurements and percentage of hemolytic erythrocytes were determined by FACS analysis, confocal microscopy and spectrophotometrically to elucidate the effect of the drug on erythrocytes and in order to explore signalling pathways involved in eryptosis. Through these experiments it could be shown that these drugs tested impair erythrocyte survival by stimulation of eryptosis, the suicidal death of erythrocytes.

13. MATERIALS AND METHODS

13.1 Erythrocytes, solutions and chemicals

Fresh Li-Heparin-anticoagulated blood samples were kindly provided by the blood bank of the University of Tübingen. The study is approved by the ethics committee of the University of Tübingen (184/2003 V). The blood was centrifuged at 120 g for 20 min at 21 °C and the platelets and leukocytes-containing supernatant was disposed. Erythrocytes were incubated in vitro at a hematocrit of 0.4% in Ringer solution containing (in mM) 125 NaCl, 5 KCl, 1 MgSO₄, 32 N-2-hydroxyethylpiperazine-N-2-ethanesulfonic acid (HEPES; pH 7.4), 5 glucose, 1 CaCl₂, at 37°C for 48 hours. Erythrocytes were exposed for 48 hours to Combretastatin A4 phosphate disodium (CA4P), Nocodazole, Terfenadine, Ceranib-2 and Sclareol (Sigma Aldrich, Hamburg, Germany). Where indicated, erythrocytes were exposed for 48 hours to Pazopanib or Piceatannol (MedChem 90 Express, Princeton, USA). Water was used to dissolve Combretastatin A4 phosphate disodium and Terfenadine powder, whereas DMSO was used to dissolve Nocodazole, Pazopanib, Piceatannol, Ceranib-2 and Sclareol. Solvents used to dissolve the powders were added to the controls. In order to estimate the impact of Pazopanib on eryptosis due to high [Ca²⁺]_i, erythrocytes were exposed for 1 hour to a combination of Pazopanib and the Ca²⁺ ionophore ionomycin (Merck Millipore, Darmstadt, Germany). To test for an involvement of p38 kinase or casein kinase 1α, erythrocytes were exposed for 48 hours to a combination of Sclareol and p38 kinase inhibitor skepinone [253] or casein kinase 1α inhibitor D4476 (Tocris bioscience, Bristol, UK), respectively. To test for an involvement of pancaspase, erythrocytes were exposed for 48 hours to a combination of Nocodazole and pancaspase inhibitor zVAD-FMK (Enzo Life Sciences, Lörrach, Germany).

13.2 Annexin-V-binding and forward scatter

After incubation under the respective experimental condition, a 100 µl cell suspension was washed in Ringer solution containing 5 mM CaCl₂ and then stained with Annexin-V-FITC (1:200 dilution; ImmunoTools, Friesoythe, Germany) in this solution at 37°C for 20 min under protection from light [98-104]. The annexin-V-abundance at the erythrocyte surface was subsequently determined on a FACS Calibur (BD, Heidelberg, Germany). Annexin-V-binding was measured with an excitation wavelength of 488 nm and an emission wavelength of 530 nm. A marker (M1) was placed to set an arbitrary threshold between annexin-V-binding cells and control cells. The same threshold was used for untreated and CA4P treated erythrocytes. A dot plot of forward scatter (FSC) vs. side scatter (SSC) was set to linear scale for both parameters. The threshold of forward scatter was set at the default value of "52".

13.3 Intracellular Ca²⁺

After incubation, erythrocytes were washed in Ringer solution and loaded with Fluo-3/AM (Biotium, Hayward, USA) in Ringer solution containing 5 µM Fluo-3/AM [98-104]. The cells were incubated at 37°C for 30 min. Fluo3-dependent fluorescence was measured with an excitation wavelength of 488 nm and an emission wavelength of 530 nm on a FACS Calibur.

13.4 Hemolysis

For the determination of hemolysis, the samples were centrifuged (10 min at 2000 rpm, room temperature) after incubation under the respective experimental conditions and the supernatants were harvested [98-104]. As a measure of hemolysis, the hemoglobin (Hb) concentration of the supernatants was determined photometrically at 405 nm. The absorption of the supernatant of erythrocytes lysed in distilled water was defined as 100% hemolysis.

13.5 Reduced glutathione

The content of reduced glutathione was determined using 5-chloromethylfluorescein diacetate (CMFDA) staining [98]. After treatment, cells were spun down, incubated in Ringer solution containing 1 µM of CMFDA (Santa Cruz Biotechnology, USA) for 45 min, washed once, and resuspended in 200 µL of Ringer solution. The fluorescence intensity was measured with flow cytometry (FACS-calibur from Becton Dickinson; Heidelberg, Germany) at an excitation wavelength of 488 nm and an emission wavelength of 530 nm.

13.6 Reactive oxygen species (ROS)

Oxidative stress was determined utilizing 2',7'-dichlorodihydrofluorescein diacetate (DCFDA). After incubation, a 100 µl suspension of erythrocytes was washed in Ringer solution and then stained with DCFDA (Sigma, Schnelldorf, Germany) in Ringer solution containing DCFDA at a final concentration of 10 µM [98-104]. Erythrocytes were incubated at 37°C for 30 min in the dark and then washed in PBS. The DCFDA-loaded erythrocytes were resuspended in 200 µl Ringer solution, and DCF-dependent fluorescence intensity was measured at an excitation wavelength of 488 nm and an emission wavelength of 530 nm on a FACS Calibur (BD).

13.7 Ceramide abundance

For the determination of ceramide, a monoclonal antibody-based assay was used. After incubation, cells were stained for 1 hour at 37°C with 1 µg/ml anti ceramide antibody (clone MID 15B4, Alexis, Grünberg, Germany) in PBS containing 0.1% bovine serum albumin (BSA) at a dilution of 1:10 [98-104]. The samples were washed twice with PBS-BSA. Subsequently, the cells were stained for 30 minutes with polyclonal fluorescein isothiocyanate (FITC) conjugated goat anti-mouse IgG and IgM specific antibody (Pharmingen, Hamburg, Germany) diluted 1:50 in PBS-BSA. Unbound secondary antibody was removed by repeated washing with PBS-BSA. The samples were then analyzed by flow cytometric analysis with an excitation wavelength of 488 nm and an emission wavelength of 530 nm.

13.8 Intracellular ATP concentration

For the determination of intracellular ATP, 80 µl of erythrocyte pellets were incubated for 48 h at 37°C in Ringer solution (final hematocrit 4.7%) with or without 50 and 100 µM Combretastatin A4 phosphate [98]. All subsequent manipulations were performed at 4°C to avoid ATP degradation. Cells were lysed in distilled water, and proteins were precipitated by addition of HClO₄ (6%). After centrifugation, an aliquot of the supernatant (400 µl) was adjusted to pH 7.7 by addition of saturated KHCO₃ solution. After dilution of the supernatant, the ATP concentrations of the aliquots were determined utilizing the luciferin-luciferase assay kit (Roche Diagnostics) on a luminometer (BertholdBiolumat LB9500, Bad Wildbad, Germany) according to the manufacturer's protocol.

13.9 Tubulin abundance

For studying the effect of Nocodazole on tubulin in human erythrocytes TubulinTracker™ Green reagent (Oregon Green® 488 Taxol; bis-acetate, Thermo Fisher Scientific, MA, USA) was used [101]. Briefly, treated samples were stained with TubulinTracker (250 nM) for 30 min in the dark at 37°C. The erythrocytes were washed twice and finally resuspended in 200 µl Ringer solution containing 5 mM CaCl₂. For flow cytometry, TubulinTracker-dependent fluorescence of the samples was measured with an excitation wavelength of 488 nm and an emission wavelength of 530 nm on a FACS Calibur (BD). For confocal microscopy, 60 µl of each sample were spread onto a glass slide and dried for 15 minutes on RT. The slides were covered with PROlong Gold antifade reagent (Invitrogen, Darmstadt Germany). Images were taken on a Zeiss LSM 5 EXCITER confocal laser-

scanning microscope or with the phase light (Carl Zeiss MicroImaging, Germany) with a water immersion Plan-Neofluar 63/1.3 NA DIC.

13.10 Statistics

Data are expressed as arithmetic means \pm SEM. As indicated in the figure legends, statistical analysis was made using ANOVA with Tukey's test as post-test and t test as appropriate. n denotes the number of different erythrocyte specimens studied. Since different erythrocyte specimens used in distinct experiments are differently susceptible to triggers of eryptosis, the same erythrocyte specimens have been used for control and experimental conditions.

14. RESULTS

14.1 CA4P

The present study explored whether CA4P stimulates eryptosis, the suicidal erythrocyte death characterized by cell shrinkage and phosphatidylserine translocation to the cell surface. Erythrocyte cell volume was estimated from forward scatter, which was determined by flow cytometry. Prior to measurements, the erythrocytes were incubated for 48 hours in Ringer solution without or with CA4P (10 - 100 μM). As illustrated in Fig. 35, a 48 hours exposure to CA4P decreased erythrocyte forward scatter, an effect reaching statistical significance at 50 and 100 μM CA4P concentration. CA4P treatment was followed by a significant increase of the percentage of shrunken erythrocytes (Fig. 35C), an effect reaching statistical significance at 25 μM CA4P concentration. CA4P treatment simultaneously increased the percentage of swollen erythrocytes (Fig. 35D), an effect reaching statistical significance at 50 μM CA4P concentration.

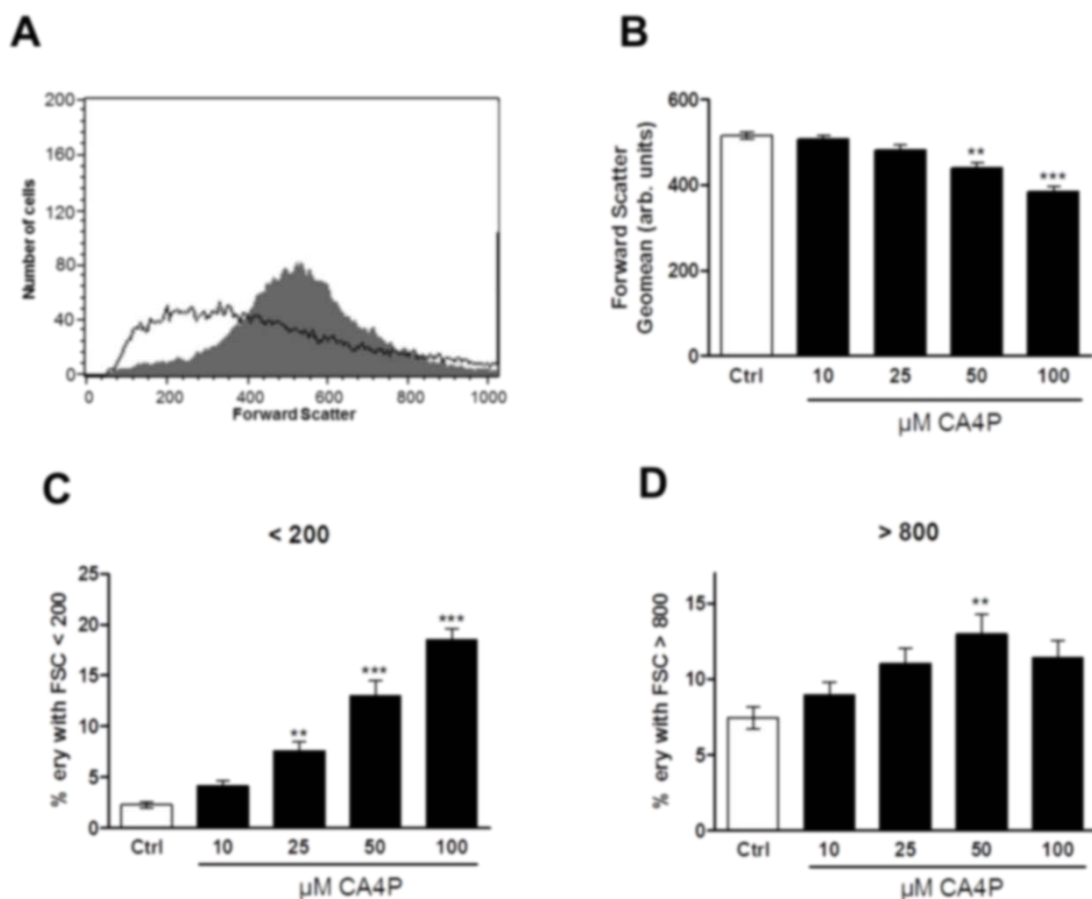


Fig. 35: Effect of CA4P on erythrocyte forward scatter. A. Original histogram of forward scatter of erythrocytes following exposure for 48 hours to Ringer solution without (grey area) and with (black line) presence of 100 μM CA4P. B. Arithmetic means \pm SEM ($n = 13$) of the erythrocyte forward scatter (FSC)

following incubation for 48 hours to Ringer solution without (white bar) or with (black bars) CA4P (10 – 100 μM). **C.** Arithmetic means \pm SEM ($n = 13$) of the percentage erythrocytes with forward scatter (FSC) <200 following incubation for 48 hours to Ringer solution without (white bar) or with (black bars) CA4P (10 – 100 μM). **D.** Arithmetic means \pm SEM ($n = 13$) of the percentage erythrocytes with forward scatter (FSC) >800 following incubation for 48 hours to Ringer solution without (white bar) or with (black bars) CA4P (10 – 100 μM). ******($p<0.01$), *******($p<0.001$) indicates significant difference from the absence of CA4P (ANOVA).

The translocation of phosphatidylserine to the erythrocyte surface was detected utilizing annexin-V-binding, as determined by flow cytometry. Prior to measurements, the erythrocytes were again incubated for 48 hours in Ringer solution without or with CA4P (10 - 100 μM). As shown in Fig. 36, a 48 hours exposure to CA4P increased the percentage of phosphatidylserine exposing erythrocytes, an effect reaching statistical significance at 50 μM CA4P.

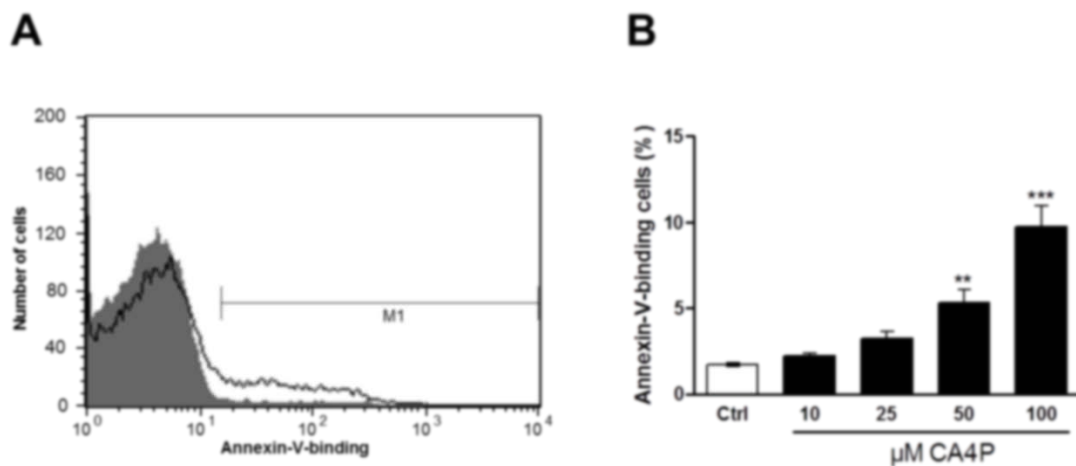


Fig. 36: Effect of CA4P on phosphatidylserine exposure. **A.** Original histogram of annexin-V-binding of erythrocytes following exposure for 48 hours to Ringer solution without (grey area) and with (black line) presence of 100 μM CA4P. **B.** Arithmetic means \pm SEM ($n = 13$) of erythrocyte annexin-V-binding following incubation for 48 hours to Ringer solution without (white bar) or with (black bars) CA4P (10 - 100 μM). ******($p<0.01$), *******($p<0.001$) indicates significant difference from the absence of CA4P (ANOVA).

In order to test whether CA4P induces hemolysis, the hemoglobin concentration was measured in the supernatant. As a result, the percentage of hemolytic erythrocytes was not significantly different between exposure to Ringer solution (1.9 ± 0.2 %, $n = 13$), and following exposure to 10 μM (1.8 ± 0.2 %, $n = 13$), 25 μM (1.9 ± 0.3 %, $n = 13$), 50 μM (2.5 ± 0.3 %, $n = 13$), and 100 μM (2.7 ± 0.3 %, $n = 13$) CA4P concentration.

Fluo3-fluorescence was utilized to estimate the effect of CA4P treatment on cytosolic Ca^{2+} activity ($[\text{Ca}^{2+}]_i$). Prior to measurements, the erythrocytes were incubated for 48 hours in Ringer solution without or with CA4P (10 - 100 μM). As shown in Fig. 37, a 48 hours exposure to 100 μM CA4P significantly increased the Fluo3-fluorescence.

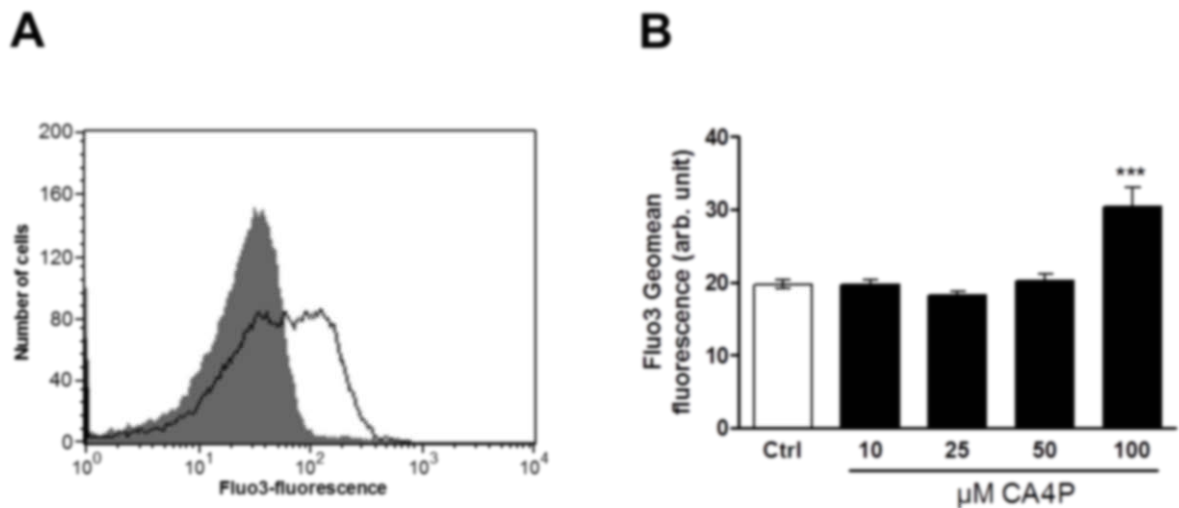


Fig. 37: Effect of CA4P on Fluo3-fluorescence. **A.** Original histogram of Fluo3-fluorescence reflecting cytosolic Ca^{2+} activity in erythrocytes following exposure for 48 hours to Ringer solution without (grey area) and with (black line) presence of 100 μM CA4P. **B.** Arithmetic means \pm SEM ($n = 13$) of erythrocyte Fluo3-fluorescence following incubation for 48 hours to Ringer solution without (white bar) or with (black bars) CA4P (10 - 100 μM). ***($p < 0.001$) indicates significant difference from the absence of CA4P (ANOVA).

Further experiments were performed in order to test whether the CA4P-induced cell membrane scrambling required entry of extracellular Ca^{2+} . Erythrocytes were incubated for 48 hours in the absence or presence of 50 or 100 μM CA4P in the presence or nominal absence of extracellular Ca^{2+} . As shown in Fig. 38, CA4P increased the percentage of annexin-V-binding erythrocytes. The effect of 100 μM CA4P was significantly blunted following removal of extracellular Ca^{2+} . However, even in the absence of extracellular Ca^{2+} , CA4P significantly increased the percentage of annexin-V-binding erythrocytes. CA4P-induced cell membrane scrambling was in large part but not exclusively due to mechanisms dependent on entry of extracellular Ca^{2+} .

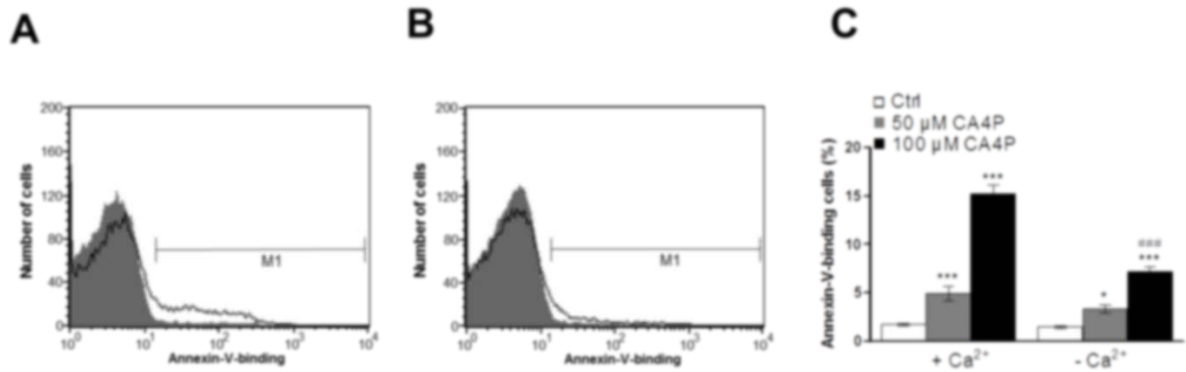


Fig. 38: Ca^{2+} sensitivity of CA4P-induced phosphatidylserine exposure. A,B. Original histogram of annexin-V-binding of erythrocytes following exposure for 48 hours to Ringer solution without (grey areas) and with (black lines) CA4P (100 μ M) in the presence (A) and absence (B) of extracellular Ca^{2+} . C. Arithmetic means \pm SEM (n = 10) of annexin-V-binding of erythrocytes after a 48 hours treatment with Ringer solution without (white bars) or with (grey, black bars) 50 and 100 μ M CA4P, respectively, in the presence (left bars, + Ca^{2+}) and absence (right bars, - Ca^{2+}) of Ca^{2+} . *(p<0.05),**(p<0.001) indicates significant difference from the absence of CA4P, ###(p<0.001) indicates significant difference from the presence of Ca^{2+} (ANOVA).

A further series of experiments were performed to investigate the effect of CA4P treatment on the erythrocyte glutathione (GSH) abundance. Erythrocytes were incubated for 48 hours in the absence or presence of 50 and 100 μ M CA4P. As shown in Fig. 39, CA4P (50, 100 μ M CA4P) significantly decreased the content of GSH.

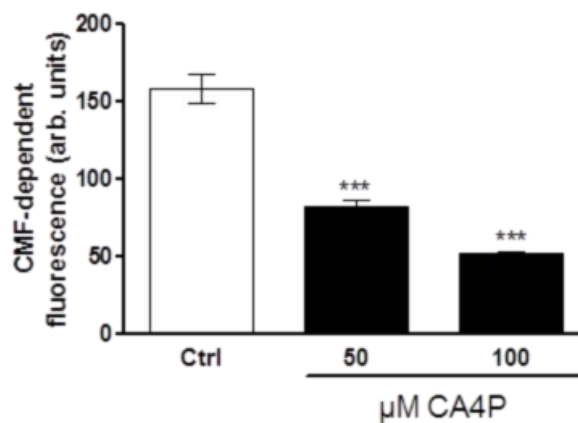


Fig. 39: Effect of CA4P on erythrocyte glutathione (GSH) abundance. Arithmetic means \pm SEM (n = 10) of the CMF-fluorescence (arbitrary units) in erythrocytes exposed for 48 hours to Ringer solution without (white bar) or with (black bars) 50 and 100 μ M CA4P. ***(p<0.001) indicates significant difference from the absence of CA4P (ANOVA).

Further series of experiments examined the influence of CA4P treatment on oxidative stress. To this end, reactive oxygen species (ROS) were determined utilizing 2',7'-dichlorodihydrofluorescein diacetate (DCFDA). As a result, the DCF-fluorescence was significantly ($p < 0.001$) lower following exposure to 50 μM (16.3 ± 0.9 a.u., $n = 13$) or 100 μM (15.6 ± 0.8 a.u., $n = 13$) CA4P concentration than following exposure to Ringer solution (23.1 ± 1.1 a.u., $n = 13$). Thus, a 48 hours exposure to CA4P decreased but did not increase ROS formation.

Eryptosis could further be stimulated by ceramide. Ceramide abundance at the erythrocyte surface was determined by flow cytometry utilizing specific antibodies. The ceramide abundance was similar following exposure to 50 μM (9.9 ± 0.1 a.u., $n = 10$) or 100 μM (10.6 ± 0.2 a.u., $n = 10$) CA4P concentration and following exposure to Ringer solution (10.4 ± 0.1 a.u., $n = 10$). Accordingly, a 48 hours exposure to CA4P (50 and 100 μM) did not significantly modify ceramide abundance.

In order to investigate whether CA4P fosters energy depletion, ATP levels were measured utilizing a luciferin–luciferase assay. As shown in Fig. 40, a 48 hours exposure to 100 μM CA4P significantly decreased the cytosolic ATP levels.

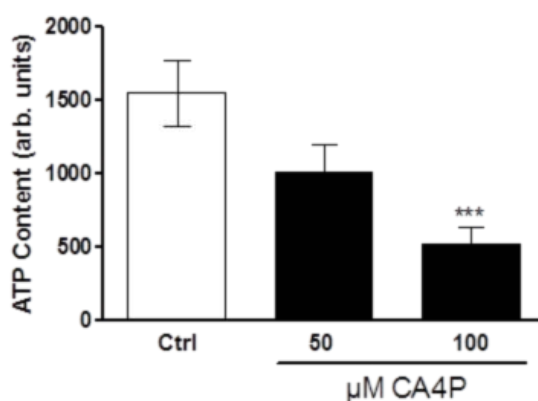


Fig. 40: Effect of CA4P on erythrocyte ATP concentration. Arithmetic means \pm SEM ($n = 5$) of the cytosolic ATP concentrations (arb. units) in erythrocytes exposed for 48 hours to Ringer solution without (white bar) or with (black bars) 50 and 100 μM CA4P. ***($p < 0.001$) indicate significant difference from the absence of CA4P (ANOVA).

14.2 PAZOPANIB

The present study investigated whether Pazopanib triggers eryptosis, the suicidal erythrocyte death characterized by phosphatidylserine translocation to the cell surface and cell shrinkage. Phosphatidylserine translocation to the erythrocyte surface was estimated from annexin-V-binding, which was determined by flow cytometry. Prior to measurements, the erythrocytes were incubated for 48 hours in Ringer solution without or with Pazopanib (10 – 50 $\mu\text{g}/\text{ml}$). As shown in Fig. 41, a 48 hours exposure to Pazopanib increased the percentage of phosphatidylserine exposing erythrocytes, an effect reaching statistical significance at 25 $\mu\text{g}/\text{ml}$ Pazopanib.

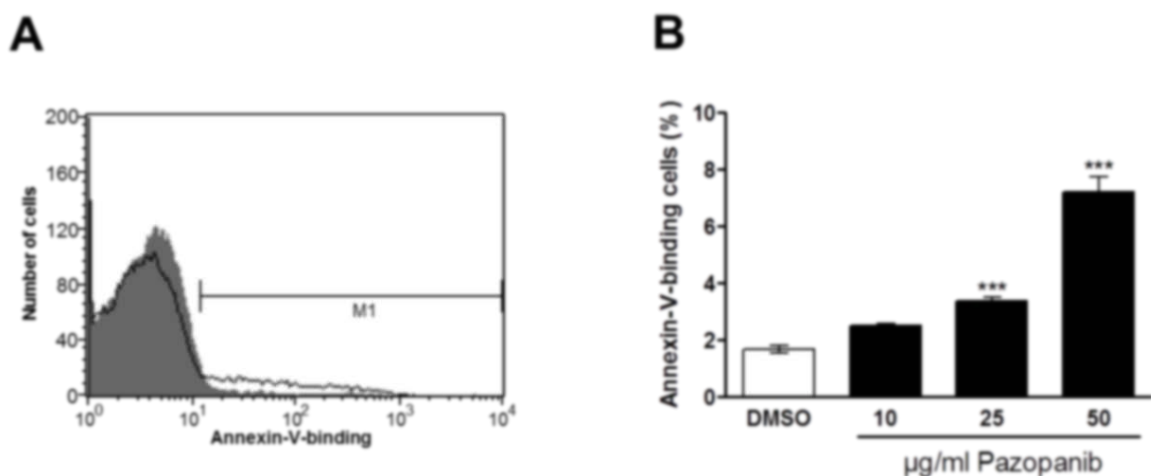


Fig. 41: Effect of Pazopanib on phosphatidylserine exposure. **A.** Original histogram of annexin-V-binding of erythrocytes following exposure for 48 hours to Ringer solution without (grey area) and with (black line) presence of 50 $\mu\text{g}/\text{ml}$ Pazopanib. **B.** Arithmetic means \pm SEM ($n = 16$) of erythrocyte annexin-V-binding following incubation for 48 hours to Ringer solution without (white bar) or with (black bars) Pazopanib (10 - 50 $\mu\text{g}/\text{ml}$). ***($p < 0.001$) indicates significant difference from the absence of Pazopanib (ANOVA).

Forward scatter was taken as a measure of erythrocyte cell volume and was determined by flow cytometry. Following a 48 hours exposure to Pazopanib (10 – 50 $\mu\text{g}/\text{ml}$), the average erythrocyte forward scatter was similar without Pazopanib treatment (497 ± 5.6 , $n = 16$) and following treatment with 10 $\mu\text{g}/\text{ml}$ (511 ± 4.8 , $n = 16$), 25 $\mu\text{g}/\text{ml}$ (505 ± 5.0 , $n = 16$), and 50 $\mu\text{g}/\text{ml}$ (476 ± 7.0 , $n = 16$) Pazopanib. Moreover, the percentage of cells with forward scatter > 800 was similar without Pazopanib treatment (96.4 ± 0.6 , $n = 16$) and following treatment with 10 $\mu\text{g}/\text{ml}$ (95.5 ± 0.5 , $n = 16$), 25 $\mu\text{g}/\text{ml}$ (95.1 ± 0.6 , $n = 16$), and 50 $\mu\text{g}/\text{ml}$ (94.9 ± 0.7 , $n = 16$) Pazopanib. Pazopanib increased the percentage of severely shrunken erythrocytes (Fig. 42A,B), an effect reaching statistical significance

at 50 $\mu\text{g/ml}$ Pazopanib concentration. Dot blots of annexin-V-binding versus forward scatter shows that the shrunken cells coincide with the annexin-V-binding cells (Fig. 42C,D).

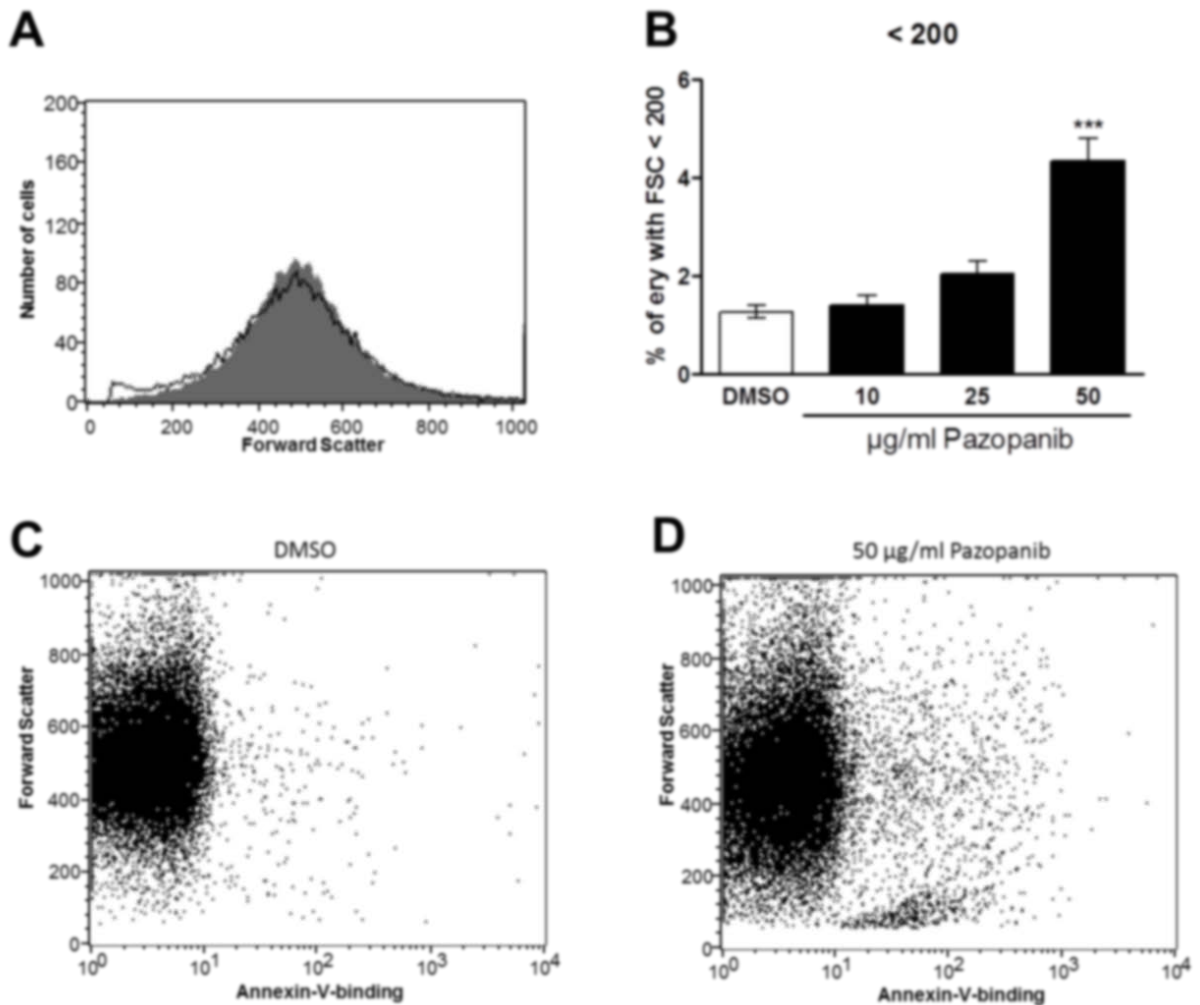


Fig. 42: Effect of Pazopanib on erythrocyte forward scatter. **A.** Original histogram of forward scatter of erythrocytes following exposure for 48 hours to Ringer solution without (grey area) and with (black line) presence of 50 $\mu\text{g/ml}$ Pazopanib. **B.** Arithmetic means \pm SEM ($n = 16$) of the percentage erythrocytes with forward scatter (FSC) < 200 following incubation for 48 hours to Ringer solution without (white bar) or with (black bars) Pazopanib (10 - 50 $\mu\text{g/ml}$). **C,D.** Original dot plots of forward scatter vs annexin-V-abundance without (**C**) and with (**D**) prior treatment with 50 $\mu\text{g/ml}$ Pazopanib. ***($p < 0.001$) indicates significant difference from the absence of Pazopanib (ANOVA).

In order to investigate the effect of Pazopanib on hemolysis, the percentage of haemolytic erythrocytes was determined from the hemoglobin concentration in the supernatant. As shown in

Fig. 43, Pazopanib increased the percentage of haemolytic erythrocytes, an effect reaching statistical significance at 25 µg/ml Pazopanib.

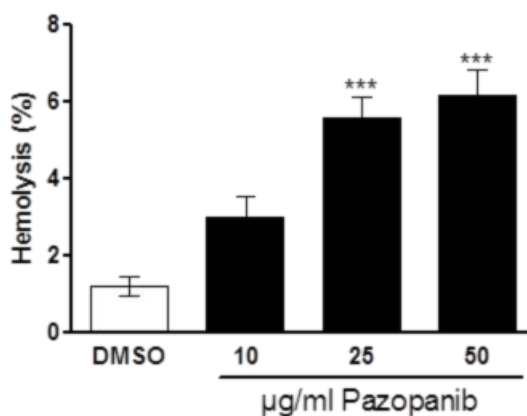


Fig. 43: Effect of Pazopanib on hemolysis. Arithmetic means \pm SEM (n = 8) of hemolytic erythrocytes following incubation for 48 hours to Ringer solution without (white bar) or with (black bars) Pazopanib (10 - 50 µg/ml). ***($p < 0.001$) indicates significant difference from the absence of Pazopanib (ANOVA).

Additional experiments explored the effect of CA4P on $[Ca^{2+}]_i$. Following a 48 hours incubation in Ringer solution without or with Pazopanib (10 – 50 µg/ml), the erythrocytes were loaded with Fluo-3 AM and the Fluo3-fluorescence was determined by flow cytometry. As a result, following a 48 hours incubation the Fluo3-fluorescence was lower in the presence of 50 µg/ml Pazopanib (17.8 ± 2.7 a.u., n = 12) than in the absence of Pazopanib (20.1 ± 3.6 a.u., n = 12). Further experiments were performed in order to investigate whether Pazopanib affects Fluo3-fluorescence of erythrocytes treated with the Ca^{2+} ionophore ionomycin (1 µM) and thus containing saturating $[Ca^{2+}]_i$. As a result, 50 µg/ml Pazopanib treatment decreased the Fluo3-fluorescence from 23.1 ± 3.2 a.u. (n = 5) to 16.5 ± 1.3 a.u. (n = 5) in the absence of ionomycin and from 46.1 ± 7.8 a.u. (n = 5) to 33.3 ± 3.8 a.u. (n = 5) in the presence of ionomycin. This results suggests that Pazopanib interferes with Fluo3-fluorescence by mechanisms other than decreasing $[Ca^{2+}]_i$, such as quenching of the Fluo3-fluorescence or leakage of dye thus reducing Fluo3-fluorescence.

Further experiments were performed in order to test whether the Pazopanib-induced cell membrane scrambling required entry of extracellular Ca^{2+} . Erythrocytes were incubated for 48 hours in the absence or presence of 50 µg/ml Pazopanib in the presence or nominal absence of extracellular Ca^{2+} . As shown in Fig. 44, removal of extracellular Ca^{2+} significantly blunted the effect

of Pazopanib on annexin-V-binding. However, even in the absence of extracellular Ca^{2+} , Pazopanib significantly increased the percentage of annexin-V-binding erythrocytes. Pazopanib-induced cell membrane scrambling was in part but not fully dependent on entry of extracellular Ca^{2+} .

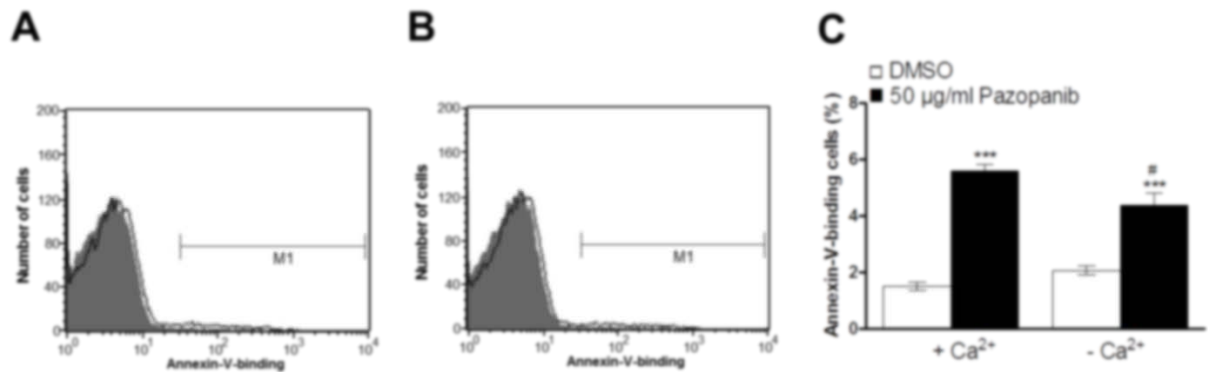


Fig. 44: Ca^{2+} sensitivity of Pazopanib-induced phosphatidylserine exposure. **A,B.** Original histogram of annexin-V-binding of erythrocytes following exposure for 48 hours to Ringer solution without (grey area) and with (black line) Pazopanib (50 $\mu\text{g}/\text{ml}$) in the presence (**A**) and absence (**B**) of extracellular Ca^{2+} . **C.** Arithmetic means \pm SEM ($n = 8$) of annexin-V-binding of erythrocytes after a 48 hours treatment with Ringer solution without (white bars) or with (black bars) Pazopanib (50 $\mu\text{g}/\text{ml}$) in the presence (left bars, + Ca^{2+}) and absence (right bars, - Ca^{2+}) of Ca^{2+} . **C.** Arithmetic means \pm SEM ($n = 8$) of annexin-V-binding of erythrocytes after a 48 hours treatment with Ringer solution without (white bars) or with (black bars) Pazopanib (50 $\mu\text{g}/\text{ml}$) in the presence (left bars, + Ca^{2+}) and absence (right bars, - Ca^{2+}) of Ca^{2+} . ***($p < 0.001$) indicates significant difference from the absence of Pazopanib, #($p < 0.05$) indicates significant difference from the presence of Ca^{2+} (ANOVA).

Other mechanisms known to induce eryptosis include oxidative stress. Reactive oxygen species (ROS) were thus quantified using 2',7'-dichlorodihydrofluorescein diacetate (DCFDA). As shown in Fig. 45, Pazopanib increased the DCF-fluorescence in erythrocytes, an effect reaching statistical significance at 50 $\mu\text{g}/\text{ml}$ Pazopanib.

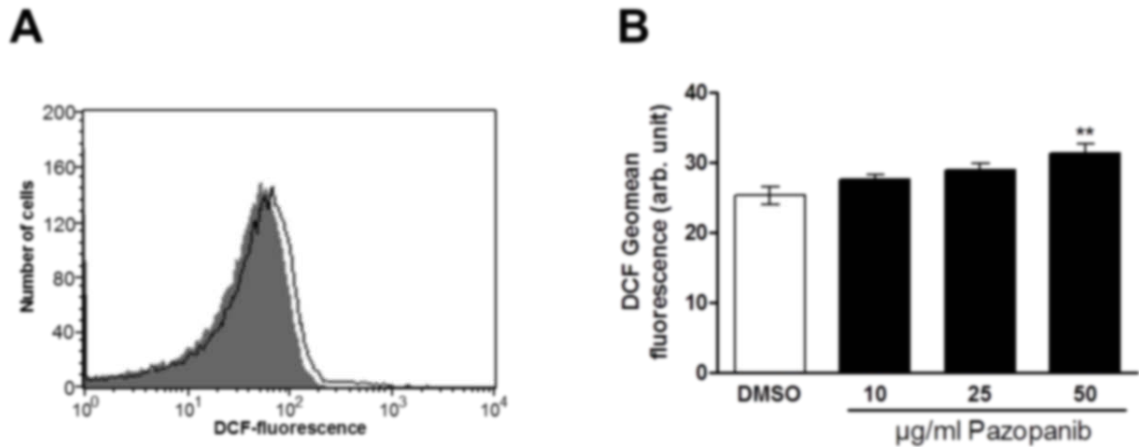


Fig. 45: Effect of Pazopanib on ROS formation. **A.** Original histogram of DCF-fluorescence in erythrocytes following exposure for 48 hours to Ringer solution without (grey area) and with (black line) presence of Pazopanib (50 µg/ml). **B.** Arithmetic means \pm SEM (n = 12) of the DCF-fluorescence (arbitrary units) in erythrocytes exposed for 48 hours to Ringer solution without (white bar) or with (black bars) Pazopanib (10 - 50 µg/ml). **($p < 0.01$) indicates significant difference from the absence of Pazopanib (ANOVA).

Eryptosis could further be stimulated by ceramide. Ceramide abundance at the erythrocyte surface was measured utilizing specific antibodies. As shown in Fig. 46, 50 µg/ml Pazopanib significantly increased the ceramide abundance at the erythrocyte surface.

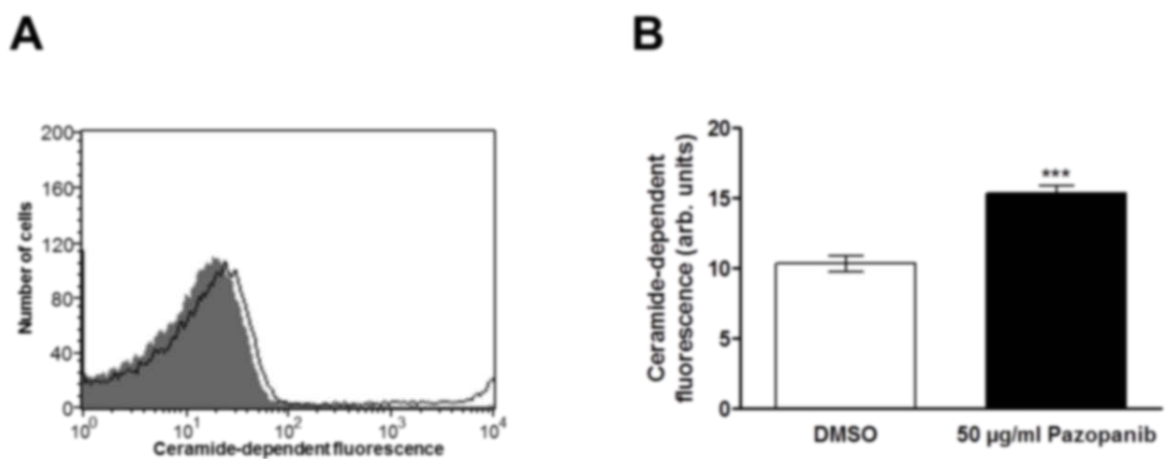


Fig. 46: Effect of Pazopanib on ceramide abundance at the erythrocyte surface. **A.** Original histogram of ceramide abundance in erythrocytes following exposure for 48 hours to Ringer solution without (grey area) and with (black line) presence of 50 µg/ml Pazopanib. **B.** Arithmetic means \pm SEM (n = 8) of the ceramide abundance (arbitrary units) in erythrocytes exposed for 48 hours to Ringer solution without (white bar) or with (black bar) presence of 50 µg/ml Pazopanib. ***($p < 0.001$) indicates significant difference from the absence of Pazopanib (ANOVA).

14.3 NOCODAZOLE

Flow cytometry was employed to explore whether Nocodazole triggers eryptosis, the suicidal erythrocyte death characterized by cell shrinkage and cell membrane scrambling with phosphatidylserine translocation to the cell surface. In order to identify phosphatidylserine exposing erythrocytes, the erythrocytes were incubated with annexin-V which tightly binds to surface phosphatidylserine. Annexin-V-abundance was determined by flow cytometry. The measurements were performed following a 48 hours incubation in Ringer solution without or with Nocodazole (15 - 60 $\mu\text{g}/\text{ml}$). As shown in Fig. 47, a 48 hours exposure to Nocodazole increased the percentage of phosphatidylserine exposing erythrocytes, an effect reaching statistical significance at 30 $\mu\text{g}/\text{ml}$ Nocodazole.

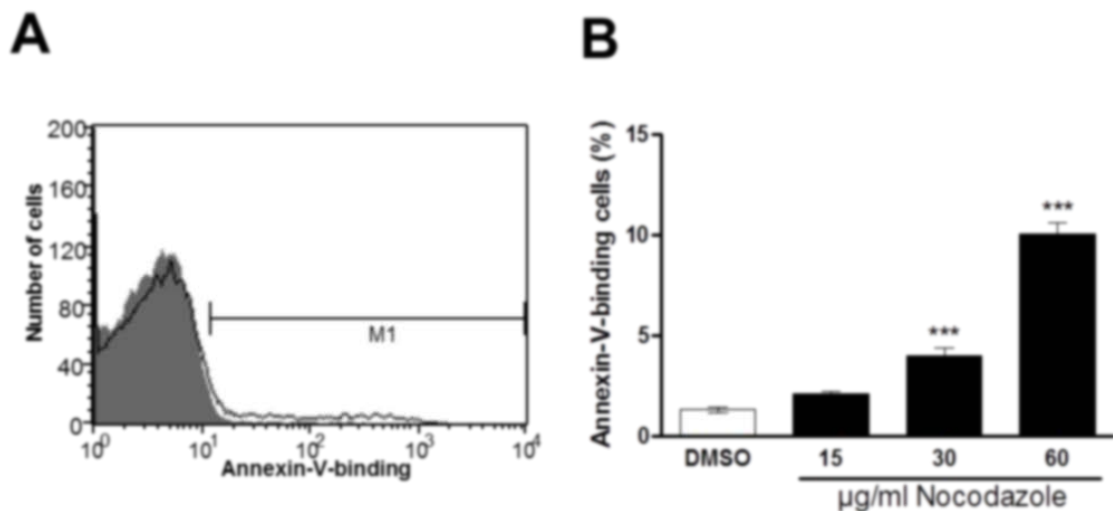


Fig. 47: Effect of Nocodazole on phosphatidylserine exposure. **A.** Original histogram of annexin-V-binding of erythrocytes following exposure for 48 hours to Ringer solution with solvent DMSO (grey area) and with presence of 60 $\mu\text{g}/\text{ml}$ Nocodazole (black line). **B.** Arithmetic means \pm SEM ($n = 8$) of erythrocyte annexin-V-binding (black bars) following incubation for 48 hours to Ringer solution without or with presence of Nocodazole (15 - 60 $\mu\text{g}/\text{ml}$). ***($p < 0.001$) indicates significant difference from the absence of Nocodazole (ANOVA).

Cell volume of human erythrocytes was estimated from forward scatter in flow cytometry, following a 48 hours incubation in Ringer solution without or with Nocodazole (15 – 60 $\mu\text{g}/\text{ml}$). As illustrated in Fig. 48, Nocodazole did not modify the average erythrocyte forward scatter. However, exposure of erythrocytes to Nocodazole was followed by an increase of the percentage of both

small (Fig. 48C) and large (Fig. 48D) erythrocytes, alterations reaching significance at Nocodazole concentrations of 60 µg/ml.

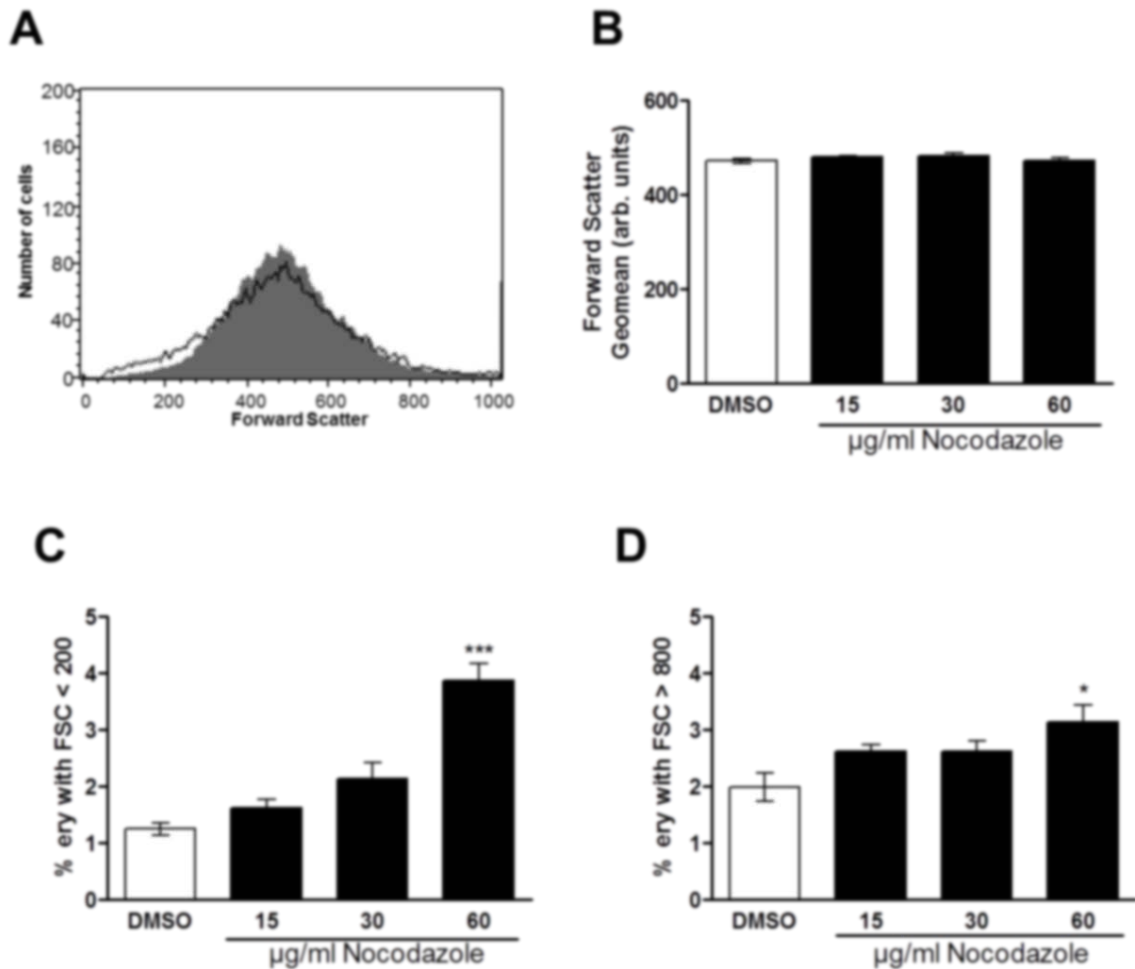


Fig. 48: Effect of Nocodazole on erythrocyte forward scatter. A. Original histogram of forward scatter of erythrocytes following exposure for 48 hours to Ringer solution with solvent DMSO (grey area) and with presence of 60 µg/ml Nocodazole (black line). B. Arithmetic means ± SEM (n = 8) of the erythrocyte forward scatter (FSC) following incubation for 48 hours to Ringer solution without (white bar) or with (black bars) Nocodazole (15 - 60 µg/ml). C. Arithmetic means ± SEM (n = 8) of the percentage erythrocytes with forward scatter (FSC) < 200 following incubation for 48 hours to Ringer solution without (white bar) or with (black bars) Nocodazole (15 - 60 µg/ml). D. Arithmetic means ± SEM (n = 8) of the percentage erythrocytes with forward scatter (FSC) > 800 following incubation for 48 hours to Ringer solution without (white bar) or with (black bars) Nocodazole (15 - 60 µg/ml). *(p<0.05),***(p<0.001) indicate significant difference from the absence of Nocodazole (ANOVA).

In order to test whether Nocodazole induces hemolysis, the hemoglobin concentration was determined in the supernatant. Following a 48 hours incubation, the percentage of hemolytic

erythrocytes was similar in the absence of Nocodazole ($3.4 \pm 0.2\%$ $n = 12$) and in the presence of 15 $\mu\text{g}/\text{ml}$ ($4.4 \pm 0.2\%$ $n = 12$) or 30 $\mu\text{g}/\text{ml}$ ($4.7 \pm 0.2\%$ $n = 12$) Nocodazole. Exposure to 60 $\mu\text{g}/\text{ml}$ Nocodazole was, however, followed by a significant increase of hemolysis ($11.1 \pm 0.9\%$ $n = 12$).

Fluo3-fluorescence was employed in order to test, whether Nocodazole influences the cytosolic Ca^{2+} activity. As shown in Fig. 49, a 48 hours exposure to Nocodazole increased the Fluo3-fluorescence, an effect reaching statistical significance at 60 $\mu\text{g}/\text{ml}$ Nocodazole.

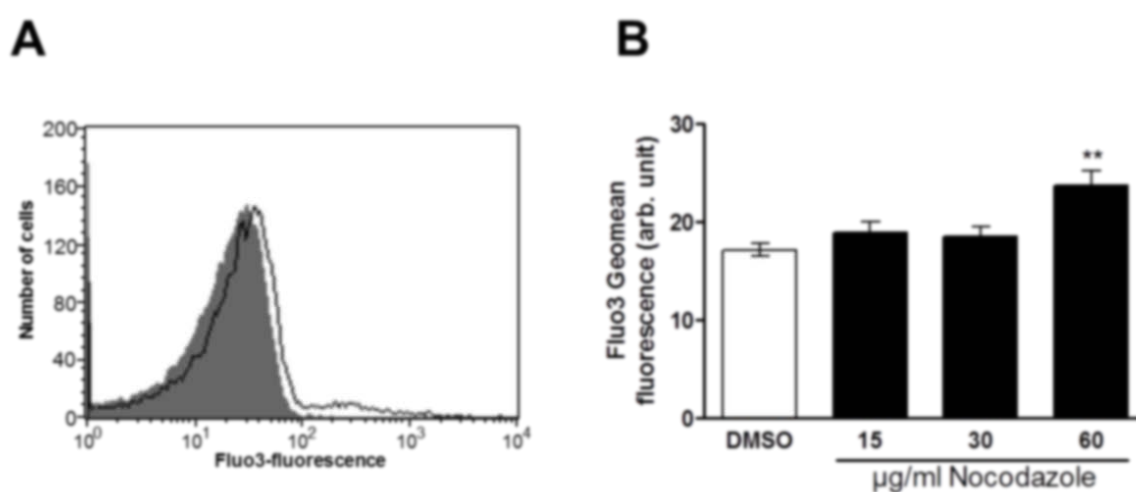


Fig. 49: Effect of Nocodazole on erythrocyte Ca^{2+} activity. **A.** Original histogram of Fluo3-fluorescence in erythrocytes following exposure for 48 hours to Ringer solution with solvent DMSO (grey area) and with presence of 60 $\mu\text{g}/\text{ml}$ Nocodazole (black line). **B.** Arithmetic means \pm SEM ($n = 8$) of the Fluo3-fluorescence (arbitrary units) in erythrocytes exposed for 48 hours to Ringer solution without (white bar) or with (black bars) Nocodazole (15 – 60 $\mu\text{g}/\text{ml}$). **($p < 0.01$) indicate significant difference from the absence of Nocodazole (ANOVA).

Further experiments were performed in order to test whether the Nocodazole-induced cell membrane scrambling required entry of extracellular Ca^{2+} . Prior to measurements, erythrocytes were incubated for 48 hours in the absence or presence of 60 $\mu\text{g}/\text{ml}$ Nocodazole in the presence or nominal absence of extracellular Ca^{2+} . As illustrated in Fig. 50, removal of extracellular Ca^{2+} significantly blunted the effect of Nocodazole on annexin-V-binding. Nevertheless, even in the absence extracellular Ca^{2+} Nocodazole significantly increased the percentage of annexin-V-binding erythrocytes. Nocodazole-induced cell membrane scrambling was in part but not fully due to entry of extracellular Ca^{2+} . Neither in the presence nor in the absence of extracellular Ca^{2+} did Nocodazole significantly modify average forward scatter.

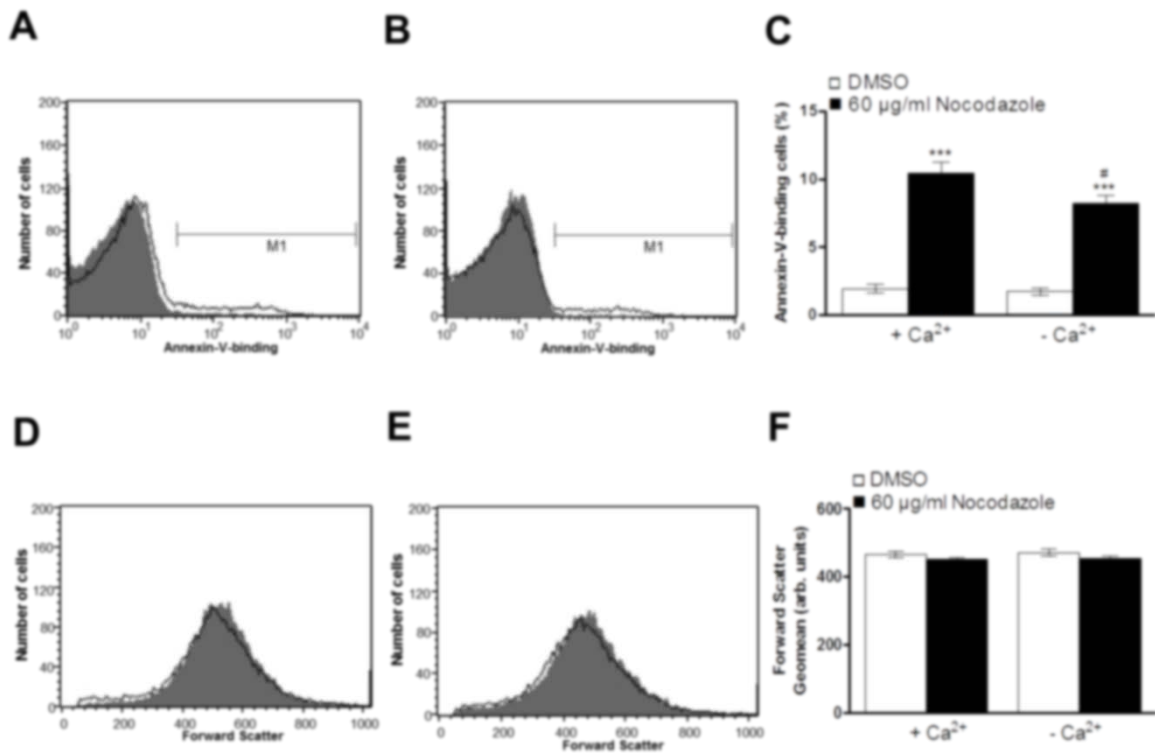


Fig. 50: Ca^{2+} sensitivity of Nocodazole-induced phosphatidylserine exposure and erythrocyte shrinkage. A,B. Original histogram of annexin-V-binding of erythrocytes following exposure for 48 hours to Ringer solution with solvent DMSO (grey area) and with presence of 60 $\mu\text{g/ml}$ Nocodazole (black line) in the presence (A) and absence (B) of extracellular Ca^{2+} . C. Arithmetic means \pm SEM ($n = 12$) of annexin-V-binding of erythrocytes after a 48 hours treatment with Ringer solution without (white bars) or with (black bars) Nocodazole (60 $\mu\text{g/ml}$) in the presence (left bars, + Ca^{2+}) and absence (right bars, - Ca^{2+}) of Ca^{2+} . D,E. Original histogram of erythrocyte forward scatter following exposure for 48 hours to Ringer solution with solvent DMSO (grey area) and with presence of 60 $\mu\text{g/ml}$ Nocodazole (black line) in the presence (D) and absence (E) of extracellular Ca^{2+} . F. Arithmetic means \pm SEM ($n = 12$) of erythrocyte forward scatter after a 48 hours treatment with Ringer solution without (white bars) or with (black bars) Nocodazole (60 $\mu\text{g/ml}$) in the presence (left bars, + Ca^{2+}) and absence (right bars, - Ca^{2+}) of Ca^{2+} . ***($P < 0.001$) indicates significant difference from the absence of Nocodazole, #($p < 0.05$) indicates significant difference from the presence of Ca^{2+} (ANOVA).

To investigate whether a 48 hours incubation with Nocodazole modified the effect of excessive $[Ca^{2+}]_i$ on cell membrane scrambling or forward scatter, erythrocytes were exposed for 60 min to Ca^{2+} ionophore ionomycin (1 μM). Ionomycin increased the percentage of annexin-V-binding erythrocytes to similarly high levels in erythrocytes incubated with Nocodazole (from $4.8 \pm 0.3\%$ to $35.8 \pm 1.6\%$ $n = 4$) and in erythrocytes incubated without Nocodazole (from $1.6 \pm 0.2\%$ to $38.7 \pm 1.8\%$ $n = 4$). Ionomycin decreased the forward scatter to similarly low levels in erythrocytes

incubated with Nocodazole (from $432 \pm 8.8\%$ to $124 \pm 1.9\%$, $n = 4$) and in erythrocytes incubated without Nocodazole (from $440 \pm 8.8\%$ to $123 \pm 4.4\%$, $n = 4$).

Further experiments were performed to clarify the effect of Nocodazole on oxidative stress. Reactive oxygen species (ROS) were determined utilizing 2',7'-dichlorodihydrofluorescein diacetate (DCFDA). As shown in Fig. 51, a 48 hours exposure to Nocodazole increased the DCF-fluorescence, an effect reaching statistical significance at 30 $\mu\text{g}/\text{ml}$ Nocodazole.

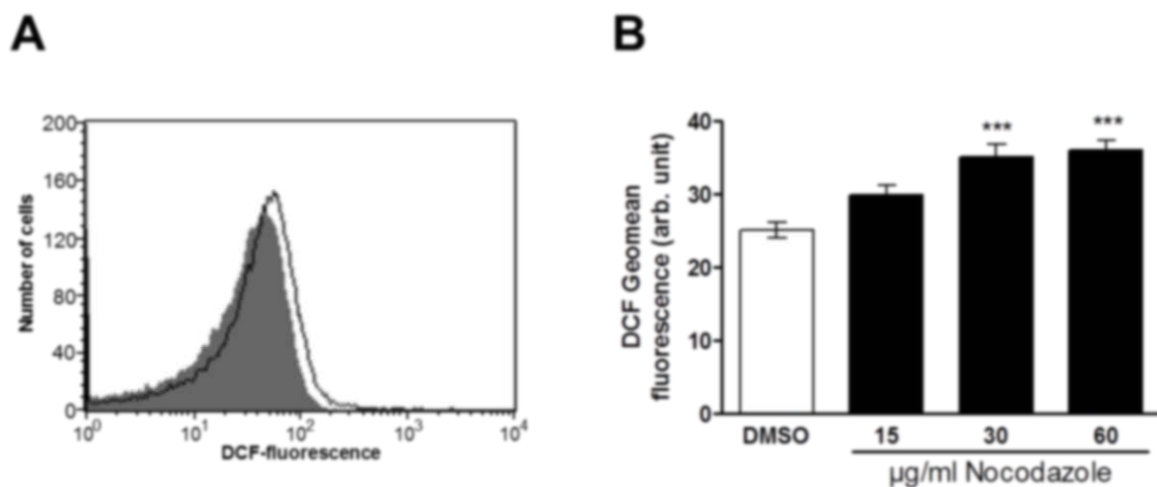


Fig. 51: Effect of Nocodazole on erythrocyte ROS formation. **A.** Original histogram of DCF-fluorescence in erythrocytes following exposure for 48 hours to Ringer solution with solvent DMSO (grey area) and with presence of 60 $\mu\text{g}/\text{ml}$ Nocodazole (black line). **B.** Arithmetic means \pm SEM ($n = 8$) of the DCF-fluorescence (arbitrary units) in erythrocytes exposed for 48 hours to Ringer solution without (white bar) or with (black bars) Nocodazole (15 – 60 $\mu\text{g}/\text{ml}$). ***($p < 0.001$) indicates significant difference from the absence of Nocodazole (ANOVA).

Eryptosis could further be stimulated by ceramide. Ceramide abundance at the erythrocyte surface was measured utilizing specific antibodies. As shown in Fig. 52, a 48 hours exposure to Nocodazole (60 $\mu\text{g}/\text{ml}$) significantly increased the ceramide abundance.

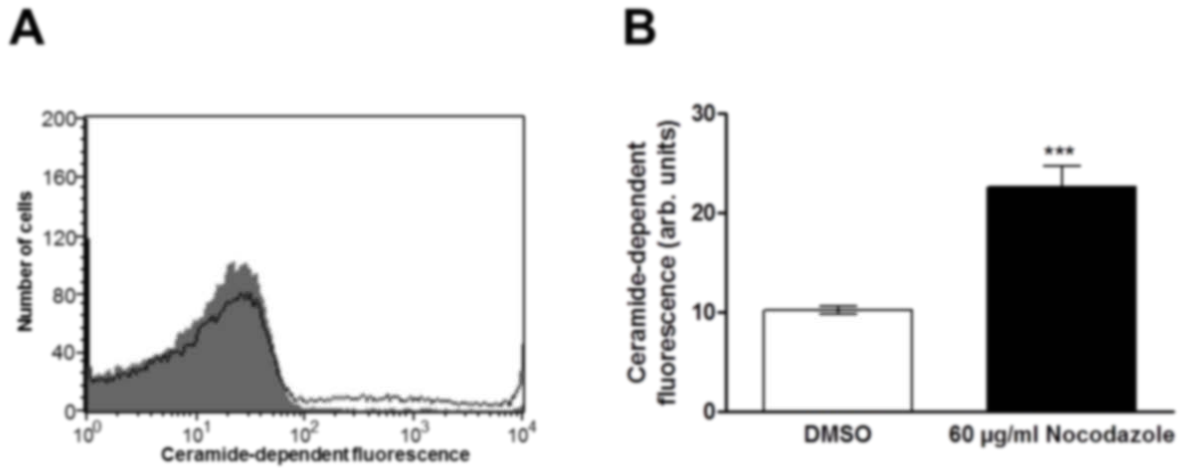


Fig. 52: Effect of Nocodazole on ceramide abundance at the erythrocyte surface. **A.** Original histogram of ceramide abundance in erythrocytes following exposure for 48 hours to Ringer solution with solvent DMSO (grey area) and with presence of 60 µg/ml Nocodazole (black line). **B.** Arithmetic means \pm SEM ($n = 9$) of the ceramide abundance (arbitrary units) in erythrocytes exposed for 48 hours to Ringer solution without (white bar) or with (black bars) Nocodazole (60 µg/ml). ***($p < 0.001$) indicates significant difference from the absence of Nocodazole (Paired t test).

To clarify the effect of Nocodazole on tubulin in erythrocytes, TubulinTracker reagent was utilized in both flow cytometry and confocal microscopy. As shown in Fig. 53, 48 hours treatment of erythrocytes with Nocodazole (60 µg/ml) significantly reduced the TubulinTracker-dependent fluorescence.

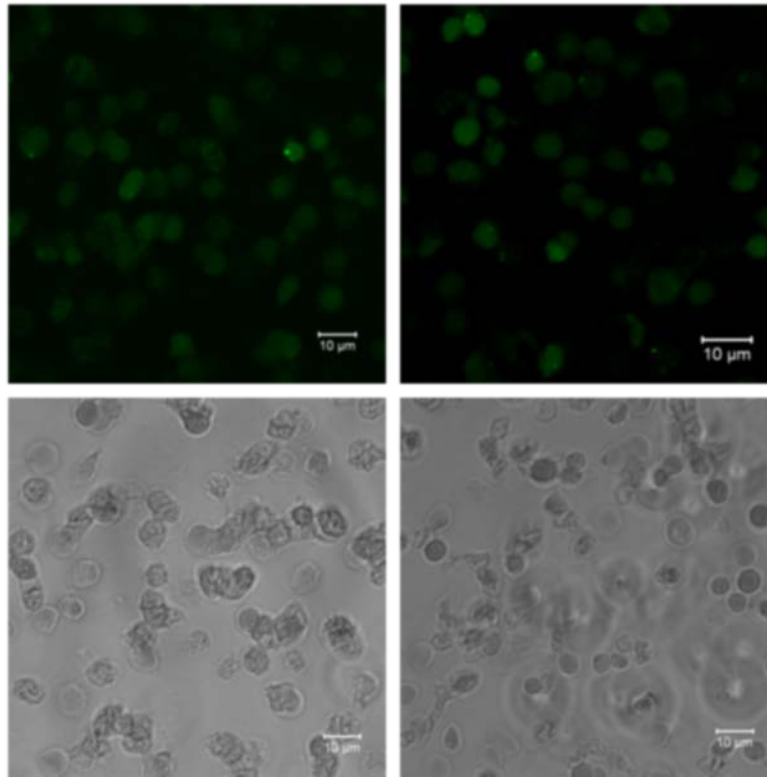
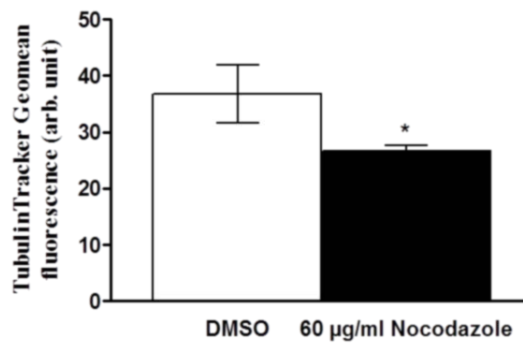
A**B**

Fig. 53: Effect of Nocodazole on tubulin abundance. **A.** Confocal images of tubulin abundance in erythrocytes following exposure for 48 hours to Ringer solution with solvent DMSO (left panel) and with presence of 60 µg/ml Nocodazole (right panel). **B.** Arithmetic means ± SEM (n = 4) of the TubulinTracker abundance (arbitrary units) in erythrocytes exposed for 48 hours to Ringer solution without (white bar) or with (black bars) Nocodazole (60 µg/ml). *(p<0.05) indicates significant difference from the absence of Nocodazole (Paired t test).

To investigate whether the stimulation of cell membrane scrambling by Nocodazole required caspase activity, erythrocytes were exposed for 48 hours to 60 $\mu\text{g}/\text{mL}$ Nocodazole either in the absence or presence of the pancaspase inhibitor zVAD (1 μM). As shown in Fig. 54, zVAD did not significantly modify the effect of Nocodazole on annexin-V-binding.

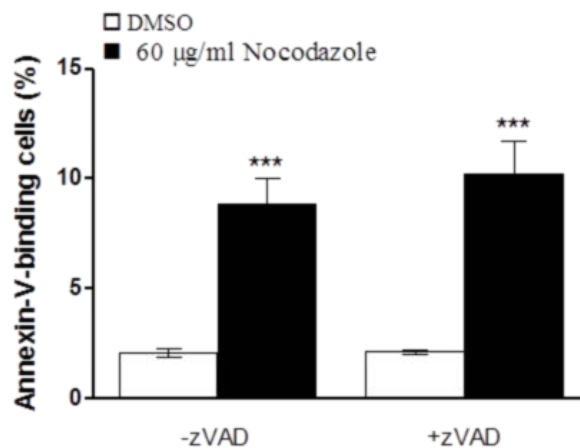


Fig. 54: Insensitivity of Nocodazole induced phosphatidylserine exposure on caspase inhibitor zVAD. Arithmetic means \pm SEM (n = 9) of erythrocyte annexin-V-binding following incubation for 48 hours to Ringer solution without (white bars) or with (black bars) Nocodazole (60 $\mu\text{g}/\text{ml}$) treatment in the absence (-zVAD) or presence (+zVAD) of the pancaspase inhibitor zVAD (1 μM). ***($p < 0.001$) indicates significant difference from the absence of Nocodazole (ANOVA).

14.4 TERFENADINE

The present study explored whether Terfenadine influences eryptosis, the suicidal erythrocyte death characterized by cell shrinkage and phosphatidylserine translocation to the cell surface. Forward scatter was determined by flow cytometry as a measure of erythrocyte cell volume. The measurements were performed after incubation of the erythrocytes 48 hours in Ringer solution without or with Terfenadine (1 – 10 μM). As illustrated in Fig. 55, Terfenadine did not significantly

modify the average erythrocyte forward scatter and did significantly modify the percentage of severely shrunken or swollen erythrocytes (Fig. 55C, D).

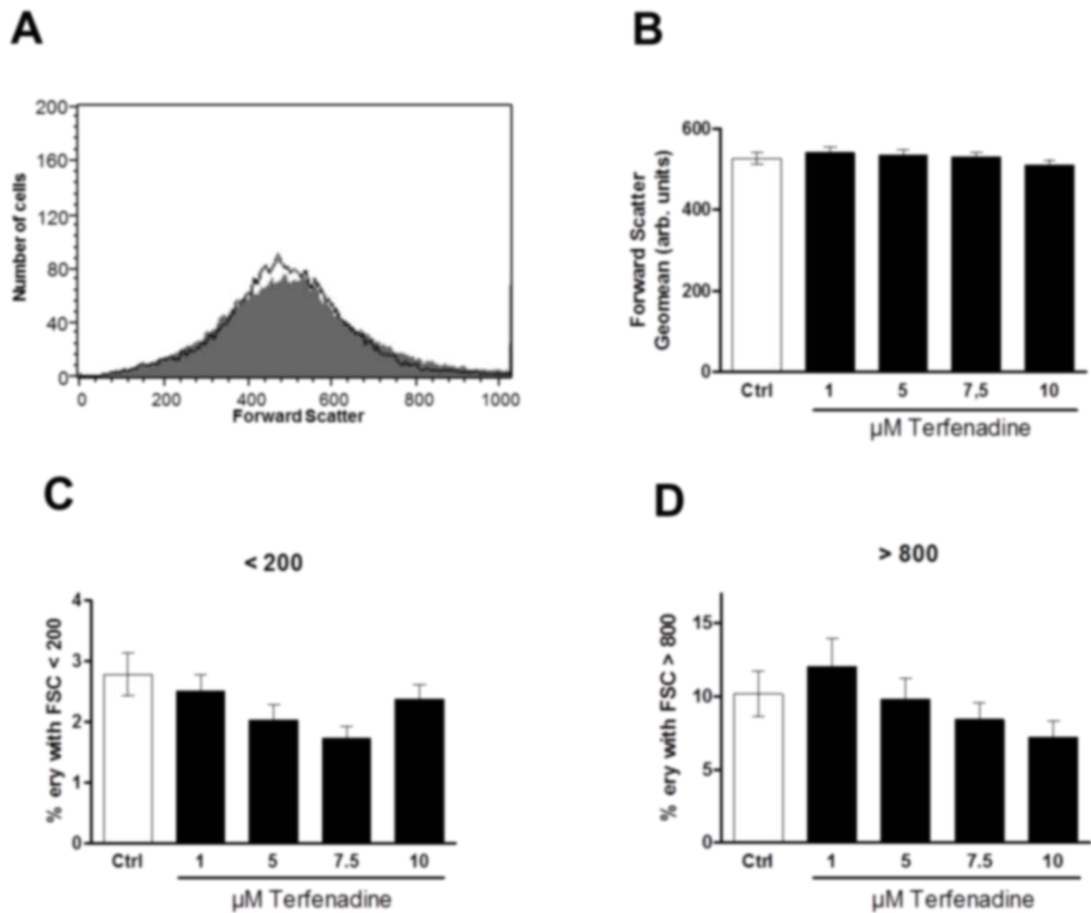


Fig. 55: Effect of Terfenadine on erythrocyte forward scatter. **A.** Original histogram of forward scatter of erythrocytes following exposure for 48 hours to Ringer solution without (grey area) and with (black line) presence of 10 μM Terfenadine. **B.** Arithmetic means \pm SEM ($n = 14$) of the erythrocyte forward scatter (FSC) following incubation for 48 hours to Ringer solution without (white bar) or with (black bars) Terfenadine (1 - 10 μM). **C.** Arithmetic means \pm SEM ($n = 14$) of the percentage erythrocytes with forward scatter (FSC) < 200 following incubation for 48 hours to Ringer solution without (white bar) or with (black bars) Terfenadine (1 - 10 μM). **D.** Arithmetic means \pm SEM ($n = 14$) of the percentage erythrocytes with forward scatter (FSC) > 800 following incubation for 48 hours to Ringer solution without (white bar) or with (black bars) Terfenadine (1 - 10 μM).

The translocation of phosphatidylserine to the erythrocyte surface was detected utilizing annexin-V-binding, as determined by flow cytometry. The erythrocytes were incubated for 48 hours in Ringer solution without or with Terfenadine (1 - 10 μM). As illustrated in Fig. 56, a 48 hours

exposure to Terfenadine increased the percentage of phosphatidylserine exposing erythrocytes, an effect reaching statistical significance at 5 μM Terfenadine.

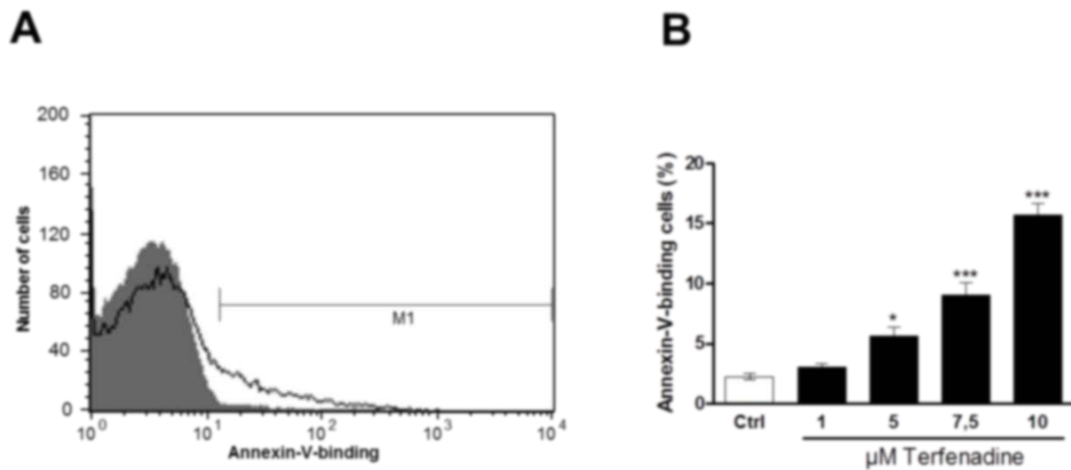


Fig. 56: Effect of Terfenadine on phosphatidylserine exposure. **A.** Original histogram of annexin-V-binding of erythrocytes following exposure for 48 hours to Ringer solution without (grey area) and with (black line) presence of 10 μM Terfenadine. **B.** Arithmetic means \pm SEM ($n = 14$) of erythrocyte annexin-V-binding following incubation for 48 hours to Ringer solution without (white bar) or with (black bars) Terfenadine (1 - 10 μM). *($p < 0.05$), ***($p < 0.001$) indicates significant difference from the absence of Terfenadine (ANOVA).

In order to test whether Terfenadine induces hemolysis, the hemoglobin concentration was determined in the supernatant. As shown in Fig. 57, a 48 hours exposure to Terfenadine increased the percentage of hemolytic erythrocytes, an effect reaching statistical significance at 5 μM Terfenadine concentration. Thus, Terfenadine increased $[\text{Ca}^{2+}]_i$.

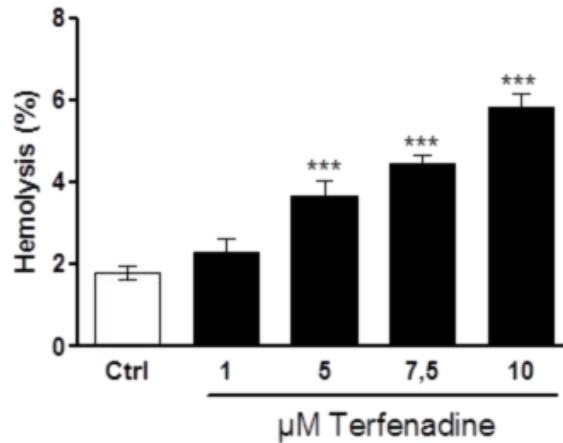


Fig. 57: Effect of Terfenadine on hemolysis. Arithmetic means \pm SEM (n = 14) of erythrocyte annexin-V-binding following incubation for 48 hours to Ringer solution without (white bar) or with (black bars) Terfenadine (1 - 10 μ M). ***($p < 0.001$) indicates significant difference from the absence of Terfenadine (ANOVA).

Fluo3-fluorescence was employed in order to test, whether Terfenadine influences the cytosolic Ca^{2+} activity. As shown in Fig. 58, a 48 hours exposure to Terfenadine increased the Fluo3-fluorescence, an effect reaching statistical significance at 7.5 μ M Terfenadine concentration. Thus, Terfenadine increased $[Ca^{2+}]_i$.

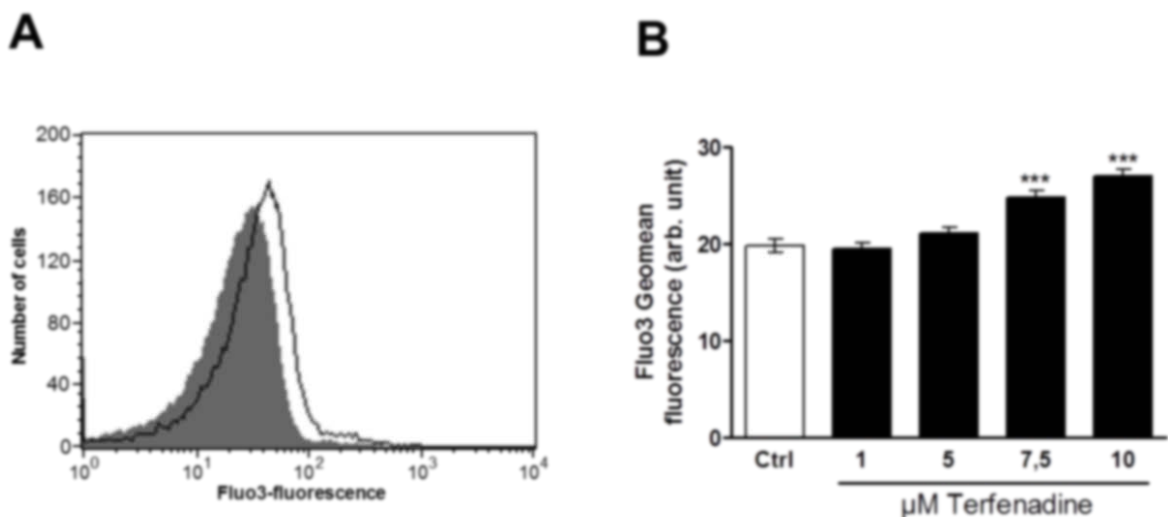


Fig. 58: Effect of Terfenadine on cytosolic Ca^{2+} activity. **A.** Original histogram of Fluo3-fluorescence in erythrocytes following exposure for 48 hours to Ringer solution without (grey area) and with (black line) presence of 10 μ M Terfenadine. **B.** Arithmetic means \pm SEM (n = 14) of erythrocyte annexin-V-binding

following incubation for 48 hours to Ringer solution without (white bar) or with (black bars) Terfenadine (1 - 10 μ M). ***($p < 0.001$) indicates significant difference from the absence of Terfenadine (ANOVA).

Further experiments were performed in order to test whether the Terfenadine-induced cell membrane scrambling required entry of extracellular Ca^{2+} . To this end, erythrocytes were incubated for 48 hours in the absence or presence of 10 μ M Terfenadine in the presence or nominal absence of extracellular Ca^{2+} . As illustrated in Fig. 59, removal of extracellular Ca^{2+} significantly blunted the effect of Terfenadine on the percentage of annexin-V-binding erythrocytes. However, even in the absence of extracellular Ca^{2+} , Terfenadine significantly increased the percentage of annexin-V-binding erythrocytes. Terfenadine was effective in part, but not fully due to entry of extracellular Ca^{2+} .

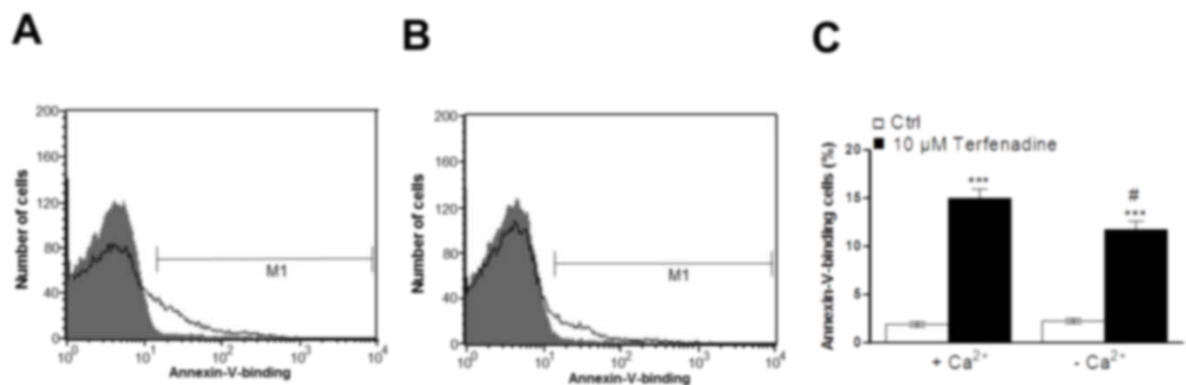


Fig. 59: Ca^{2+} sensitivity of Terfenadine-induced phosphatidylserine exposure. A,B. Original histograms of annexin-V-binding of erythrocytes following exposure for 48 hours to Ringer solution without (grey area) and with (black line) Terfenadine (10 μ M) in the presence (A) and absence (B) of extracellular Ca^{2+} . C. Arithmetic means \pm SEM ($n = 16$) of annexin-V-binding of erythrocytes after a 48 hours treatment with Ringer solution without (white bars) or with (black bars) Terfenadine (10 μ M) in the presence (left bars, + Ca^{2+}) and absence (right bars, - Ca^{2+}) of Ca^{2+} . ***($p < 0.001$) indicates significant difference from the absence of Terfenadine, #($p < 0.05$) indicates significant difference from the presence of Ca^{2+} (ANOVA).

In order to investigate whether Terfenadine enhanced the Ca^{2+} sensitivity of cell membrane scrambling, erythrocytes were incubated for 48 hours in the absence or presence of 10 μ M Terfenadine and subsequently loaded with Ca^{2+} by a 15 minute treatment with the Ca^{2+} ionophore ionomycin (1 μ M). As illustrated in Fig. 60, the pretreatment with 10 μ M Terfenadine significantly increased the percentage of annexin-V-binding erythrocytes and significantly augmented the stimulating effect of ionomycin on the percentage of annexin-V-binding erythrocytes. Terfenadine sensitized the erythrocytes for the scrambling effect of Ca^{2+} entry.

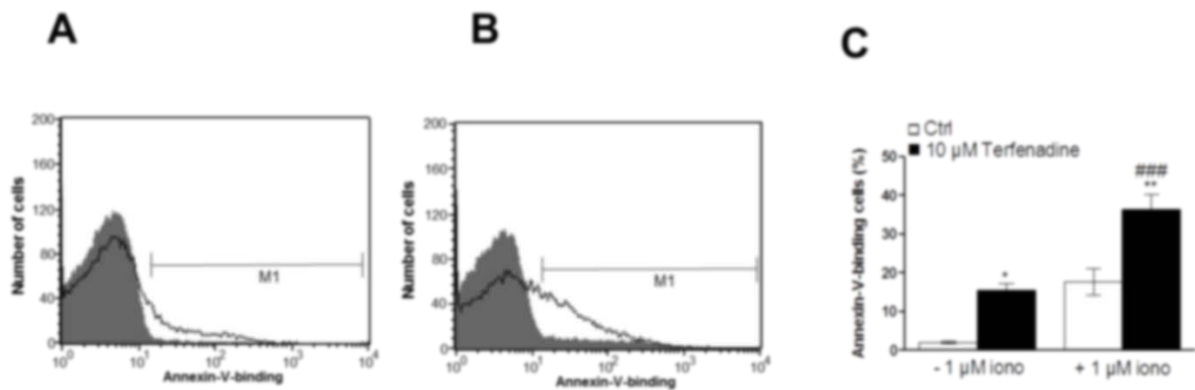


Fig. 60: Terfenadine-sensitivity of ionomycin-induced phosphatidylserine exposure. A,B. Original histograms of annexin-V-binding of erythrocytes without (grey area) and with (black line) a 48 hours Terfenadine (10 μM) pretreatment and without (A) and with (B) a 15 min exposure to ionomycin (1 μM). C. Arithmetic means ± SEM (n = 5) of annexin-V-binding of erythrocytes without (left bars, - 1 μM iono) and with (right bars, + 1 μM iono) a 15 min exposure to ionomycin (1 μM) without (white bars) and with (black bars) a 48 hours Terfenadine (10 μM) pretreatment. *(p<0.05),**(p<0.01) indicates significant difference from the absence of ionomycin, ###(p<0.001) indicates significant difference from the absence of Terfenadine (ANOVA).

Other mechanisms known to induce eryptosis include oxidative stress. To this end, the abundance of reactive oxygen species (ROS) was quantified utilizing 2',7'-dichlorodihydrofluorescein diacetate (DCFDA). The DCF-fluorescence was similar following a 48 hours incubation in Ringer with 10 μM Terfenadine (22.2 ± 4.2 a.u., n = 10) and without Terfenadine (24.7 ± 3.2 a.u., n = 10). Thus, Terfenadine did not appreciably induce oxidative stress.

In order to quantify ceramide abundance at the erythrocyte surface specific antibodies were used. As a result, the ceramide abundance was similar following a 48 hours incubation in Ringer with 10 μM Terfenadine (9.9 ± 0.27 a.u., n = 5) and in the absence of Terfenadine (11.26 ± 0.44 a.u., n = 5). Terfenadine did not appreciably induce ceramide abundance.

14.5 PICEATANNOL

The present study explored whether Piceatannol influences eryptosis, the suicidal erythrocyte death characterized by cell shrinkage and phosphatidylserine translocation to the cell surface. Erythrocyte cell volume was estimated from forward scatter, which was determined by flow cytometry after a 48 hours incubation of human erythrocytes in Ringer solution without or with Piceatannol (5 – 20 μM). As shown in Fig. 61A, B, Piceatannol slightly decreased the average

erythrocyte forward scatter, an effect reaching statistical significance at 20 μM Piceatannol. As illustrated in Fig. 61C, D, Piceatannol significantly increased the percentage of both severely swollen and severely shrunken erythrocytes.

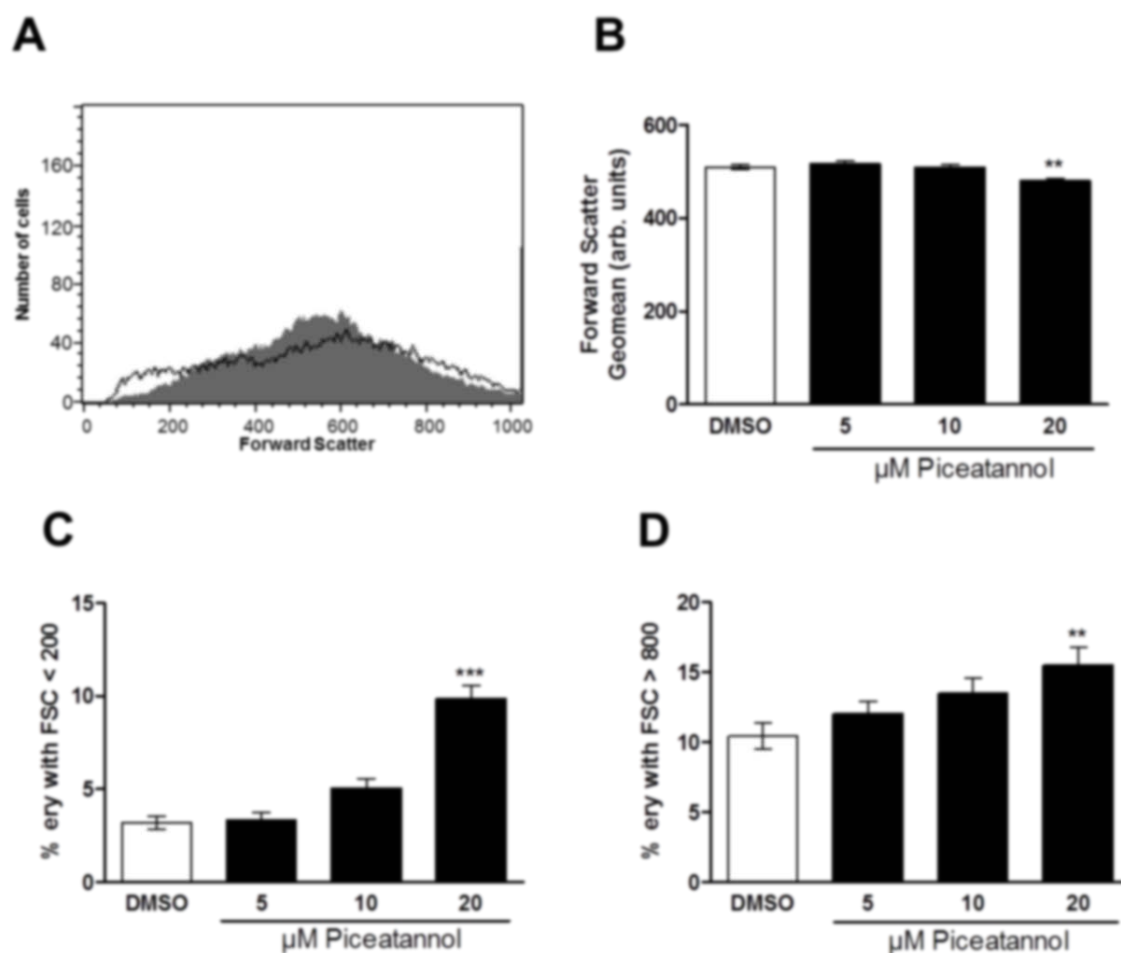


Fig. 61: Effect of Piceatannol on erythrocyte forward scatter. **A.** Original histogram of forward scatter of erythrocytes following exposure for 48 hours to Ringer solution without (grey area) and with (black line) presence of 20 μM Piceatannol. **B.** Arithmetic means \pm SEM ($n = 10$) of the erythrocyte forward scatter (FSC) following incubation for 48 hours to Ringer solution without (white bar) or with (black bars) Piceatannol (5 - 20 μM). **C.** Arithmetic means \pm SEM ($n = 10$) of the percentage erythrocytes with forward scatter (FSC) <200 following incubation for 48 hours to Ringer solution without (white bar) or with (black bars) Piceatannol (5 - 20 μM). **D.** Arithmetic means \pm SEM ($n = 10$) of the percentage erythrocytes with forward scatter (FSC) >800 following incubation for 48 hours to Ringer solution without (white bar) or with (black bars) Piceatannol (5 - 20 μM). **($p < 0.01$), ***($p < 0.001$) indicates significant difference from the absence of Piceatannol (ANOVA).

Phosphatidylserine exposing erythrocytes were detected utilizing annexin-V-binding, as determined by flow cytometry. The erythrocytes were again incubated for 48 hours in Ringer solution without

or with Piceatannol (5 – 20 μM). As shown in Fig. 62, a 48 hours exposure to Piceatannol increased the percentage of phosphatidylserine exposing erythrocytes, an effect reaching statistical significance at 10 μM Piceatannol. For comparison, the percentage of hemolysis after 48 hours exposure in Ringer solution without or with Piceatannol (5 – 20 μM) is shown in the same bar chart (Fig. 50B; grey bars).

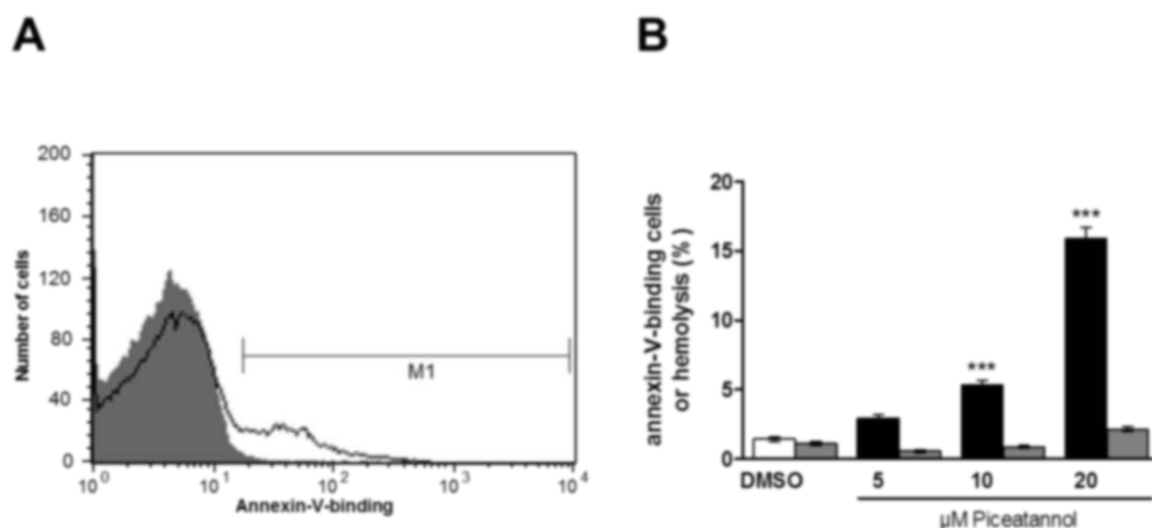


Fig. 62: Effect of Piceatannol on phosphatidylserine exposure and hemolysis. **A.** Original histogram of annexin-V-binding of erythrocytes following exposure for 48 hours to Ringer solution without (grey area) and with (black line) presence of 20 μM Piceatannol. **B.** Arithmetic means \pm SEM ($n = 10$) of erythrocyte annexin-V-binding following incubation for 48 hours to Ringer solution without (white bar) or with (black bars) Piceatannol (5 - 20 μM). For comparison, arithmetic means \pm SEM ($n = 10$) of the percentage of hemolysis is shown as grey bars. ***($p < 0.001$) indicates significant difference from the absence of Piceatannol (ANOVA).

Fluo-3 fluorescence was employed in order to test, whether Piceatannol influences the cytosolic Ca^{2+} activity. As a result, the average Fluo3-fluorescence was similar following a 48 hours incubation without Piceatannol as in the presence of Piceatannol (5 - 20 μM) (Table 1).

Table 1: Fluo3-fluorescence following incubation for 48 hours without or with Piceatannol treatment.

| | DMSO | 5 μM | 10 μM | 20 μM |
|---------------------------|------------------------------|------------------------------|------------------------------|------------------------------|
| Fluo3-fluorescence | 22.5 \pm 0.9 a.u., n=10 | 20.3 \pm 0.6 a.u., n=10 | 21.0 \pm 0.5 a.u., n=10 | 20.1 \pm 0.5 a.u., n=10 |

Further experiments were performed in order to investigate whether the Piceatannol-induced translocation of phosphatidylserine or erythrocyte shrinkage required entry of extracellular Ca^{2+} . Erythrocytes were again incubated for 48 hours in the absence or presence of 20 μM Piceatannol in the presence or nominal absence of extracellular Ca^{2+} . As shown in Fig. 63, removal of extracellular Ca^{2+} slightly, but significantly blunted the effect of Piceatannol on forward scatter. However, even in the absence of extracellular Ca^{2+} , Piceatannol significantly decreased the erythrocyte forward scatter. Furthermore, removal of extracellular Ca^{2+} slightly, but significantly blunted the effect of Piceatannol on annexin-V-binding. However, even in the absence of extracellular Ca^{2+} , Piceatannol significantly increased the percentage of annexin-V-binding erythrocytes (Fig. 63). Thus, Piceatannol-induced cell membrane scrambling was in large part triggered by mechanisms insensitive to entry of extracellular Ca^{2+} .

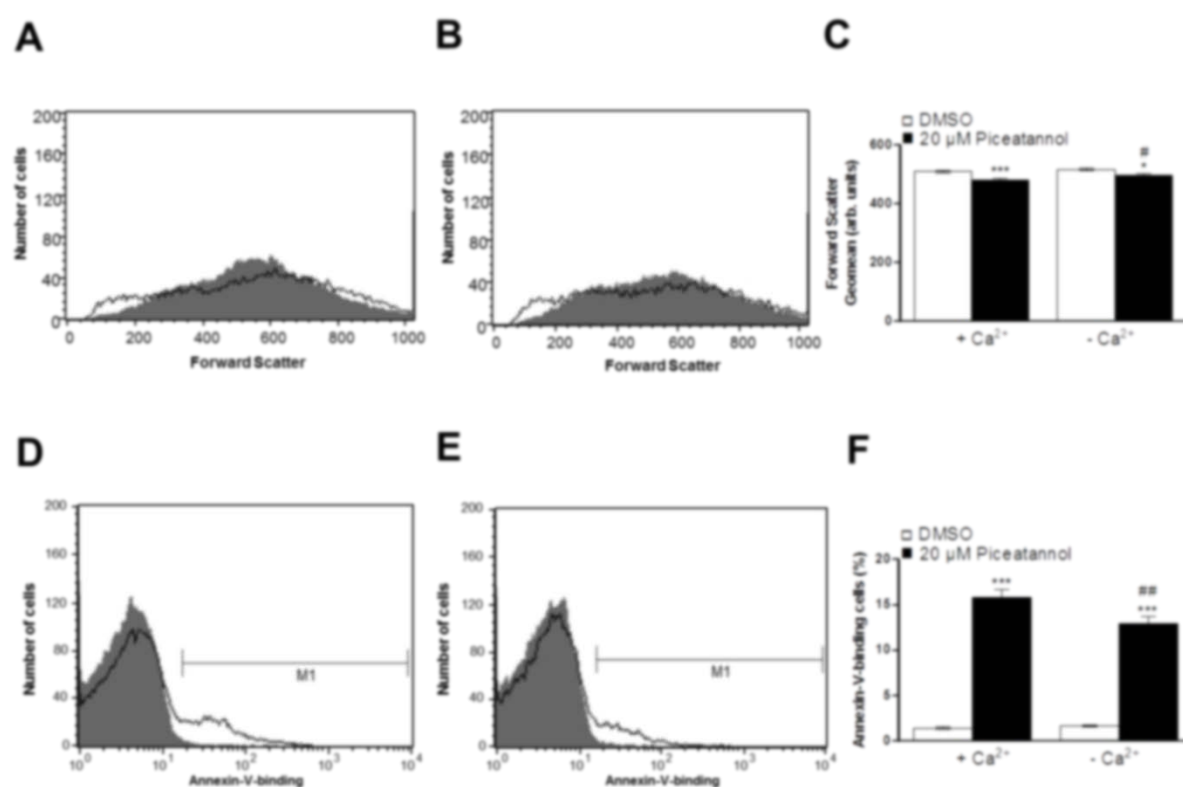


Fig. 63: Ca^{2+} sensitivity of Piceatannol-induced erythrocyte shrinkage and phosphatidylserine exposure. A,B. Original histogram of forward scatter of erythrocytes following exposure for 48 hours to Ringer solution without (grey area) and with (black line) Piceatannol (20 μM) in the presence (A) and absence (B) of extracellular Ca^{2+} . C. Arithmetic means \pm SEM (n = 10) of forward scatter of erythrocytes after a 48 hours treatment with Ringer solution without (white bars) or with (black bars) Piceatannol (20 μM) in the presence (left bars, + Ca^{2+}) and absence (right bars, - Ca^{2+}) of Ca^{2+} . D,E. Original histogram of annexin-V-binding of erythrocytes following exposure for 48 hours to Ringer solution without (grey area) and with (black line) Piceatannol (20 μM) in the presence (D) and absence (F) of extracellular Ca^{2+} . F. Arithmetic means \pm SEM (n =

10) of annexin-V-binding of erythrocytes after a 48 hours treatment with Ringer solution without (white bars) or with (black bars) Piceatannol (20 μM) in the presence (left bars, $+\text{Ca}^{2+}$) and absence (right bars, $-\text{Ca}^{2+}$) of Ca^{2+} . *($p < 0.05$), ***($p < 0.001$) indicates significant difference from the absence of Piceatannol, #($p < 0.05$), ##($p < 0.01$) indicates significant difference from the nominal absence of Ca^{2+} (ANOVA).

Further experiments were performed in order to investigate whether Piceatannol modified cell shrinkage and translocation of phosphatidylserine following increase of cytosolic Ca^{2+} activity by treatment of the erythrocytes with Ca^{2+} ionophore ionomycin (1 μM). Erythrocytes were incubated for 48 hours in the absence or presence of 20 μM Piceatannol and subsequently treated for 30 minutes with ionomycin (1 μM). As shown in Fig. 64A following Piceatannol pretreatment, ionomycin increased cytosolic Ca^{2+} activity to similar values in erythrocytes with or without Piceatannol treatment. The effect of ionomycin on forward scatter was significantly blunted (Fig. 64C) and the effect of ionomycin on annexin-V-binding significantly stronger following Piceatannol pretreatment (Fig. 64B).

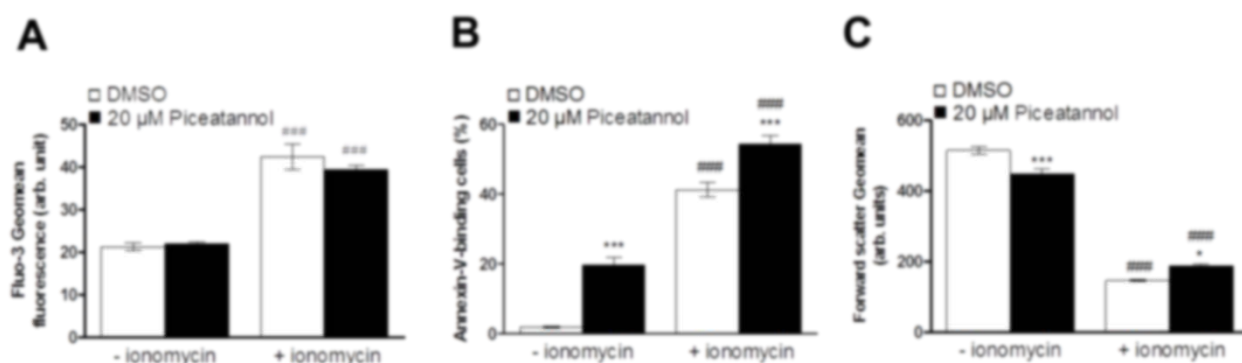


Fig. 64: Effect of Ca^{2+} ionophore ionomycin on phosphatidylserine exposure in the presence and absence of Piceatannol. A-C. Arithmetic means \pm SEM ($n = 10$) of (A.) the Fluo3-fluorescence, (B.) the percentage of annexin-V-binding erythrocytes, and (C.) the forward scatter following incubation for 30 min in the absence (left bars, -ionomycin) or presence (right bars, +ionomycin) of Ca^{2+} ionophore ionomycin (1 μM) after a 48 hours preincubation in the absence (white bars) or presence (black bars) of 20 μM Piceatannol. *($p < 0.05$), ***($p < 0.001$) indicates significant difference from the absence of Piceatannol. ###($p < 0.001$) indicates significant difference from the absence of ionomycin (ANOVA).

Further experiments were performed to clarify the effect of Piceatannol on oxidative stress. Reactive oxygen species (ROS) were determined utilizing 2',7'-dichlorodihydrofluorescein diacetate (DCFDA). As illustrated in Fig. 65, the DCF-fluorescence was higher following exposure to

Piceatannol than in the absence of Piceatannol, a difference reaching statistical significance at 10 μ M Piceatannol concentration.

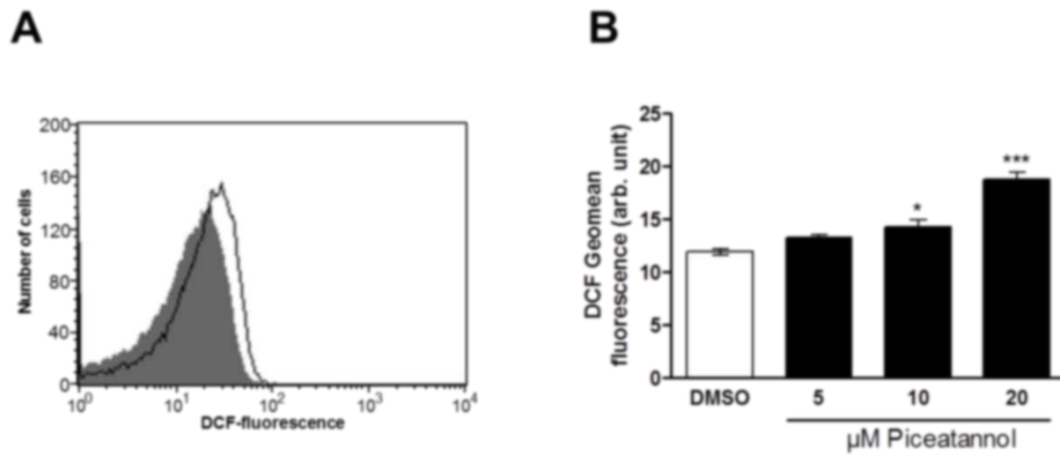


Fig. 65: Effect of Piceatannol on erythrocyte ROS formation. **A.** Original histogram of DCF-fluorescence in erythrocytes following exposure for 48 hours to Ringer solution without (grey area) and with (black line) presence of Piceatannol (20 μ M). **B.** Arithmetic means \pm SEM (n = 10) of the DCF-fluorescence (arbitrary units) in erythrocytes exposed for 48 hours to Ringer solution without (white bar) or with (black bars) Piceatannol (5– 20 μ M). *(p<0.05), ***(p<0.001) indicate significant difference from the absence of Piceatannol (ANOVA).

A further stimulator of eryptosis is ceramide. Ceramide abundance at the erythrocyte surface was thus determined utilizing specific antibodies. As illustrated in Fig. 66, the ceramide abundance was significantly higher following exposure to 20 μ M Piceatannol than in the absence of Piceatannol.

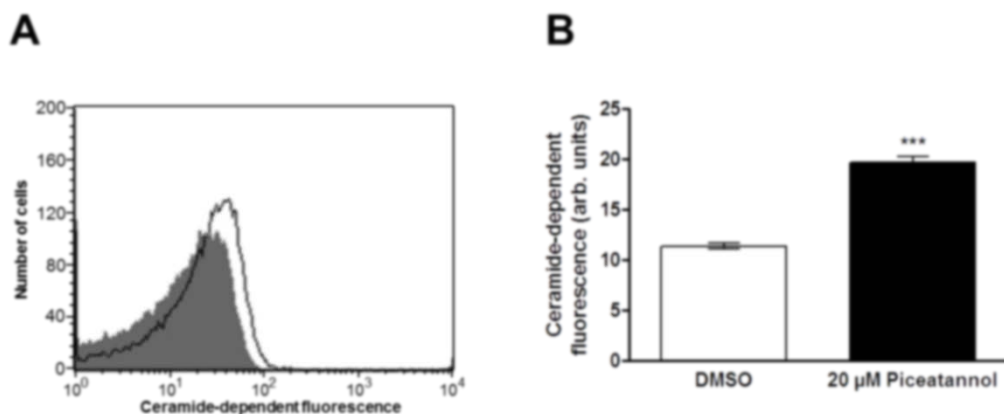


Fig. 66: Effect of Piceatannol on ceramide abundance at the erythrocyte surface. **A.** Original histogram of ceramide abundance in erythrocytes following exposure for 48 hours to Ringer solution without (grey area) and with (black line) presence of 20 μ M Piceatannol. **B.** Arithmetic means \pm SEM (n = 10) of the ceramide abundance (arbitrary units) in erythrocytes exposed for 48 hours to Ringer solution without (white bar) or

with (black bar) presence of 20 μM Piceatannol. ***($p < 0.001$) indicates significant difference from the absence of Piceatannol (ANOVA).

14.6 CERANIB-2

The present study explored whether Ceranib-2 influences eryptosis. The translocation of phosphatidylserine to the erythrocyte surface was detected utilizing annexin-V-binding, as determined by flow cytometry. Prior to measurements, the erythrocytes were incubated for 48 hours in Ringer solution without or with Ceranib-2 (10 – 100 μM). As shown in Fig. 67, 48 hours exposure to Ceranib-2 increased the percentage of phosphatidylserine exposing erythrocytes, an effect reaching statistical significance at 50 μM Ceranib-2.

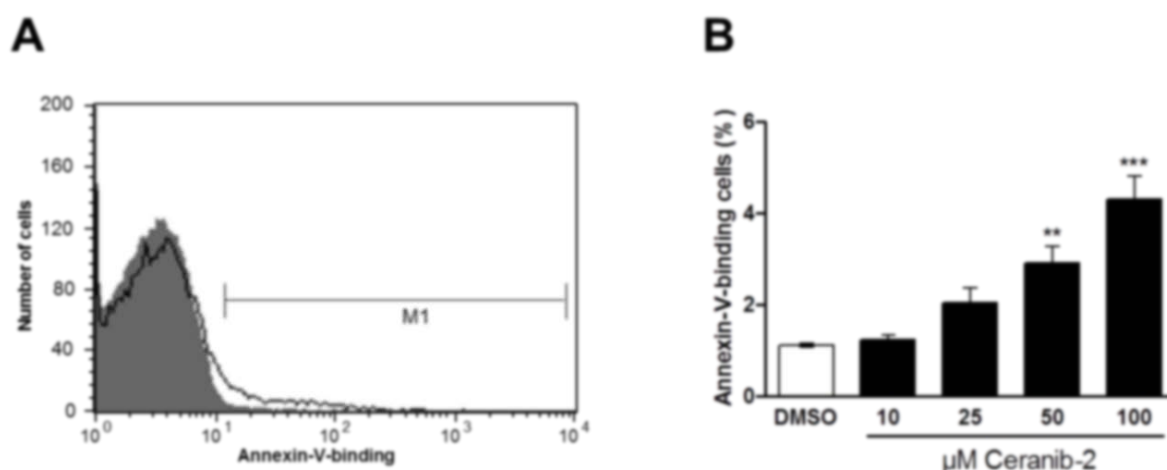


Fig. 67: Effect of Ceranib-2 on phosphatidylserine exposure. **A.** Original histogram of annexin-V-binding to erythrocytes following exposure for 48 hours to Ringer solution without (grey area) and with (black line) presence of 100 μM Ceranib-2. **B.** Arithmetic means \pm SEM ($n = 10$) of erythrocyte annexin-V-binding following incubation for 48 hours to Ringer solution without (white bar) or with (black bars) Ceranib-2 (10 - 100 μM). **($p < 0.01$), ***($p < 0.001$) indicates significant difference from the absence of Ceranib-2 (ANOVA).

Erythrocyte cell volume was estimated from forward scatter, which was determined by flow cytometry. The erythrocytes were again incubated for 48 hours in Ringer solution without or with Ceranib-2 (10 – 100 μM). As shown in Fig. 68, Ceranib-2 did not significantly modify average erythrocyte forward scatter. The percentage of shrunken erythrocytes (< 200) was not significantly different following incubation in Ringer ($3.7 \pm 0.6\%$, $n = 10$), and following incubation with 10 μM ($4.1 \pm 0.3\%$, $n = 10$), 25 μM ($3.1 \pm 0.4\%$, $n = 10$), 50 μM ($2.4 \pm 0.3\%$, $n = 10$), or 100 μM ($2.7 \pm 0.3\%$, $n = 10$) Ceranib-2. Furthermore, the percentage of markedly swollen erythrocytes (> 800) was not

significantly different following incubation in Ringer ($6.2 \pm 0.9\%$, $n = 10$), and following incubation with $10 \mu\text{M}$ ($8.7 \pm 1.2\%$, $n = 10$), $25 \mu\text{M}$ ($7.2 \pm 0.7\%$, $n = 10$), $50 \mu\text{M}$ ($6.3 \pm 0.9\%$, $n = 10$), or $100 \mu\text{M}$ ($6.3 \pm 0.8\%$, $n = 10$) Ceranib-2.

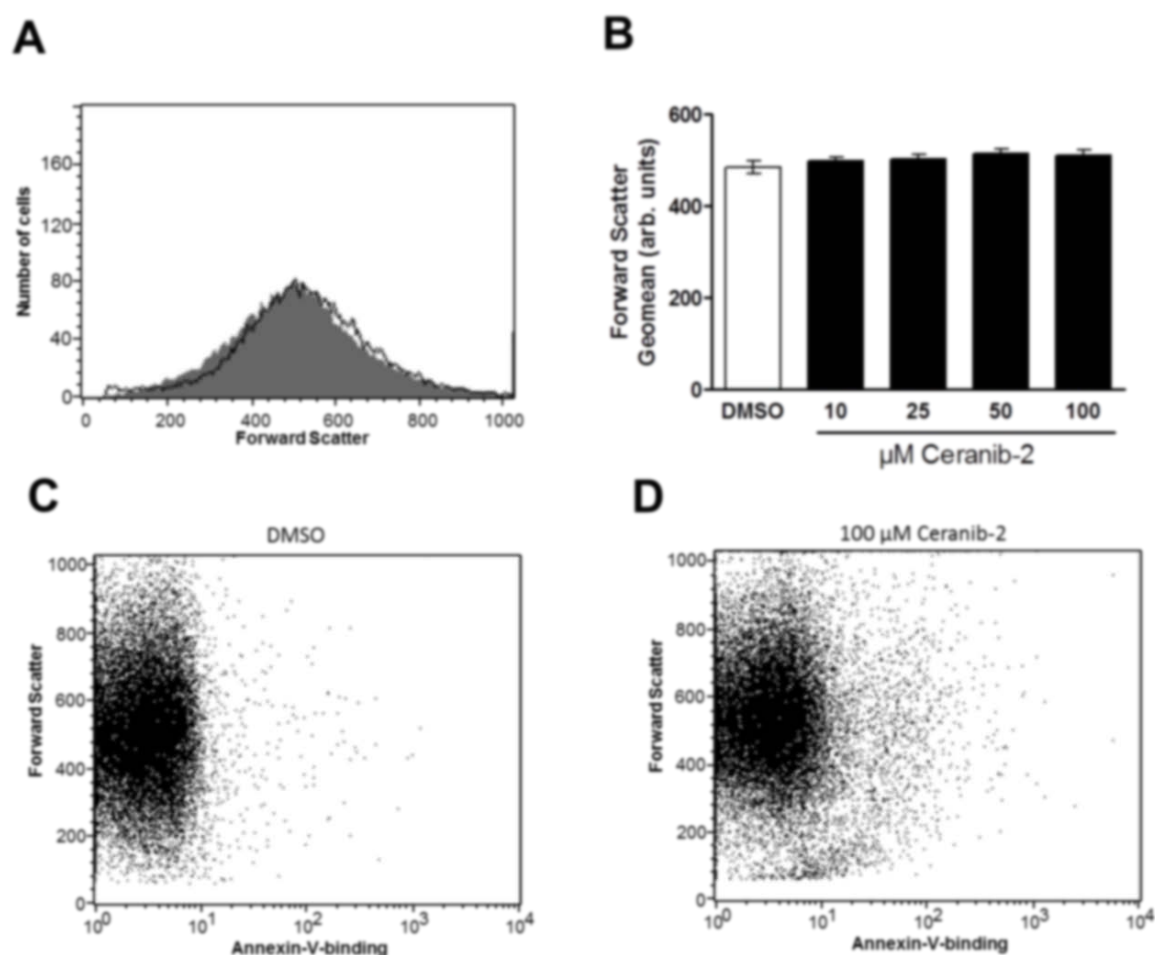


Fig. 68: Effect of Ceranib-2 on erythrocyte forward scatter. **A.** Original histogram of forward scatter of erythrocytes following exposure for 48 hours to Ringer solution without (grey area) and with (black line) presence of $100 \mu\text{M}$ Ceranib-2. **B.** Arithmetic means \pm SEM ($n = 10$) of the erythrocyte forward scatter (FSC) following incubation for 48 hours to Ringer solution without (white bar) or with (black bars) Ceranib-2 ($10 - 100 \mu\text{M}$). **C,D.** Original dot plots of forward scatter vs annexin-V-abundance without (**C**) and with (**D**) prior treatment with $100 \mu\text{M}$ Ceranib-2.

In order to investigate the effect of Ceranib-2 on hemolysis, the percentage of haemolytic erythrocytes was determined from the hemoglobin concentration in the supernatant. As shown in Fig. 69, 48 hours incubation with Ceranib-2 ($10 - 100 \mu\text{M}$) significantly increased the percentage of hemolysed erythrocytes.

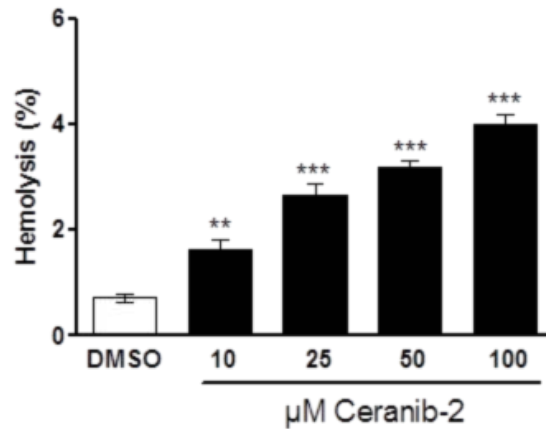


Fig. 69: Effect of Ceranib-2 on hemolysis. Arithmetic means \pm SEM (n = 10) of the percentage hemolytic erythrocytes following incubation for 48 hours to Ringer solution without (white bar) or with (black bars) Ceranib-2 (10 - 100 μ M). **($p < 0.01$), ***($p < 0.001$) indicates significant difference from the absence of Ceranib-2 (ANOVA).

Fluo3-fluorescence was employed in order to test, whether Ceranib-2 influences the cytosolic Ca^{2+} activity ($[\text{Ca}^{2+}]_i$). As shown in Fig. 70, 48 hours incubation with Ceranib-2 was followed by an increase of the Fluo3-fluorescence, an effect reaching statistical significance at 25 μ M Ceranib-2.

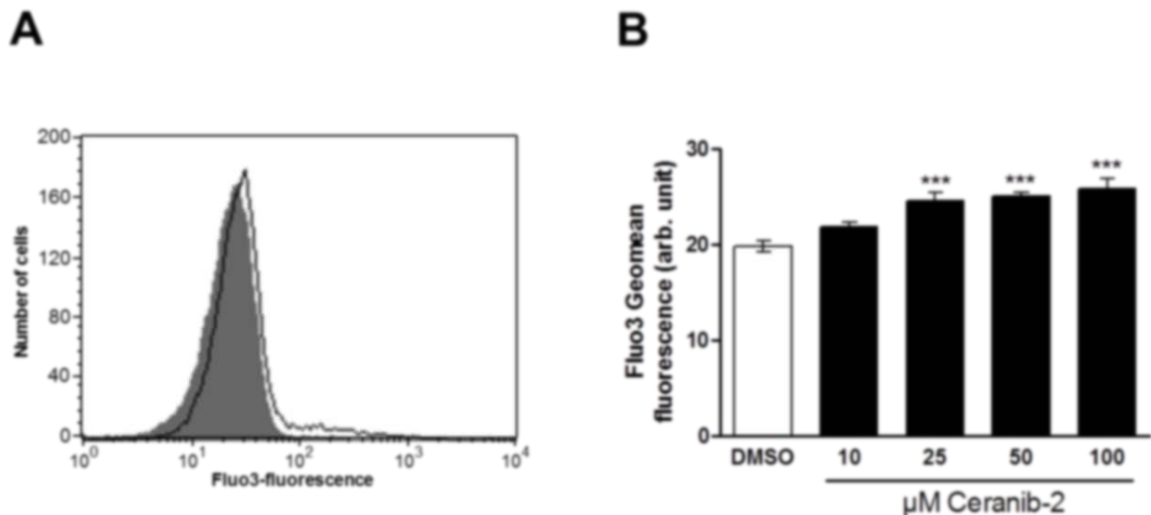


Fig. 70: Effect of Ceranib-2 on Fluo3-fluorescence. **A.** Original histogram of Fluo3-fluorescence reflecting cytosolic Ca^{2+} activity in erythrocytes following exposure for 48 hours to Ringer solution without (grey area) and with (black line) presence of 100 μ M Ceranib-2. **B.** Arithmetic means \pm SEM (n = 10) of erythrocyte Fluo3-fluorescence following incubation for 48 hours to Ringer solution without (white bar) or with (black bars)

Ceranib-2 (10 - 100 μM). ***($p < 0.001$) indicates significant difference from the absence of Ceranib-2 (ANOVA).

Further experiments were performed in order to investigate whether the Ceranib-2-induced translocation of phosphatidylserine was dependent on the presence of extracellular Ca^{2+} . Prior to measurements, erythrocytes were incubated for 48 hours in the absence or presence of 100 μM Ceranib-2 in the presence or nominal absence of extracellular Ca^{2+} . As shown in Fig. 71, removal of extracellular Ca^{2+} did not significantly blunt the effect of Ceranib-2 on annexin-V-binding and in the absence of extracellular Ca^{2+} , Ceranib-2 significantly increased the percentage of annexin-V-binding erythrocytes. Ceranib-2-induced cell membrane scrambling was in large part triggered by mechanisms not requiring presence of extracellular Ca^{2+} .

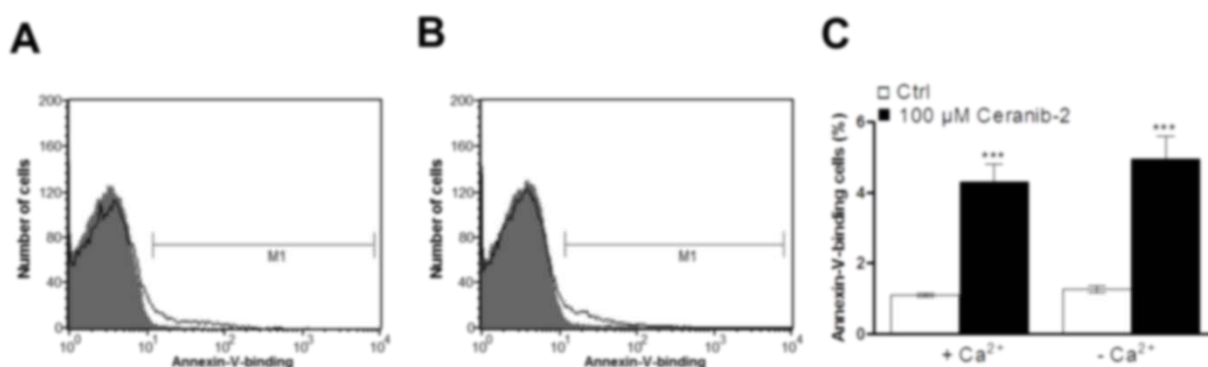


Fig. 71: Ca^{2+} insensitivity of Ceranib-2-induced phosphatidylserine exposure. A,B. Original histogram of annexin-V-binding to erythrocytes following exposure for 48 hours to Ringer solution without (grey area) and with (black line) Ceranib-2 (100 μM) in the presence (A) and absence (B) of extracellular Ca^{2+} . C. Arithmetic means \pm SEM ($n = 10$) of annexin-V-binding of erythrocytes after a 48 hours treatment with Ringer solution without (white bars) or with (black bars) Ceranib-2 (100 μM) in the presence (left bars, + Ca^{2+}) and absence (right bars, - Ca^{2+}) of Ca^{2+} . ***($p < 0.001$) indicates significant difference from the absence of Ceranib-2 (ANOVA).

Further experiments were performed to clarify the effect of Ceranib-2 on oxidative stress. Reactive oxygen species (ROS) were determined utilizing 2',7'-dichlorodihydrofluorescein diacetate (DCFDA). As shown in Fig. 72, 48 hours incubation with Ceranib-2 was followed by an increase of the DCF-fluorescence, an effect reaching statistical significance at 50 μM Ceranib-2.

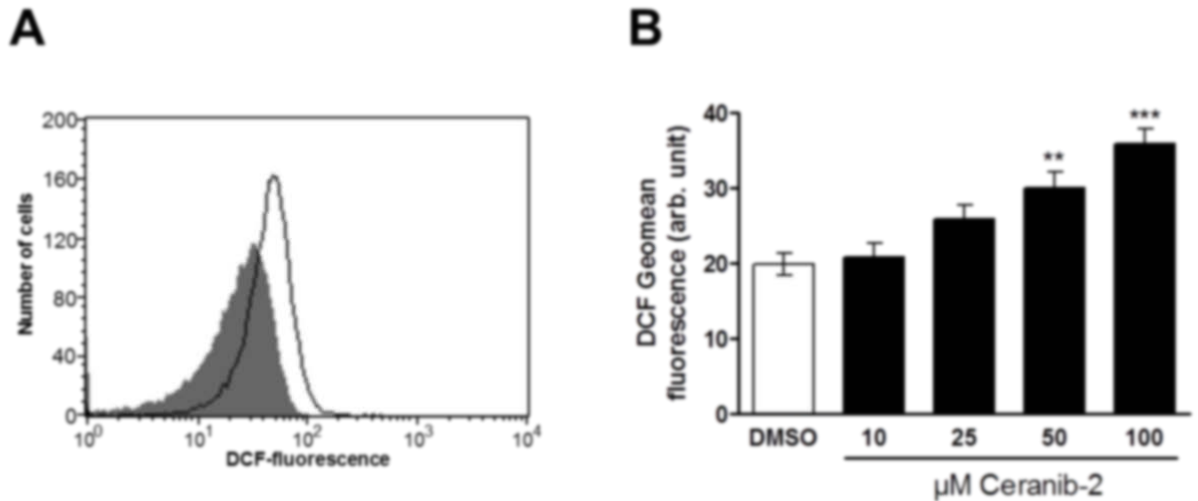


Fig. 72: Effect of Ceranib-2 on ROS formation. **A.** Original histogram of DCF-fluorescence in erythrocytes following exposure for 48 hours to Ringer solution without (grey area) and with (black line) presence of Ceranib-2 (100 μM). **B.** Arithmetic means ± SEM (n = 10) of the DCF-fluorescence (arbitrary units) in erythrocytes exposed for 48 hours to Ringer solution without (white bar) or with (black bars) Ceranib-2 (10 - 100 μM). **($p < 0.01$), ***($p < 0.001$) indicates significant difference from the absence of Ceranib-2 (ANOVA).

Ceramide abundance at the erythrocyte surface was quantified utilizing specific antibodies. As shown in Fig. 73, 48 hours incubation with 100 μM Ceranib-2 was followed by a significant increase of the ceramide abundance at the erythrocyte surface.

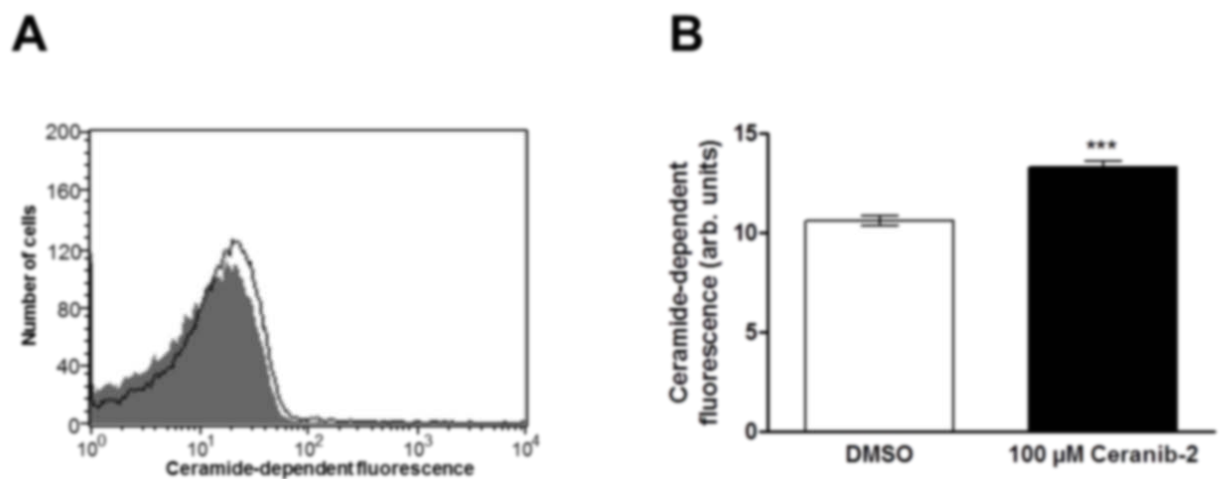


Fig. 73: Effect of Ceranib-2 on ceramide abundance at the erythrocyte surface. **A.** Original histogram of ceramide abundance in erythrocytes following exposure for 48 hours to Ringer solution without (grey area) and with (black line) presence of 100 μM Ceranib-2. **B.** Arithmetic means ± SEM (n = 10) of the ceramide abundance (arbitrary units) in erythrocytes exposed for 48 hours to Ringer solution without (white bar) or with (black bars) Ceranib-2 (100 μM). ***($p < 0.001$) indicates significant difference from the absence of Ceranib-2 (ANOVA).

14.7 SCLAREOL

The present study addressed the putative effect of Sclareol on eryptosis, the suicidal erythrocyte death. In order to quantify cell membrane scrambling, phosphatidylserine exposing erythrocytes were identified utilizing annexin-V-binding, as determined by flow cytometry. Prior to measurements, the erythrocytes were incubated for 48 hours in Ringer solution without or with Sclareol (10 - 100 μ M). As shown in Fig. 74, a 48 hours exposure to Sclareol increased the percentage of phosphatidylserine exposing erythrocytes, an effect reaching statistical significance at 100 μ M Sclareol.

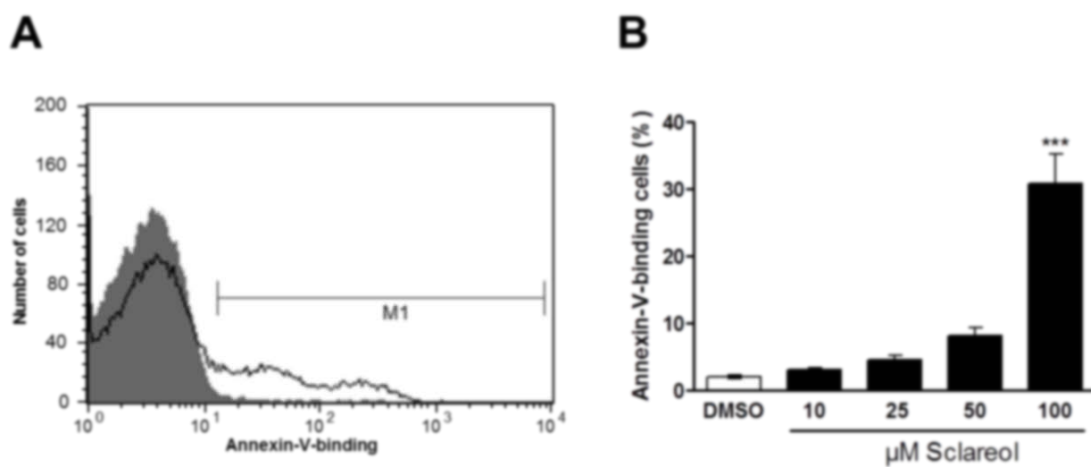


Fig. 74: Effect of Sclareol on phosphatidylserine exposure. **A.** Original histogram of annexin-V-binding of erythrocytes following exposure for 48 hours to Ringer solution without (grey area) and with (black line) presence of 100 μ M Sclareol. **B.** Arithmetic means \pm SEM ($n = 10$) of erythrocyte annexin-V-binding following incubation for 48 hours to Ringer solution without (white bar) or with (black bars) Sclareol (10 – 100 μ M). ***($p < 0.001$) indicates significant difference from the absence of Sclareol (ANOVA).

Erythrocyte cell volume was quantified utilizing forward scatter determined with flow cytometry. The erythrocytes were again incubated for 48 hours in Ringer solution without or with Sclareol (10 – 100 μ M). As illustrated in Fig. 75, Sclareol did not significantly modify the average erythrocyte forward scatter, but at a concentration of 100 μ M significantly decreased the percentage of large erythrocytes (>800).

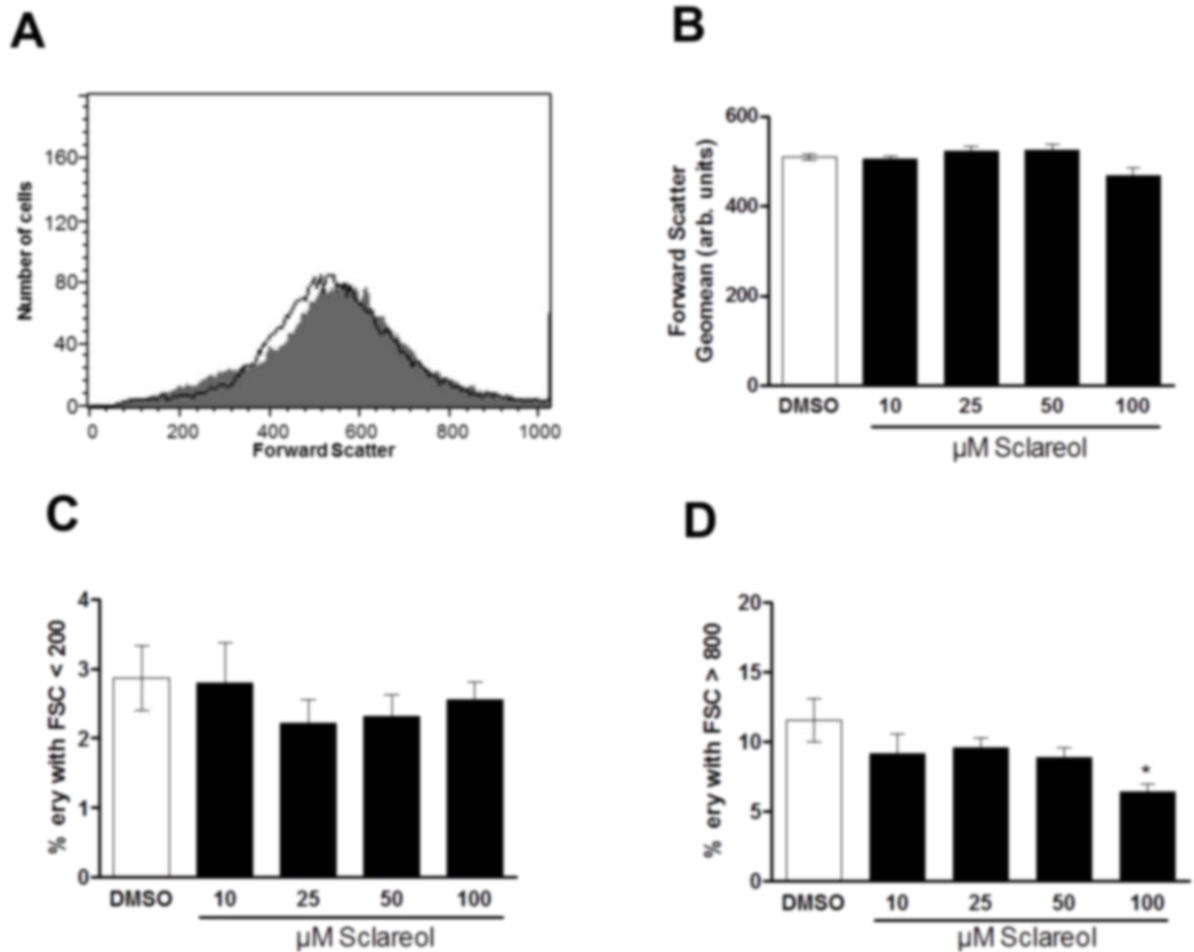


Fig. 75: Effect of Sclareol on erythrocyte forward scatter. **A.** Original histogram of forward scatter of erythrocytes following exposure for 48 hours to Ringer solution without (grey area) and with (black line) presence of 100 μM Sclareol. **B.** Arithmetic means \pm SEM ($n = 10$) of the erythrocyte forward scatter (FSC) following incubation for 48 hours to Ringer solution without (white bar) or with (black bars) Sclareol (10 - 100 μM). **C.** Arithmetic means \pm SEM ($n = 10$) of the percentage erythrocytes with forward scatter (FSC) < 200 following incubation for 48 hours to Ringer solution without (white bar) or with (black bars) Sclareol (10 - 100 μM). **D.** Arithmetic means \pm SEM ($n = 10$) of the percentage erythrocytes with forward scatter (FSC) > 800 following incubation for 48 hours to Ringer solution without (white bar) or with (black bars) Sclareol (10 - 100 μM). *($p < 0.05$) indicates significant difference from the absence of Sclareol (ANOVA).

The hemoglobin concentration in the supernatant was determined in order to estimate the percentage of hemolysed erythrocytes. As illustrated in Fig. 76, Sclareol exposure was further followed by hemolysis, an effect reaching statistical significance at 50 μM Sclareol.

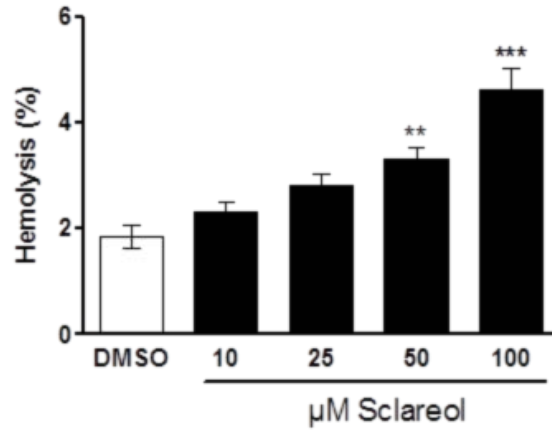


Fig. 76: Effect of Sclareol on hemolysis. Arithmetic means \pm SEM (n = 10) of the percentage hemolytic erythrocytes following incubation for 48 hours to Ringer solution without (white bar) or with (black bars) Sclareol (10 - 100 μ M). **($p < 0.01$), ***($p < 0.001$) indicates significant difference from the absence of Sclareol (ANOVA).

Fluo3-fluorescence was quantified as a measure of cytosolic Ca^{2+} activity ($[Ca^{2+}]_i$). As shown in Fig. 77, a 48 hours exposure to 100 μ M Sclareol significantly increased the Fluo3-fluorescence, an observation pointing to increase of $[Ca^{2+}]_i$.

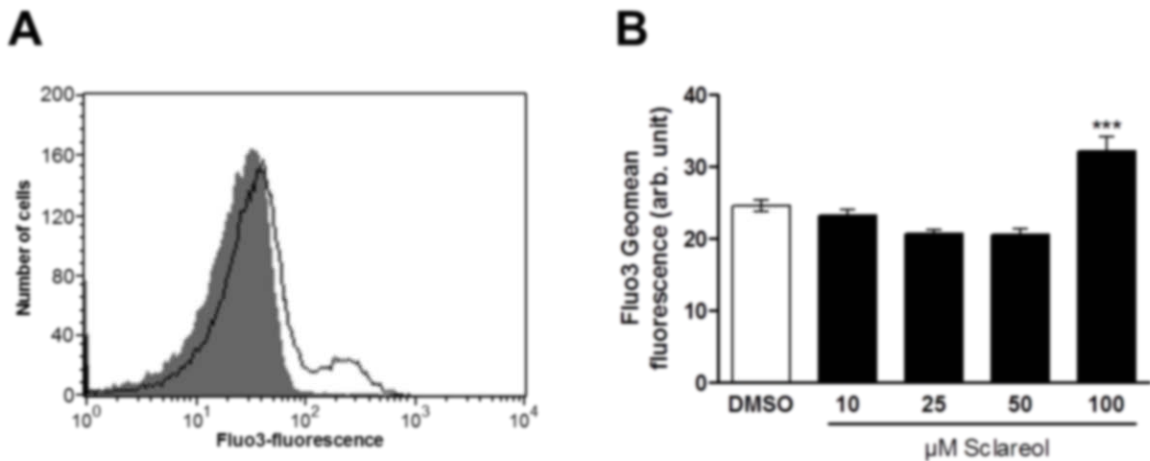


Fig. 77: Effect of Sclareol on cytosolic Ca^{2+} activity. A. Original histogram of Fluo3-fluorescence of erythrocytes following exposure for 48 hours to Ringer solution without (grey area) and with (black line) presence of 100 μ M Sclareol. B. Arithmetic means \pm SEM (n = 10) of erythrocyte annexin-V-binding following incubation for 48 hours to Ringer solution without (white bar) or with (black bars) Sclareol (10 - 100 μ M). ***($p < 0.001$) indicates significant difference from the absence of Sclareol (ANOVA).

Further experiments were performed in order to test whether the Sclareol-induced translocation of phosphatidylserine was sensitive to extracellular Ca^{2+} . To this end, erythrocytes were incubated for 48 hours in the absence or presence of 50 or 100 μM Sclareol in the presence or nominal absence of extracellular Ca^{2+} . As illustrated in Fig. 78, removal of extracellular Ca^{2+} did not significantly blunt the effect of Sclareol on the percentage of annexin-V-binding erythrocytes. Sclareol significantly increased the percentage of annexin-V-binding erythrocytes, even in the absence of extracellular Ca^{2+} . Sclareol-induced cell membrane scrambling was not dependent on entry of extracellular Ca^{2+} .

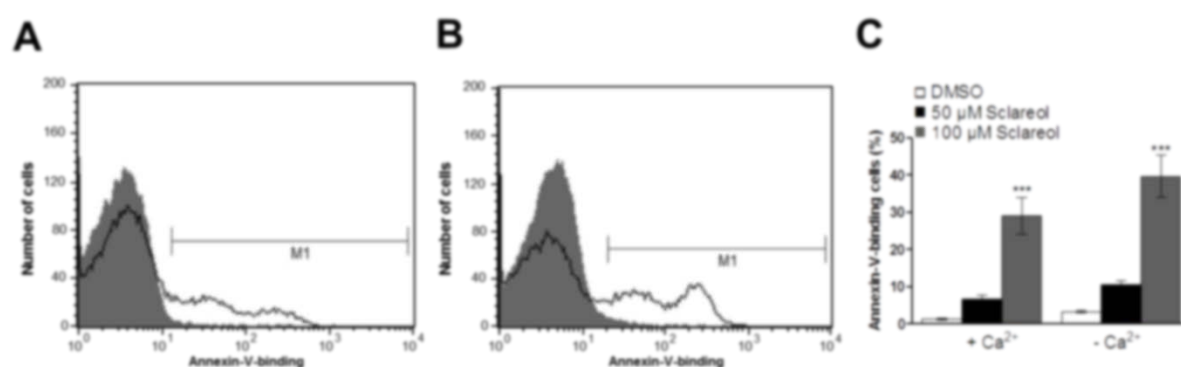


Fig. 78: Ca^{2+} sensitivity of Sclareol-induced phosphatidylserine exposure. A,B. Original histogram of annexin-V-binding of erythrocytes following exposure for 48 hours to Ringer solution without (grey area) and with (black line) Sclareol (100 μM) in the presence (A) and absence (B) of extracellular Ca^{2+} . C. Arithmetic means \pm SEM ($n = 10$) of annexin-V-binding of erythrocytes after a 48 hours treatment with Ringer solution without (white bars) or with 50 μM (black bars) or 100 μM (grey bars) Sclareol in the presence (left bars, + Ca^{2+}) and absence (right bars, - Ca^{2+}) of Ca^{2+} . ***($p < 0.001$) indicates significant difference from the absence of Sclareol (ANOVA).

Eryptosis is further stimulated by oxidative stress. Reactive oxygen species (ROS) were thus quantified utilizing 2',7'-dichlorodihydrofluorescein (DCF) diacetate. The DCF-fluorescence was similar following exposure to 10 μM Sclareol (15.1 ± 0.4 a.u., $n = 5$), 25 μM Sclareol (13.6 ± 0.6 a.u., $n = 5$) 50 μM Sclareol (12.8 ± 0.4 a.u., $n = 5$) and 100 μM Sclareol (17.4 ± 2.5 a.u., $n = 5$) as in the absence of Sclareol (17.3 ± 2.6 a.u., $n = 5$). Thus, Sclareol did not appreciably induce oxidative stress.

Eryptosis is further stimulated by ceramide. Ceramide abundance at the erythrocyte surface was determined utilizing specific antibodies. The ceramide abundance was similar following exposure to 50 μM Sclareol (10.9 ± 0.2 a.u., $n = 5$) and 100 μM Sclareol (11.4 ± 0.2 a.u., $n = 5$) as in the absence of Sclareol (11.2 ± 0.3 a.u., $n = 5$). Thus, Sclareol did not appreciably induce ceramide abundance.

To investigate, whether the effects of Sclareol involved p38 kinase activity, the influence of Sclareol on annexin-V-binding was measured in the absence or presence of p38 kinase inhibitor skepinone (2 μ M). As shown in Fig. 79A, the effect of 100 μ M Sclareol was significantly blunted in the presence of skepinone. However, even in the presence of skepinone, Sclareol significantly increased the percentage of annexin-V-binding erythrocytes. Sclareol-induced cell membrane scrambling was apparently in part but not fully due to activation of p38 kinase. To clarify, whether the effects of Sclareol required casein kinase 1 α activity, the effect of Sclareol on annexin-V-binding was measured in the absence or presence of casein kinase 1 α inhibitor D4476 (10 μ M). As shown in Fig. 79B, the effect of 100 μ M Sclareol was significantly blunted in the presence of D4476. However, even in the presence of D4476, Sclareol significantly increased the percentage of annexin-V-binding erythrocytes. Sclareol-induced cell membrane scrambling was again in part due to activation of casein kinase 1 α .

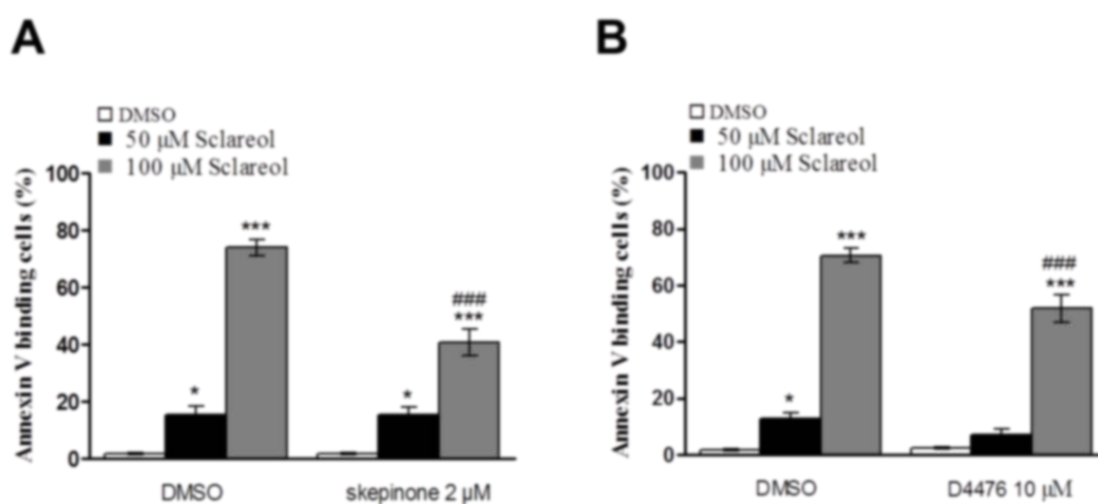


Fig. 79: Effect of p38 kinase inhibitor skepinone and of casein kinase 1 α inhibitor D4476 on Sclareol-induced phosphatidylserine exposure. A. Arithmetic means \pm SEM (n = 10) of annexin-V-binding of erythrocytes after a 48 hours treatment with Ringer solution without (white bars) or with 50 μ M (black bars) or 100 μ M (grey bars) Sclareol in the absence (left bars, DMSO) and presence (right bars, skepinone) of p38 kinase inhibitor skepinone (2 μ M). **B.** Arithmetic means \pm SEM (n = 15) of annexin-V-binding of erythrocytes after a 48 hours treatment with Ringer solution without (white bars) or with 50 μ M (black bars) or 100 μ M (grey bars) Sclareol in the absence (left bars, DMSO) and presence (right bars, D4476) of casein kinase 1 α inhibitor D4476 (10 μ M). *(p<0.05), ***(p<0.001) indicates significant difference from the absence of Sclareol, ###(p<0.001) indicates significant difference from the absence of kinase inhibitors (ANOVA).

15. DISCUSSION

15.1 CA4P

The present study demonstrates that exposure of human erythrocytes to CA4P triggers eryptosis, the suicidal erythrocyte death [98]. CA4P treatment is followed by cell shrinkage and by cell membrane scrambling with phosphatidylserine translocation to the erythrocyte surface. The CA4P concentrations required for those effects are in the range of concentrations encountered in the plasma of patients [140]. However, the higher concentrations utilized in the present study (50 and 100 μM) would be approached only following intake of toxic drug doses. The removal of extracellular Ca^{2+} significantly blunted CA4P induced phosphatidylserine translocation. Furthermore, the effect of CA4P on cell shrinkage was presumably in part due to Ca^{2+} entry. An intracellular increase of Ca^{2+} may activate Ca^{2+} -sensitive K^+ channels, leading to K^+ exit, cell membrane hyperpolarization, Cl^- exit and thus cellular loss of KCl with water [105]. Eryptosis is a physiological mechanism which allow the clearance of defective erythrocytes from circulating blood prior to hemolysis [105]. Hemolysis is important in order to prevent lysis with subsequent release of hemoglobin into the blood flow [121]. Hemolysis of defective erythrocytes leads to release of hemoglobin, which may pass the renal glomerular filter, precipitates in the acidic lumen of renal tubules, occludes nephrons and could trigger renal failure [134]. As phosphatidylserine exposing erythrocytes are rapidly cleared from circulating blood, excessive eryptosis may result in anemia, which could develop whether the generation of new erythrocytes fails to replenish the loss of erythrocytes by eryptosis [105]. Anemia may result from blood loss, impaired erythropoiesis caused by inadequate production of erythropoietin, decreased availability of iron or from decreased lifespan of erythrocytes [121]. Phosphatidylserine-exposing erythrocytes may adhere to the vascular wall [254], stimulate blood clotting and trigger thrombosis [133, 255, 256], thus impairing microcirculation [133, 257-261]. The sensitivity of erythrocytes to CA4P treatment could be enhanced in several clinical conditions, such as dehydration [262], hyperphosphatemia [263], chronic kidney disease (CKD) [264-267], hemolytic-uremic syndrome [268], diabetes [269], hepatic failure [270], malignancy [105], sepsis [271], sickle-cell disease [105] as well as beta-thalassemia [105]. The possibility of enhanced CA4P toxicity in those clinical conditions should be taken into consideration. From these results it can be concluded that CA4P stimulates calcium entry into human erythrocytes with subsequent erythrocyte shrinkage and erythrocyte cell membrane scrambling. Thus, CA4P elicits eryptosis, the suicidal erythrocyte death.

15.2 PAZOPANIB

The present study reveals a novel xenobiotic triggering suicidal erythrocyte death or eryptosis, such as Pazopanib [104]. Exposure of human erythrocytes to Pazopanib is followed by increase of the percentage shrunken and phosphatidylserine exposing erythrocytes. The Pazopanib concentrations required for those effects are in the range of the plasma concentrations encountered in the plasma of the patients under Pazopanib treatment [151, 272]. Removal of extracellular Ca^{2+} significantly blunted the effect of Pazopanib on cell membrane scrambling. Fluo3-fluorescence decreased following Pazopanib treatment, indicating the substance may interact with Fluo3-fluorescence. Pazopanib treatment increases ROS and ceramide abundance, both well-known trigger of eryptosis [121]. Pazopanib treatment increased the percentage of the shrunken erythrocytes. The shrinkage could have been due to activation of K^+ channels, K^+ exit, cell membrane hyperpolarization, Cl^- exit and thus cellular loss of KCl with water [121]. Pazopanib treatment increases also the percentage of hemolysis. Eryptosis could be important in order to clear defective erythrocytes from circulating blood prior to hemolysis [121]. Hemolysis is followed by release of hemoglobin into blood vessels or extravascularly, which may pass the renal glomerular filter, precipitate in the acidic lumen of renal tubules, occlude nephrons and thus trigger renal failure [134]. As phosphatidylserine exposing erythrocytes are rapidly cleared from circulating blood, excessive eryptosis may result in anemia, if the rate of eryptosis with subsequent clearance from circulating blood exceeds the formation of new erythrocytes [121]. Enhanced eryptosis may lead to anemia, as phosphatidylserine exposing erythrocytes are rapidly cleared from circulating blood [121]. Moreover, phosphatidylserine exposing erythrocytes may adhere to the vascular wall [254], trigger blood clotting and thus induce thrombosis [133, 255, 256]. Eryptotic erythrocytes could impair microcirculation [133, 257-261]. The effect of Pazopanib on eryptosis could be particularly relevant in clinical conditions characterized by enhanced eryptosis, such as dehydration [262], hyperphosphatemia [263], chronic kidney disease (CKD) [264-267], hemolytic-uremic syndrome [268], diabetes [269], hepatic failure [270], malignancy [121], sepsis [271], sickle-cell disease [121], beta-thalassemia [121], Hb-C and G6PD-deficiency [121] and Wilson's disease [273]. From these results it can be concluded that Pazopanib stimulates eryptosis, the suicidal erythrocyte death.

15.3 NOCODAZOLE

The present study demonstrates that exposure of human erythrocytes to Nocodazole treatment triggers eryptosis [101]. The concentrations required for the toxic effect are higher than those required for disassembly of microtubules [171] but are similar to those previously employed to

trigger cell cycle arrest [274]. Nocodazole treatment is followed by cell membrane scrambling and was in part due to increase of cytosolic Ca^{2+} activity ($[\text{Ca}^{2+}]_i$) and was significantly blunted by removal of extracellular Ca^{2+} . Nocodazole increased oxidative stress and ceramide abundance. Furthermore, Nocodazole treatment increased the percentage of shrunken and swollen erythrocytes. The cell shrinkage could be explained at least partially by increase of $[\text{Ca}^{2+}]_i$ with subsequent activation of Ca^{2+} sensitive K^+ channels, K^+ exit, cell membrane hyperpolarization, Cl^- exit and thus cellular loss of KCl with water [275]. A candidate mechanism to explain Nocodazole induced erythrocyte swelling could be impairment of Na^+/K^+ ATPase with subsequent cellular accumulation of Na^+ with Cl^- . However, Nocodazole treatment leads to swelling of only a small subset of erythrocytes. Further experiments demonstrate a moderate decrease of tubulin abundance following Nocodazole treatment. The Nocodazole induced eryptosis was insensitive to zVAD and the stimulation of cell membrane scrambling by Nocodazole does apparently not involve caspases. Suicidal death of nucleated cells may similarly be independent from caspase activation [276-278] and may involve activation of other enzymes. Eryptosis may involve activation of calpain [279]. Stimulation of eryptosis may lead to anemia due to rapid clearance of eryptotic erythrocytes from circulating blood [279]. Eryptosis further leads to adherence of phosphatidylserine exposing erythrocytes to the vascular wall [254], to stimulation of blood clotting and to triggering of thrombosis [133, 255, 256]. Enhanced eryptosis may lead to impairment of microcirculation [133, 257-261]. To conclude, Nocodazole triggers eryptosis with cell membrane scrambling, an effect in part due to increase of cytosolic Ca^{2+} activity, oxidative stress and ceramide.

15.4 TERFENADINE

The present study demonstrates that exposure of human erythrocytes to Terfenadine triggers eryptosis, the suicidal erythrocyte death [99]. The Terfenadine concentrations required for the stimulation of eryptosis are in the range of concentrations required to trigger apoptosis of human melanoma cells [184]. Terfenadine effect could be particularly effective in clinical conditions characterized by accelerated eryptosis, such as dehydration [262], hyperphosphatemia [263], chronic kidney disease (CKD) [264-267], hemolytic-uremic syndrome [268], diabetes [269], hepatic failure [270], malignancy [105], sepsis [271], sickle-cell disease [105], beta-thalassemia [105], Hb-C and G6PD-deficiency [105] and Wilson's disease [273]. Furthermore, Terfenadine could increase the eryptotic effect of other compounds [105, 280-308], possibly leading to of serious drug-drug interactions [309, 310]. The effect of Terfenadine on cell membrane scrambling was paralleled by an increase of cytosolic Ca^{2+} concentration ($[\text{Ca}^{2+}]_i$) and blunted by removal of Ca^{2+} from

extracellular space, indicating that entry of extracellular Ca^{2+} contributed to the stimulating effect of Terfenadine on phosphatidylserine translocation. Terfenadine triggered cell membrane scrambling even in the absence of extracellular Ca^{2+} . Furthermore, Terfenadine augmented the cell membrane scrambling triggered by ionomycin. Thus, Terfenadine sensitizes apparently the cell membrane scrambling to the stimulating effects of Ca^{2+} . Additional mechanisms able to trigger eryptosis include oxidative stress and ceramide [105]. Nevertheless, Terfenadine triggered eryptosis without enhancing the abundance of ROS or ceramide. Terfenadine treatment increases also the percentage of hemolytic erythrocytes. Eryptosis could be important for the clearance of defective erythrocytes from circulating blood prior to hemolysis [69]. Haemolysis may cause major harmful outcomes that could eventually progress to renal dysfunction, vascular disease, or chronic inflammation [134]. Eryptosis may counteract development of parasitemia in malaria, as infected erythrocytes enter eryptosis and are thus cleared from circulating blood [105]. Stimulation of eryptosis may lead to anemia due to rapid clearance of eryptotic erythrocytes from circulating blood [105]. Phosphatidylserine exposing erythrocytes may adhere to the vascular wall [254], stimulate blood clotting and thus foster thrombosis [133, 255, 256]. Stimulation of eryptosis may thus impair microcirculation [133, 257-261]. To conclude, Terfenadine treatment triggers cell membrane scrambling with phosphatidylserine translocation to the erythrocyte surface, an effect in part due to Ca^{2+} entry.

15.5 PICEATANNOL

The present observations unveil that exposure of human erythrocytes to Piceatannol is followed by cell shrinkage and cell membrane scrambling with phosphatidylserine translocation to the erythrocyte surface [100]. Piceatannol did not increase cytosolic Ca^{2+} activity ($[\text{Ca}^{2+}]_i$). Instead, it slightly tended to decrease Fluo3-fluorescence, but we cannot rule out an artifact, such as cellular loss of fluorescent dye. Nevertheless, the effect of Piceatannol treatment on cell membrane scrambling was significantly blunted following removal of extracellular Ca^{2+} . Furthermore, Piceatannol augmented cell membrane scrambling in erythrocytes loaded with Ca^{2+} by ionomycin treatment. The sensitivity of cell membrane scrambling to Ca^{2+} could be enhanced by ceramide [5]. Piceatannol increased ceramide abundance, which may contribute to or even account for the sensitization of cell membrane scrambling to $[\text{Ca}^{2+}]_i$. The stimulation of cell membrane scrambling by Piceatannol was paralleled by oxidative stress [105]. The effect of Piceatannol on cell shrinkage was significantly blunted by removal of extracellular Ca^{2+} . Moreover, Piceatannol significantly blunted the effect of the Ca^{2+} ionophore ionomycin on cell shrinkage. At low concentrations

Piceatannol decreases and at high concentrations Piceatannol increases hemolysis and thus release of hemoglobin. Hemoglobin released into blood vessels could pass the renal glomerular filter, precipitate in the acidic lumen of renal tubules, occlude nephrons and thus lead to renal failure [134]. Another important function of eryptosis could be the clearance of defective erythrocytes prior to hemolysis. Eryptosis may foster elimination of erythrocytes infected with the pathogen *Plasmodium* [105]. Excessive eryptosis could result in anemia if the loss of eryptotic erythrocytes outcasts the formation of new erythrocytes by erythropoiesis [105]. Phosphatidylserine exposing erythrocytes further adhere to the vascular wall [254], stimulate blood clotting and trigger thrombosis [133, 255, 256], thus impairing microcirculation [133, 257-261]. The effect of Piceatannol contrasts that of the analogue substance resveratrol [311-313], which has been shown to inhibit eryptosis [314]. To conclude, Piceatannol triggers eryptosis with cell shrinkage and cell membrane scrambling, an effect involving oxidative stress and ceramide.

15.6 CERANIB-2

The present study shows that Ceranib-2 triggers cell membrane scrambling in human RBCs [103]. The concentration required for the stimulation of eryptosis was similar to that triggering apoptosis of prostate tumor cells [315]. Removal of extracellular Ca^{2+} did not significantly modify Ceranib-2 induced eryptosis. Ceranib-2 treatment did not appreciably decrease forward scatter. Further experiments shown that Ceranib-2 treatment increased ceramide abundance. Ceramide could sensitize erythrocytes for the scrambling effect of Ca^{2+} [105]. A further mechanism presumably contributing to the stimulation of cell membrane scrambling by Ceranib-2 is oxidative stress, another stimulator of eryptosis [105]. Ceranib-2 increased also the percentage of hemolysis. Eryptosis is a physiological mechanism which allow the clearance of defective erythrocytes from circulating blood prior to hemolysis [105]. Failure of eryptosis to inhibit hemolysis leads to release of hemoglobin, which may pass the renal glomerular filter, precipitates in the acidic lumen of renal tubules, occludes nephrons and thus triggers renal failure [134]. Another case in which eryptosis is presumed to provide advantageous effects is malaria. The rapid clearance of phosphatidylserine exposing RBCs is followed by anaemia if the loss of erythrocytes surpasses the formation of new erythrocytes by erythropoiesis [105]. Phosphatidylserine exposing erythrocytes further adhere to the vascular wall [254, 257], stimulate blood clotting and trigger thrombosis [133, 255, 256]. Stimulation of eryptosis may thus be followed by impairment of microcirculation [133, 257-261]. To conclude, exposure of erythrocytes to Ceranib-2 triggers cell membrane scrambling, an effect apparently independent from Ca^{2+} entry, but involving oxidative stress and ceramide.

15.7 SCLAREOL

The present observations reveal that exposure of human erythrocytes drawn from healthy individuals to Sclareol is followed by cell membrane scrambling with phosphatidylserine translocation to the erythrocyte surface. Thus, Sclareol stimulates the suicidal erythrocyte death or eryptosis [102]. The Sclareol concentrations (10-100 μM) required for this effect were in the range of those required for induction of apoptosis and cell cycle arrest in human breast cancer cells [228]. The effect of 100 μM Sclareol on cell membrane scrambling was paralleled by an increase of $[\text{Ca}^{2+}]_i$. Sclareol treatment did not increase oxidative stress and ceramide abundance at the erythrocyte surface. Instead, the effect of Sclareol treatment on cell membrane scrambling was significantly blunted by pharmacological inhibition of p38 kinase and of casein kinase 1 α . It is well-known that these kinases could be involved in the machinery stimulating eryptosis [105]. Sclareol did not modify the average forward scatter. An increase of $[\text{Ca}^{2+}]_i$ could activate non-selective cation channels leading to K^+ exit, cell membrane hyperpolarization, Cl^- exit and thus cellular loss of KCl with water [275]. Probably, the effect of K^+ channel activation on cell volume was abrogated by impairment of Na^+/K^+ ATPase with respective dissipation of chemical K^+ , Na^+ and Cl^- gradients. Sclareol may further trigger hemolysis with the subsequent release of hemoglobin. To conclude, exposure of erythrocytes to Sclareol triggers cell membrane scrambling, an effect apparently independent from oxidative stress and ceramide.

16. BIBLIOGRAPHY

96. Kempe DS, Lang PA, Durantón C, Akel A, Lang KS, Huber SM, Wieder T, Lang F: **Enhanced programmed cell death of iron-deficient erythrocytes.** *Faseb j* 2006, **20**(2):368-370.
97. Lang F, Lang E, Foller M: **Physiology and pathophysiology of eryptosis.** *Transfus Med Hemother* 2012, **39**(5):308-314.
98. Signoretto E, Bissinger R, Castagna M, Lang F: **Stimulation of Eryptosis by Combretastatin A4 Phosphate Disodium (CA4P).** *Cell Physiol Biochem* 2016, **38**(3):969-981.
99. Signoretto E, Castagna M, Al Mamun Bhuyan A, Lang F: **Stimulating Effect of Terfenadine on Erythrocyte Cell Membrane Scrambling.** *Cell Physiol Biochem* 2016, **38**(4):1425-1434.
100. Signoretto E, Castagna M, Lang F: **Stimulation of Eryptosis, the Suicidal Erythrocyte Death by Piceatannol.** *Cell Physiol Biochem* 2016, **38**(6):2300-2310.
101. Signoretto E, Honisch S, Briglia M, Faggio C, Castagna M, Lang F: **Nocodazole Induced Suicidal Death of Human Erythrocytes.** *Cell Physiol Biochem* 2016, **38**(1):379-392.
102. Signoretto E, Laufer SA, Lang F: **Stimulating Effect of Sclareol on Suicidal Death of Human Erythrocytes.** *Cell Physiol Biochem* 2016, **39**(2):554-564.
103. Signoretto E, Zierle J, Bhuyan AA, Castagna M, Lang F: **Ceranib-2-induced suicidal erythrocyte death.** *Cell Biochem Funct* 2016, **34**(5):359-366.
104. Signoretto E, Zierle J, Bissinger R, Castagna M, Bossi E, Lang F: **Triggering of Suicidal Erythrocyte Death by Pazopanib.** *Cell Physiol Biochem* 2016, **38**(3):926-938.
105. Lang E, Lang F: **Mechanisms and pathophysiological significance of eryptosis, the suicidal erythrocyte death.** *Semin Cell Dev Biol* 2015, **39**:35-42.
106. Palis J: **Primitive and definitive erythropoiesis in mammals.** *Front Physiol* 2014, **5**:3.
107. Ghezzi P, Brines M: **Erythropoietin as an antiapoptotic, tissue-protective cytokine.** *Cell death and differentiation* 2004, **11 Suppl 1**:S37-44.
108. Mohandas N, Gallagher PG: **Red cell membrane: past, present, and future.** *Blood* 2008, **112**(10):3939-3948.
109. Atukorale PU, Yang YS, Bekdemir A, Carney RP, Silva PJ, Watson N, Stellacci F, Irvine DJ: **Influence of the glycocalyx and plasma membrane composition on amphiphilic gold nanoparticle association with erythrocytes.** *Nanoscale* 2015, **7**(26):11420-11432.
110. Ballas SK, Krasnow SH: **Structure of erythrocyte membrane and its transport functions.** *Annals of clinical and laboratory science* 1980, **10**(3):209-219.
111. Zwaal RF, Schroit AJ: **Pathophysiologic implications of membrane phospholipid asymmetry in blood cells.** *Blood* 1997, **89**(4):1121-1132.

112. Salomao M, Zhang X, Yang Y, Lee S, Hartwig JH, Chasis JA, Mohandas N, An X: **Protein 4.1R-dependent multiprotein complex: new insights into the structural organization of the red blood cell membrane.** *Proceedings of the National Academy of Sciences of the United States of America* 2008, **105**(23):8026-8031.
113. Smith JE: **Erythrocyte membrane: structure, function, and pathophysiology.** *Veterinary pathology* 1987, **24**(6):471-476.
114. Zidova Z, Kapralova K, Koralkova P, Mojzikova R, Dolezal D, Divoky V, Horvathova M: **DMT1-mutant erythrocytes have shortened life span, accelerated glycolysis and increased oxidative stress.** *Cellular physiology and biochemistry : international journal of experimental cellular physiology, biochemistry, and pharmacology* 2014, **34**(6):2221-2231.
115. Nagababu E, Gulyani S, Earley CJ, Cutler RG, Mattson MP, Rifkind JM: **Iron-deficiency anaemia enhances red blood cell oxidative stress.** *Free radical research* 2008, **42**(9):824-829.
116. Lang E, Bissinger R, Gulbins E, Lang F: **Ceramide in the regulation of eryptosis, the suicidal erythrocyte death.** *Apoptosis* 2015, **20**(5):758-767.
117. Ganz T: **Macrophages and systemic iron homeostasis.** *Journal of innate immunity* 2012, **4**(5-6):446-453.
118. Mackenzie B, Hediger MA: **SLC11 family of H⁺-coupled metal-ion transporters NRAMP1 and DMT1.** *Pflugers Archiv : European journal of physiology* 2004, **447**(5):571-579.
119. Lang E, Lang F: **Triggers, inhibitors, mechanisms, and significance of eryptosis: the suicidal erythrocyte death.** *Biomed Res Int* 2015, **2015**:513518.
120. Lang F, Gulbins E, Lang PA, Zappulla D, Foller M: **Ceramide in suicidal death of erythrocytes.** *Cellular physiology and biochemistry : international journal of experimental cellular physiology, biochemistry, and pharmacology* 2010, **26**(1):21-28.
121. Lang F, Qadri SM: **Mechanisms and significance of eryptosis, the suicidal death of erythrocytes.** *Blood Purif* 2012, **33**(1-3):125-130.
122. Gatidis S, Zelenak C, Fajol A, Lang E, Jilani K, Michael D, Qadri SM, Lang F: **p38 MAPK activation and function following osmotic shock of erythrocytes.** *Cell Physiol Biochem* 2011, **28**(6):1279-1286.
123. Zelenak C, Eberhard M, Jilani K, Qadri SM, Macek B, Lang F: **Protein kinase CK1alpha regulates erythrocyte survival.** *Cellular physiology and biochemistry : international journal of experimental cellular physiology, biochemistry, and pharmacology* 2012, **29**(1-2):171-180.

124. Berg CP, Engels IH, Rothbart A, Lauber K, Renz A, Schlosser SF, Schulze-Osthoff K, Wesselborg S: **Human mature red blood cells express caspase-3 and caspase-8, but are devoid of mitochondrial regulators of apoptosis.** *Cell death and differentiation* 2001, **8**(12):1197-1206.
125. Daugas E, Cande C, Kroemer G: **Erythrocytes: death of a mummy.** *Cell death and differentiation* 2001, **8**(12):1131-1133.
126. Lang F, Jilani K, Lang E: **Therapeutic potential of manipulating suicidal erythrocyte death.** *Expert Opin Ther Targets* 2015, **19**(9):1219-1227.
127. Bissinger R, Schumacher C, Qadri SM, Honisch S, Malik A, Gotz F, Kopp HG, Lang F: **Enhanced eryptosis contributes to anemia in lung cancer patients.** *Oncotarget* 2016, **7**(12):14002-14014.
128. Borst O, Abed M, Alesutan I, Towhid ST, Qadri SM, Foller M, Gawaz M, Lang F: **Dynamic adhesion of eryptotic erythrocytes to endothelial cells via CXCL16/SR-PSOX.** *Am J Physiol Cell Physiol* 2012, **302**(4):C644-651.
129. Fadok VA, Bratton DL, Rose DM, Pearson A, Ezekewitz RA, Henson PM: **A receptor for phosphatidylserine-specific clearance of apoptotic cells.** *Nature* 2000, **405**(6782):85-90.
130. Setty BN, Betal SG: **Microvascular endothelial cells express a phosphatidylserine receptor: a functionally active receptor for phosphatidylserine-positive erythrocytes.** *Blood* 2008, **111**(2):905-914.
131. Manodori AB, Barabino GA, Lubin BH, Kuypers FA: **Adherence of phosphatidylserine-exposing erythrocytes to endothelial matrix thrombospondin.** *Blood* 2000, **95**(4):1293-1300.
132. Du VX, Huskens D, Maas C, Al Dieri R, de Groot PG, de Laat B: **New insights into the role of erythrocytes in thrombus formation.** *Semin Thromb Hemost* 2014, **40**(1):72-80.
133. Andrews DA, Low PS: **Role of red blood cells in thrombosis.** *Curr Opin Hematol* 1999, **6**(2):76-82.
134. Harrison HE, Bunting H, Ordway NK, Albrink WS: **The Pathogenesis of the Renal Injury Produced in the Dog by Hemoglobin or Methemoglobin.** *The Journal of experimental medicine* 1947, **86**(4):339-356.
135. Foller M, Bobbala D, Koka S, Huber SM, Gulbins E, Lang F: **Suicide for survival--death of infected erythrocytes as a host mechanism to survive malaria.** *Cell Physiol Biochem* 2009, **24**(3-4):133-140.
136. Greene LM, Meegan MJ, Zisterer DM: **Combretastatins: more than just vascular targeting agents?** *The Journal of pharmacology and experimental therapeutics* 2015, **355**(2):212-227.

137. Abma E, Daminet S, Smets P, Ni Y, de Rooster H: **Combretastatin A4-phosphate and its potential in veterinary oncology: a review.** *Veterinary and comparative oncology* 2015.
138. Chaplin DJ, Pettit GR, Hill SA: **Anti-vascular approaches to solid tumour therapy: evaluation of combretastatin A4 phosphate.** *Anticancer research* 1999, **19**(1a):189-195.
139. Dowlati A, Robertson K, Cooney M, Petros WP, Stratford M, Jesberger J, Rafie N, Overmoyer B, Makkar V, Stambler B *et al*: **A phase I pharmacokinetic and translational study of the novel vascular targeting agent combretastatin a-4 phosphate on a single-dose intravenous schedule in patients with advanced cancer.** *Cancer research* 2002, **62**(12):3408-3416.
140. He X, Li S, Huang H, Li Z, Chen L, Ye S, Huang J, Zhan J, Lin T: **A pharmacokinetic and safety study of single dose intravenous combretastatin A4 phosphate in Chinese patients with refractory solid tumours.** *Br J Clin Pharmacol* 2011, **71**(6):860-870.
141. Nathan P, Zweifel M, Padhani AR, Koh DM, Ng M, Collins DJ, Harris A, Carden C, Smythe J, Fisher N *et al*: **Phase I trial of combretastatin A4 phosphate (CA4P) in combination with bevacizumab in patients with advanced cancer.** *Clin Cancer Res* 2012, **18**(12):3428-3439.
142. Pettit GR, Rhodes MR: **Antineoplastic agents 389. New syntheses of the combretastatin A-4 prodrug.** *Anti-cancer drug design* 1998, **13**(3):183-191.
143. Pettit GR, Singh SB, Hamel E, Lin CM, Alberts DS, Garcia-Kendall D: **Isolation and structure of the strong cell growth and tubulin inhibitor combretastatin A-4.** *Experientia* 1989, **45**(2):209-211.
144. Pettit GR, Cragg, G. M., Herald, D. L., Schmidt, J. M., and Lohavanijaya, P.: **Isolation and structure of combretastatin.** *Can J Chem* 1982, **60**:1374-1376.
145. Vincent L, Kermani P, Young LM, Cheng J, Zhang F, Shido K, Lam G, Bompais-Vincent H, Zhu Z, Hicklin DJ *et al*: **Combretastatin A4 phosphate induces rapid regression of tumor neovessels and growth through interference with vascular endothelial-cadherin signaling.** *J Clin Invest* 2005, **115**(11):2992-3006.
146. West CM, Price P: **Combretastatin A4 phosphate.** *Anti-cancer drugs* 2004, **15**(3):179-187.
147. Greene LM, O'Boyle NM, Nolan DP, Meegan MJ, Zisterer DM: **The vascular targeting agent Combretastatin-A4 directly induces autophagy in adenocarcinoma-derived colon cancer cells.** *Biochemical pharmacology* 2012, **84**(5):612-624.
148. Ding X, Zhang Z, Li S, Wang A: **Combretastatin A4 phosphate induces programmed cell death in vascular endothelial cells.** *Oncology research* 2011, **19**(7):303-309.
149. Lin HL, Chiou SH, Wu CW, Lin WB, Chen LH, Yang YP, Tsai ML, Uen YH, Liou JP, Chi CW: **Combretastatin A4-induced differential cytotoxicity and reduced metastatic ability by**

- inhibition of AKT function in human gastric cancer cells.** *The Journal of pharmacology and experimental therapeutics* 2007, **323**(1):365-373.
150. Song J, Yoo J, Kwon A, Kim D, Nguyen HK, Lee BY, Suh W, Min KH: **Structure-Activity Relationship of Indole-Tethered Pyrimidine Derivatives that Concurrently Inhibit Epidermal Growth Factor Receptor and Other Angiokinases.** *PloS one* 2015, **10**(9):e0138823.
151. Kerklaan BM, Lolkema MP, Devriese LA, Voest EE, Nol-Boekel A, Mergui-Roelvink M, Langenberg M, Mykulowycz K, Stoebenau J, Lane S *et al*: **Phase I and pharmacological study of pazopanib in combination with oral topotecan in patients with advanced solid tumours.** *Br J Cancer* 2015, **113**(5):706-715.
152. Schutz FA, Choueiri TK, Sternberg CN: **Pazopanib: Clinical development of a potent anti-angiogenic drug.** *Critical reviews in oncology/hematology* 2011, **77**(3):163-171.
153. Sternberg CN, Davis ID, Deen KC, Sigal E, Hawkins RE: **An open-label extension study to evaluate safety and efficacy of pazopanib in patients with advanced renal cell carcinoma.** *Oncology* 2014, **87**(6):342-350.
154. Davidson BA, Secord AA: **Profile of pazopanib and its potential in the treatment of epithelial ovarian cancer.** *International journal of women's health* 2014, **6**:289-300.
155. Ahn HK, Choi JY, Kim KM, Kim H, Choi SH, Park SH, Park JO, Lim HY, Kang WK, Lee J *et al*: **Phase II study of pazopanib monotherapy in metastatic gastroenteropancreatic neuroendocrine tumours.** *British journal of cancer* 2013, **109**(6):1414-1419.
156. Reardon DA, Groves MD, Wen PY, Nabors L, Mikkelsen T, Rosenfeld S, Raizer J, Barriuso J, McLendon RE, Suttle AB *et al*: **A phase I/II trial of pazopanib in combination with lapatinib in adult patients with relapsed malignant glioma.** *Clinical cancer research : an official journal of the American Association for Cancer Research* 2013, **19**(4):900-908.
157. Pinciroli P, Won H, Iyer G, Canevari S, Colecchia M, Giannatempo P, Raggi D, Pierotti MA, De Braud FG, Solit DB *et al*: **Molecular Signature of Response to Pazopanib Salvage Therapy for Urothelial Carcinoma.** *Clinical genitourinary cancer* 2016, **14**(1):e81-90.
158. Necchi A, Pennati M, Zaffaroni N, Landoni E, Giannatempo P, Raggi D, Schwartz LH, Morosi C, Crippa F, Fare E *et al*: **Analysis of plasma cytokines and angiogenic factors in patients with pretreated urothelial cancer receiving Pazopanib: the role of circulating interleukin-8 to enhance the prognostic accuracy.** *British journal of cancer* 2014, **110**(1):26-33.
159. Amiri-Kordestani L, Tan AR, Swain SM: **Pazopanib for the treatment of breast cancer.** *Expert opinion on investigational drugs* 2012, **21**(2):217-225.

160. Nikolinakos PG, Altorki N, Yankelevitz D, Tran HT, Yan S, Rajagopalan D, Bordogna W, Ottesen LH, Heymach JV: **Plasma cytokine and angiogenic factor profiling identifies markers associated with tumor shrinkage in early-stage non-small cell lung cancer patients treated with pazopanib.** *Cancer research* 2010, **70**(6):2171-2179.
161. Craveiro RB, Ehrhardt M, Holst MI, Pietsch T, Dilloo D: **In comparative analysis of multi-kinase inhibitors for targeted medulloblastoma therapy pazopanib exhibits promising in vitro and in vivo efficacy.** *Oncotarget* 2014, **5**(16):7149-7161.
162. Paesler J, Gehrke I, Gandhirajan RK, Filipovich A, Hertweck M, Erdfelder F, Uhrmacher S, Poll-Wolbeck SJ, Hallek M, Kreuzer KA: **The vascular endothelial growth factor receptor tyrosine kinase inhibitors vatalanib and pazopanib potently induce apoptosis in chronic lymphocytic leukemia cells in vitro and in vivo.** *Clinical cancer research : an official journal of the American Association for Cancer Research* 2010, **16**(13):3390-3398.
163. Fauster A, Rebsamen M, Huber KV, Bigenzahn JW, Stukalov A, Lardeau CH, Scorzoni S, Bruckner M, Gridling M, Parapatics K *et al*: **A cellular screen identifies ponatinib and pazopanib as inhibitors of necroptosis.** *Cell death & disease* 2015, **6**:e1767.
164. Kale SS, Jedhe GS, Meshram SN, Santra MK, Hamel E, Sanjayan GJ: **Novel hybrid nocodazole analogues as tubulin polymerization inhibitors and their antiproliferative activity.** *Bioorganic & medicinal chemistry letters* 2015, **25**(9):1982-1985.
165. Beswick RW, Ambrose HE, Wagner SD: **Nocodazole, a microtubule de-polymerising agent, induces apoptosis of chronic lymphocytic leukaemia cells associated with changes in Bcl-2 phosphorylation and expression.** *Leuk Res* 2006, **30**(4):427-436.
166. Zacharaki P, Stephanou G, Demopoulos NA: **Comparison of the aneugenic properties of nocodazole, paclitaxel and griseofulvin in vitro. Centrosome defects and alterations in protein expression profiles.** *J Appl Toxicol* 2013, **33**(9):869-879.
167. Ho YS, Duh JS, Jeng JH, Wang YJ, Liang YC, Lin CH, Tseng CJ, Yu CF, Chen RJ, Lin JK: **Griseofulvin potentiates antitumorigenesis effects of nocodazole through induction of apoptosis and G2/M cell cycle arrest in human colorectal cancer cells.** *Int J Cancer* 2001, **91**(3):393-401.
168. Hsu SL, Yu CT, Yin SC, Tang MJ, Tien AC, Wu YM, Huang CY: **Caspase 3, periodically expressed and activated at G2/M transition, is required for nocodazole-induced mitotic checkpoint.** *Apoptosis* 2006, **11**(5):765-771.
169. Kitagawa K, Niikura Y: **Caspase-independent mitotic death (CIMD).** *Cell Cycle* 2008, **7**(8):1001-1005.

170. Frezzato F, Trimarco V, Martini V, Gattazzo C, Ave E, Visentin A, Cabrelle A, Olivieri V, Zambello R, Facco M *et al*: **Leukaemic cells from chronic lymphocytic leukaemia patients undergo apoptosis following microtubule depolymerization and Lyn inhibition by nocodazole.** *Br J Haematol* 2014, **165**(5):659-672.
171. Verdoodt B, Decordier I, Geleyns K, Cunha M, Cundari E, Kirsch-Volders M: **Induction of polyploidy and apoptosis after exposure to high concentrations of the spindle poison nocodazole.** *Mutagenesis* 1999, **14**(5):513-520.
172. Decordier I, Cundari E, Kirsch-Volders M: **Survival of aneuploid, micronucleated and/or polyploid cells: crosstalk between ploidy control and apoptosis.** *Mutat Res* 2008, **651**(1-2):30-39.
173. Han CR, Jun do Y, Lee JY, Kim YH: **Prometaphase arrest-dependent phosphorylation of Bcl-2 and Bim reduces the association of Bcl-2 with Bak or Bim, provoking Bak activation and mitochondrial apoptosis in nocodazole-treated Jurkat T cells.** *Apoptosis* 2014, **19**(1):224-240.
174. Song H, Kim SI, Ko MS, Kim HJ, Heo JC, Lee HJ, Lee HS, Han IS, Kwack K, Park JW: **Overexpression of DRG2 increases G2/M phase cells and decreases sensitivity to nocodazole-induced apoptosis.** *J Biochem* 2004, **135**(3):331-335.
175. Asnaghi L, Bruno P, Priulla M, Nicolin A: **mTOR: a protein kinase switching between life and death.** *Pharmacol Res* 2004, **50**(6):545-549.
176. Choi HJ, Zhu BT: **Role of cyclin B1/Cdc2 in mediating Bcl-XL phosphorylation and apoptotic cell death following nocodazole-induced mitotic arrest.** *Mol Carcinog* 2014, **53**(2):125-137.
177. Bhakta-Guha D, Saeed ME, Greten HJ, Efferth T: **Dis-organizing centrosomal clusters: specific cancer therapy for a generic spread?** *Curr Med Chem* 2015, **22**(6):685-694.
178. Agnese V, Bazan V, Fiorentino FP, Fanale D, Badalamenti G, Colucci G, Adamo V, Santini D, Russo A: **The role of Aurora-A inhibitors in cancer therapy.** *Ann Oncol* 2007, **18** Suppl 6:vi47-52.
179. Guo X, Zhang X, Li Y, Guo Y, Wang J, Li Y, Shen B, Sun D, Zhang J: **Nocodazole increases the ERK activity to enhance MKP-1 expression which inhibits p38 activation induced by TNF-alpha.** *Mol Cell Biochem* 2012, **364**(1-2):373-380.
180. Holzer M, Ziegler S, Albrecht B, Kronenberger B, Kaul A, Bartenschlager R, Kattner L, Klein CD, Hartmann RW: **Identification of terfenadine as an inhibitor of human CD81-receptor HCV-E2 interaction: synthesis and structure optimization.** *Molecules (Basel, Switzerland)* 2008, **13**(5):1081-1110.

181. Simons FE, M JS, Goritz SS, Simons KJ: **H1-antihistaminic activity of cetirizine and fexofenadine in allergic children.** *Pediatric allergy and immunology : official publication of the European Society of Pediatric Allergy and Immunology* 2003, **14**(3):207-211.
182. Nicolau-Galmes F, Asumendi A, Alonso-Tejerina E, Perez-Yarza G, Jangi SM, Gardeazabal J, Arroyo-Berdugo Y, Careaga JM, Diaz-Ramon JL, Apraiz A *et al*: **Terfenadine induces apoptosis and autophagy in melanoma cells through ROS-dependent and -independent mechanisms.** *Apoptosis* 2011, **16**(12):1253-1267.
183. Jangi SM, Diaz-Perez JL, Ochoa-Lizarralde B, Martin-Ruiz I, Asumendi A, Perez-Yarza G, Gardeazabal J, Diaz-Ramon JL, Boyano MD: **H1 histamine receptor antagonists induce genotoxic and caspase-2-dependent apoptosis in human melanoma cells.** *Carcinogenesis* 2006, **27**(9):1787-1796.
184. Jangi SM, Ruiz-Larrea MB, Nicolau-Galmes F, Andollo N, Arroyo-Berdugo Y, Ortega-Martinez I, Diaz-Perez JL, Boyano MD: **Terfenadine-induced apoptosis in human melanoma cells is mediated through Ca²⁺ homeostasis modulation and tyrosine kinase activity, independently of H1 histamine receptors.** *Carcinogenesis* 2008, **29**(3):500-509.
185. Wang WT, Chen YH, Hsu JL, Leu WJ, Yu CC, Chan SH, Ho YF, Hsu LC, Guh JH: **Terfenadine induces anti-proliferative and apoptotic activities in human hormone-refractory prostate cancer through histamine receptor-independent Mcl-1 cleavage and Bak up-regulation.** *Naunyn-Schmiedeberg's archives of pharmacology* 2014, **387**(1):33-45.
186. Rizzuto R, Pinton P, Ferrari D, Chami M, Szabadkai G, Magalhaes PJ, Di Virgilio F, Pozzan T: **Calcium and apoptosis: facts and hypotheses.** *Oncogene* 2003, **22**(53):8619-8627.
187. Diaz-Trelles R, Novelli A, Vega JA, Marini A, Fernandez-Sanchez MT: **Antihistamine terfenadine potentiates NMDA receptor-mediated calcium influx, oxygen radical formation, and neuronal death.** *Brain research* 2000, **880**(1-2):17-27.
188. Brooks CD, Karl KJ, Francom SF: **Profile of ragweed hay fever symptom control with terfenadine started before or after symptoms are established.** *Clinical and experimental allergy : journal of the British Society for Allergy and Clinical Immunology* 1990, **20**(1):21-26.
189. Ciprandi G, Iudice A, Tosca MA, Ruffoni S, Buscaglia S, Canonica GW: **Comparative effects of terfenadine and loratadine in the treatment of hay fever.** *Journal of investigational allergology & clinical immunology* 1991, **1**(6):368-372.
190. McTavish D, Goa KL, Ferrill M: **Terfenadine. An updated review of its pharmacological properties and therapeutic efficacy.** *Drugs* 1990, **39**(4):552-574.
191. Sorkin EM, Heel RC: **Terfenadine. A review of its pharmacodynamic properties and therapeutic efficacy.** *Drugs* 1985, **29**(1):34-56.

192. Larrosa M, Tomas-Barberan FA, Espin JC: **The grape and wine polyphenol piceatannol is a potent inducer of apoptosis in human SK-Mel-28 melanoma cells.** *European journal of nutrition* 2004, **43**(5):275-284.
193. Piotrowska H, Kucinska M, Murias M: **Biological activity of piceatannol: leaving the shadow of resveratrol.** *Mutat Res* 2012, **750**(1):60-82.
194. Seyed MA, Jantan I, Bukhari SN, Vijayaraghavan K: **A Comprehensive Review on the Chemotherapeutic Potential of Piceatannol for Cancer Treatment, with Mechanistic Insights.** *J Agric Food Chem* 2016, **64**(4):725-737.
195. Tang YL, Chan SW: **A review of the pharmacological effects of piceatannol on cardiovascular diseases.** *Phytother Res* 2014, **28**(11):1581-1588.
196. Munzenberger B, Heilemann J, Strack D, Kottke I, Oberwinkler F: **Phenolics of mycorrhizas and non-mycorrhizal roots of Norway spruce.** *Planta* 1990, **182**(1):142-148.
197. Ferrigni NR, McLaughlin JL, Powell RG, Smith CR, Jr.: **Use of potato disc and brine shrimp bioassays to detect activity and isolate piceatannol as the antileukemic principle from the seeds of Euphorbia lagascae.** *J Nat Prod* 1984, **47**(2):347-352.
198. Jancinova V, Perecko T, Nosal R, Svitekova K, Drabikova K: **The natural stilbenoid piceatannol decreases activity and accelerates apoptosis of human neutrophils: involvement of protein kinase C.** *Oxid Med Cell Longev* 2013, **2013**:136539.
199. Fernandez LA, Torrealba J, Yagci G, Ishido N, Tsuchida M, Tae Kim H, Dong Y, Oberley T, Fechner J, Colburn MJ *et al*: **Piceatannol in combination with low doses of cyclosporine A prolongs kidney allograft survival in a stringent rat transplantation model.** *Transplantation* 2002, **74**(11):1609-1617.
200. Geahlen RL, McLaughlin JL: **Piceatannol (3,4,3',5'-tetrahydroxy-trans-stilbene) is a naturally occurring protein-tyrosine kinase inhibitor.** *Biochem Biophys Res Commun* 1989, **165**(1):241-245.
201. Ashikawa K, Majumdar S, Banerjee S, Bharti AC, Shishodia S, Aggarwal BB: **Piceatannol inhibits TNF-induced NF-kappaB activation and NF-kappaB-mediated gene expression through suppression of IkkappaBalpha kinase and p65 phosphorylation.** *J Immunol* 2002, **169**(11):6490-6497.
202. Jin CY, Moon DO, Lee KJ, Kim MO, Lee JD, Choi YH, Park YM, Kim GY: **Piceatannol attenuates lipopolysaccharide-induced NF-kappaB activation and NF-kappaB-related proinflammatory mediators in BV2 microglia.** *Pharmacol Res* 2006, **54**(6):461-467.

203. Su L, David M: **Distinct mechanisms of STAT phosphorylation via the interferon-alpha/beta receptor. Selective inhibition of STAT3 and STAT5 by piceatannol.** *J Biol Chem* 2000, **275**(17):12661-12666.
204. Kumari AL, Ali AM, Das S, Pardhasaradhi BV, Varalakshmi C, Khar A: **Role of STAT3 and NFkappaB signaling in the serum factor-induced apoptosis in AK-5 cells.** *Biochem Biophys Res Commun* 2005, **336**(3):860-867.
205. Kim YH, Park C, Lee JO, Kim GY, Lee WH, Choi YH, Ryu CH: **Induction of apoptosis by piceatannol in human leukemic U937 cells through down-regulation of Bcl-2 and activation of caspases.** *Oncol Rep* 2008, **19**(4):961-967.
206. Draper JM, Xia Z, Smith RA, Zhuang Y, Wang W, Smith CD: **Discovery and evaluation of inhibitors of human ceramidase.** *Mol Cancer Ther* 2011, **10**(11):2052-2061.
207. Arana L, Gangoiti P, Ouro A, Trueba M, Gomez-Munoz A: **Ceramide and ceramide 1-phosphate in health and disease.** *Lipids in health and disease* 2010, **9**:15.
208. Arboleda G, Morales LC, Benitez B, Arboleda H: **Regulation of ceramide-induced neuronal death: cell metabolism meets neurodegeneration.** *Brain research reviews* 2009, **59**(2):333-346.
209. Boslem E, Meikle PJ, Biden TJ: **Roles of ceramide and sphingolipids in pancreatic beta-cell function and dysfunction.** *Islets* 2012, **4**(3):177-187.
210. Claus RA, Dorer MJ, Bunck AC, Deigner HP: **Inhibition of sphingomyelin hydrolysis: targeting the lipid mediator ceramide as a key regulator of cellular fate.** *Current medicinal chemistry* 2009, **16**(16):1978-2000.
211. Dimanche-Boitrel MT, Rebillard A, Gulbins E: **Ceramide in chemotherapy of tumors.** *Recent patents on anti-cancer drug discovery* 2011, **6**(3):284-293.
212. Galadari S, Rahman A, Pallichankandy S, Thayyullathil F: **Tumor suppressive functions of ceramide: evidence and mechanisms.** *Apoptosis : an international journal on programmed cell death* 2015, **20**(5):689-711.
213. Jana A, Hogan EL, Pahan K: **Ceramide and neurodegeneration: susceptibility of neurons and oligodendrocytes to cell damage and death.** *Journal of the neurological sciences* 2009, **278**(1-2):5-15.
214. Kolesnick R: **The therapeutic potential of modulating the ceramide/sphingomyelin pathway.** *J Clin Invest* 2002, **110**(1):3-8.
215. Colombini M: **Ceramide channels and their role in mitochondria-mediated apoptosis.** *Biochim Biophys Acta* 2010, **1797**(6-7):1239-1244.

216. Kogot-Levin A, Saada A: **Ceramide and the mitochondrial respiratory chain.** *Biochimie* 2014, **100**:88-94.
217. Novgorodov SA, Gudz TI: **Ceramide and mitochondria in ischemic brain injury.** *Int J Biochem Mol Biol* 2011, **2**(4):347-361.
218. Ueda N: **Ceramide-induced apoptosis in renal tubular cells: a role of mitochondria and sphingosine-1-phosphate.** *Int J Mol Sci* 2015, **16**(3):5076-5124.
219. Ogretmen B, Hannun YA: **Biologically active sphingolipids in cancer pathogenesis and treatment.** *Nat Rev Cancer* 2004, **4**(8):604-616.
220. Bielawska A, Linardic CM, Hannun YA: **Ceramide-mediated biology. Determination of structural and stereospecific requirements through the use of N-acyl-phenylaminoalcohol analogs.** *J Biol Chem* 1992, **267**(26):18493-18497.
221. Selzner M, Bielawska A, Morse MA, Rudiger HA, Sindram D, Hannun YA, Clavien PA: **Induction of apoptotic cell death and prevention of tumor growth by ceramide analogues in metastatic human colon cancer.** *Cancer Res* 2001, **61**(3):1233-1240.
222. Park JE, Lee KE, Jung E, Kang S, Kim YJ: **Sclareol isolated from *Salvia officinalis* improves facial wrinkles via an antiphotoreactive mechanism.** *Journal of cosmetic dermatology* 2016.
223. Ulubelen A, Topcu G, Eris C, Sonmez U, Kartal M, Kurucu S, Bozok-Johansson C: **Terpenoids from *Salvia sclarea*.** *Phytochemistry* 1994, **36**(4):971-974.
224. Sultana N, Saify ZS: **Enzymatic biotransformation of terpenes as bioactive agents.** *J Enzym Inhib Med Ch* 2013, **28**(6):1113-1128.
225. Zerbe P, Bohlmann J: **Enzymes for Synthetic Biology of Ambroxide-Related Diterpenoid Fragrance Compounds.** *Adv Biochem Eng Biot* 2015, **148**:427-447.
226. Dimas K, Hatziantoniou S, Tseleni S, Khan H, Georgopoulos A, Alevizopoulos K, Wyche JH, Pantazis P, Demetzos C: **Sclareol induces apoptosis in human HCT116 colon cancer cells in vitro and suppression of HCT116 tumor growth in immunodeficient mice.** *Apoptosis* 2007, **12**(4):685-694.
227. Dimas K, Kokkinopoulos D, Demetzos C, Vaos B, Marselos M, Malamas M, Tzavaras T: **The effect of sclareol on growth and cell cycle progression of human leukemic cell lines.** *Leukemia Res* 1999, **23**(3):217-234.
228. Dimas K, Papadaki A, Tsimplouli C, Hatziantoniou S, Alevizopoulos K, Pantazis P, Demetzos C: **Labd-14-ene-8,13-diol (sclareol) induces cell cycle arrest and apoptosis in human breast cancer cells and enhances the activity of anticancer drugs.** *Biomedicine & Pharmacotherapy* 2006, **60**(3):127-133.

229. Hatziantoniou S, Dimas K, Georgopoulos A, Sotiriadou N, Demetzos C: **Cytotoxic and antitumor activity of liposome-incorporated sclareol against cancer cell lines and human colon cancer xenografts.** *Pharmacol Res* 2006, **53**(1):80-87.
230. Mahaira LG, Tsimplouli C, Sakellaridis N, Alevizopoulos K, Demetzos C, Han ZY, Pantazis P, Dimas K: **The labdane diterpene sclareol (labd-14-ene-8, 13-diol) induces apoptosis in human tumor cell lines and suppression of tumor growth in vivo via a p53-independent mechanism of action.** *Eur J Pharmacol* 2011, **666**(1-3):173-182.
231. Noori S, Hassan ZM, Mohammadi M, Habibi Z, Sohrabi N, Bayanolhagh S: **Sclareol modulates the Treg intra-tumoral infiltrated cell and inhibits tumor growth in vivo.** *Cell Immunol* 2010, **263**(2):148-153.
232. Noori S, Hassan ZM, Salehian O: **Sclareol Reduces CD4+CD25+FoxP3+T-reg Cells in a Breast Cancer Model in Vivo.** *Iran J Immunol* 2013, **10**(1):10-21.
233. Paradissis A, Hatziantoniou S, Georgopoulos A, Psarra AMG, Dimas K, Demetzos C: **Liposomes modify the subcellular distribution of sclareol uptake by HCT-116 cancer cell lines.** *Biomed Pharmacother* 2007, **61**(2-3):120-124.
234. Sashidhara KV, Rosaiah JN, Kumar A, Bid HK, Konwar R, Chattopadhyay N: **Cell growth inhibitory action of an unusual labdane diterpene, 13-epi-Sclareol in breast and uterine cancers in vitro.** *Phytother Res* 2007, **21**(11):1105-1108.
235. Shakeel-u-Rehman, Rah B, Lone SH, Rasool RU, Farooq S, Nayak D, Chikan NA, Chakraborty S, Behl A, Mondhe DM *et al*: **Design and Synthesis of Antitumor Heck-Coupled Sclareol Analogues: Modulation of BH3 Family Members by SS-12 in Autophagy and Apoptotic Cell Death.** *J Med Chem* 2015, **58**(8):3432-3444.
236. Wang L, He HS, Yu HL, Zeng Y, Han H, He N, Liu ZG, Wang ZY, Xu SJ, Xiong M: **Sclareol, a plant diterpene, exhibits potent antiproliferative effects via the induction of apoptosis and mitochondrial membrane potential loss in osteosarcoma cancer cells.** *Mol Med Rep* 2015, **11**(6):4273-4278.
237. Huang GJ, Pan CH, Wu CH: **Sclareol Exhibits Anti-inflammatory Activity in Both Lipopolysaccharide-Stimulated Macrophages and the lambda-Carrageenan-Induced Paw Edema Model.** *J Nat Prod* 2012, **75**(1):54-59.
238. Zhong Y, Huang Y, Santoso MB, Wu LD: **Sclareol exerts anti-osteoarthritic activities in interleukin-1 beta-induced rabbit chondrocytes and a rabbit osteoarthritis model.** *Int J Clin Exp Patho* 2015, **8**(3):2365-2374.

239. Choudhary ML, Siddiqui ZA, Hussain S, Atta-ur-Rahman: **Structure elucidation and antibacterial activity of new fungal metabolites of sclareol.** *Chem Biodivers* 2006, **3**(1):54-61.
240. Ma MF, Feng JL, Li RX, Chen SW, Xu H: **Synthesis and antifungal activity of ethers, alcohols, and iodohydrin derivatives of sclareol against phytopathogenic fungi in vitro.** *Bioorg Med Chem Lett* 2015, **25**(14):2773-2777.
241. Tapia L, Torres J, Mendoza L, Urzua A, Ferreira J, Pavani M, Wilkens M: **Effect of 13-epi-sclareol on the bacterial respiratory chain.** *Planta Med* 2004, **70**(11):1058-1063.
242. Georgieva J: **Effects of the Diterpene Sclareol Glycol on Body-Temperature in Rats.** *Method Find Exp Clin* 1989, **11**(4):277-280.
243. Georgieva J: **Effects of the Diterpene Sclareol Glycol on Convulsive Seizures.** *Method Find Exp Clin* 1989, **11**(5):335-340.
244. Georgieva J: **Measures of Anxiety, Retention and Stress in the Rat Following Treatment with the Diterpene Sclareol Glycol.** *Method Find Exp Clin* 1990, **12**(1):5-10.
245. Georgieva J: **The Response of Diterpene Sclareol Glycol to Acute-Hypoxia in Mice.** *Method Find Exp Clin* 1990, **12**(9):591-593.
246. Georgieva J, Danchev N: **The Effects of the Diterpene Sclareol Glycol on Seizures Do Not Depend on Central Benzodiazepine Receptors.** *Method Find Exp Clin* 1990, **12**(10):679-683.
247. Georgieva JV: **Diterpene Sclareol Glycol Inhibits Clonidine-Induced Aggressive Responses in Mice.** *Pharmacol Biochem Be* 1989, **34**(3):503-505.
248. Georgieva JV: **Influences of Diterpene Sclareol Glycol on Some Dopamine Related Behavior.** *Gen Pharmacol* 1991, **22**(2):331-335.
249. Patel NR, Hatziantoniou S, Georgopoulos A, Demetzos C, Torchilin VP, Weissig V, D'Souza GGM: **Mitochondria-targeted liposomes improve the apoptotic and cytotoxic action of sclareol.** *J Liposome Res* 2010, **20**(3):244-249.
250. Dimas K, Demetzos C, Vaos V, Ioannidis P, Trangas T: **Labdane type diterpenes down-regulate the expression of c-Myc protein, but not of Bcl-2, in human leukemia T-cells undergoing apoptosis.** *Leuk Res* 2001, **25**(6):449-454.
251. Dimas K, Papadaki M, Tsimplouli C, Hatziantoniou S, Alevizopoulos K, Pantazis P, Demetzos C: **Labd-14-ene-8,13-diol (sclareol) induces cell cycle arrest and apoptosis in human breast cancer cells and enhances the activity of anticancer drugs.** *Biomed Pharmacother* 2006, **60**(3):127-133.

252. Kyrikou I, Georgopoulos A, Hatziantoniou S, Mavromoustakos T, Demetzos C: **A comparative study of the effects of cholesterol and sclareol, a bioactive labdane type diterpene, on phospholipid bilayers.** *Chem Phys Lipids* 2005, **133**(2):125-134.
253. Koeberle SC, Romir J, Fischer S, Koeberle A, Schattel V, Albrecht W, Grutter C, Werz O, Rauh D, Stehle T *et al*: **Skepinone-L is a selective p38 mitogen-activated protein kinase inhibitor.** *Nature Chemical Biology* 2012, **8**(2):141-143.
254. Borst O, Abed M, Alesutan I, Towhid ST, Qadri SM, Foller M, Gawaz M, Lang F: **Dynamic adhesion of eryptotic erythrocytes to endothelial cells via CXCL16/SR-PSOX.** *Am J Physiol Cell Physiol* 2012, **302**(4):C644-C651.
255. Chung SM, Bae ON, Lim KM, Noh JY, Lee MY, Jung YS, Chung JH: **Lysophosphatidic acid induces thrombogenic activity through phosphatidylserine exposure and procoagulant microvesicle generation in human erythrocytes.** *Arterioscler Thromb Vasc Biol* 2007, **27**(2):414-421.
256. Zwaal RF, Comfurius P, Bevers EM: **Surface exposure of phosphatidylserine in pathological cells.** *Cell Mol Life Sci* 2005, **62**(9):971-988.
257. Abed M, Towhid ST, Mia S, Pakladok T, Alesutan I, Borst O, Gawaz M, Gulbins E, Lang F: **Sphingomyelinase-induced adhesion of eryptotic erythrocytes to endothelial cells.** *Am J Physiol Cell Physiol* 2012, **303**(9):C991-999.
258. Clossé C, Dachary-Prigent J, Boisseau MR: **Phosphatidylserine-related adhesion of human erythrocytes to vascular endothelium.** *Br J Haematol* 1999, **107**(2):300-302.
259. Gallagher PG, Chang SH, Rettig MP, Neely JE, Hillery CA, Smith BD, Low PS: **Altered erythrocyte endothelial adherence and membrane phospholipid asymmetry in hereditary hydrocytosis.** *Blood* 2003, **101**(11):4625-4627.
260. Pandolfi A, Di Pietro N, Sirolli V, Giardinelli A, Di Silvestre S, Amoroso L, Di Tomo P, Capani F, Consoli A, Bonomini M: **Mechanisms of uremic erythrocyte-induced adhesion of human monocytes to cultured endothelial cells.** *J Cell Physiol* 2007, **213**(3):699-709.
261. Wood BL, Gibson DF, Tait JF: **Increased erythrocyte phosphatidylserine exposure in sickle cell disease: flow-cytometric measurement and clinical associations.** *Blood* 1996, **88**(5):1873-1880.
262. Abed M, Feger M, Alzoubi K, Pakladok T, Frauenfeld L, Geiger C, Towhid ST, Lang F: **Sensitization of erythrocytes to suicidal erythrocyte death following water deprivation.** *Kidney Blood Press Res* 2013, **37**(6):567-578.

263. Voelkl J, Alzoubi K, Mamar AK, Ahmed MS, Abed M, Lang F: **Stimulation of suicidal erythrocyte death by increased extracellular phosphate concentrations.** *Kidney Blood Press Res* 2013, **38**(1):42-51.
264. Abed M, Artunc F, Alzoubi K, Honisch S, Baumann D, Foller M, Lang F: **Suicidal erythrocyte death in end-stage renal disease.** *Journal of molecular medicine* 2014, **92**(8):871-879.
265. Ahmed MS, Langer H, Abed M, Voelkl J, Lang F: **The uremic toxin acrolein promotes suicidal erythrocyte death.** *Kidney & blood pressure research* 2013, **37**(2-3):158-167.
266. Polak-Jonkisz D, Purzyc L: **Ca(2+) influx versus efflux during eryptosis in uremic erythrocytes.** *Blood purification* 2012, **34**(3-4):209-210; author reply 210.
267. Calderon-Salinas JV, Munoz-Reyes EG, Guerrero-Romero JF, Rodriguez-Moran M, Bracho-Riquelme RL, Carrera-Gracia MA, Quintanar-Escorza MA: **Eryptosis and oxidative damage in type 2 diabetic mellitus patients with chronic kidney disease.** *Molecular and cellular biochemistry* 2011, **357**(1-2):171-179.
268. Lang PA, Beringer O, Nicolay JP, Amon O, Kempe DS, Hermle T, Attanasio P, Akel A, Schafer R, Friedrich B *et al*: **Suicidal death of erythrocytes in recurrent hemolytic uremic syndrome.** *Journal of molecular medicine* 2006, **84**(5):378-388.
269. Nicolay JP, Schneider J, Niemoeller OM, Artunc F, Portero-Otin M, Haik G, Jr., Thornalley PJ, Schleicher E, Wieder T, Lang F: **Stimulation of suicidal erythrocyte death by methylglyoxal.** *Cell Physiol Biochem* 2006, **18**(4-5):223-232.
270. Lang E, Gatidis S, Freise NF, Bock H, Kubitz R, Laueremann C, Orth HM, Klindt C, Schuier M, Keitel V *et al*: **Conjugated bilirubin triggers anemia by inducing erythrocyte death.** *Hepatology* 2015, **61**(1):275-284.
271. Kempe DS, Akel A, Lang PA, Hermle T, Biswas R, Muresanu J, Friedrich B, Dreischer P, Wolz C, Schumacher U *et al*: **Suicidal erythrocyte death in sepsis.** *Journal of molecular medicine* 2007, **85**(3):273-281.
272. Inada-Inoue M, Ando Y, Kawada K, Mitsuma A, Sawaki M, Yokoyama T, Sunakawa Y, Ishida H, Araki K, Yamashita K *et al*: **Phase 1 study of pazopanib alone or combined with lapatinib in Japanese patients with solid tumors.** *Cancer Chemother Pharmacol* 2014, **73**(4):673-683.
273. Lang PA, Schenck M, Nicolay JP, Becker JU, Kempe DS, Lupescu A, Koka S, Eisele K, Klarl BA, Rubben H *et al*: **Liver cell death and anemia in Wilson disease involve acid sphingomyelinase and ceramide.** *Nature medicine* 2007, **13**(2):164-170.
274. Avantaggiati ML, Ogryzko V, Gardner K, Giordano A, Levine AS, Kelly K: **Recruitment of p300/CBP in p53-dependent signal pathways.** *Cell* 1997, **89**(7):1175-1184.

275. Lang PA, Kaiser S, Myssina S, Wieder T, Lang F, Huber SM: **Role of Ca²⁺-activated K⁺ channels in human erythrocyte apoptosis.** *Am J Physiol Cell Physiol* 2003, **285**(6):C1553-C1560.
276. Lockshin RA, Zakeri Z: **Apoptosis, autophagy, and more.** *Int J Biochem Cell Biol* 2004, **36**(12):2405-2419.
277. Lockshin RA, Zakeri Z: **Caspase-independent cell death?** *Oncogene* 2004, **23**(16):2766-2773.
278. Naito M, Hashimoto C, Masui S, Tsuruo T: **Caspase-independent necrotic cell death induced by a radiosensitizer, 8-nitrocaffeine.** *Cancer Sci* 2004, **95**(4):361-366.
279. Lang E, Qadri SM, Lang F: **Killing me softly - suicidal erythrocyte death.** *Int J Biochem Cell Biol* 2012, **44**(8):1236-1243.
280. Alzoubi K, Calabrò S, Bissinger R, Abed M, Faggio C, Lang F: **Stimulation of Suicidal Erythrocyte Death by Artesunate.** *Cellular physiology and biochemistry : international journal of experimental cellular physiology, biochemistry, and pharmacology* 2014, **34**:2232-2244.
281. Alzoubi K, Egler J, Abed M, Lang F: **Enhanced Eryptosis Following Auranofin Exposure.** *Cellular physiology and biochemistry : international journal of experimental cellular physiology, biochemistry, and pharmacology* 2015, **37**(3):1018-1028.
282. Arnold M, Bissinger R, Lang F: **Mitoxantrone-induced suicidal erythrocyte death.** *Cellular physiology and biochemistry : international journal of experimental cellular physiology, biochemistry, and pharmacology* 2014, **34**(5):1756-1767.
283. Arnold M, Lang E, Modicano P, Bissinger R, Faggio C, Abed M, Lang F: **Effect of nitazoxanide on erythrocytes.** *Basic & clinical pharmacology & toxicology* 2014, **114**(5):421-426.
284. Bissinger R, Barking S, Alzoubi K, Liu G, Liu G, Lang F: **Stimulation of Suicidal Erythrocyte Death by the Antimalarial Drug Mefloquine.** *Cellular physiology and biochemistry : international journal of experimental cellular physiology, biochemistry, and pharmacology* 2015, **36**(4):1395-1405.
285. Bissinger R, Bouguerra G, Stockinger K, Abbas S, Lang F: **Triggering of Suicidal Erythrocyte Death by Topotecan.** *Cellular physiology and biochemistry : international journal of experimental cellular physiology, biochemistry, and pharmacology* 2015, **37**(4):1607-1618.
286. Bissinger R, Fischer S, Jilani K, Lang F: **Stimulation of Erythrocyte Death by Phloretin.** *Cellular physiology and biochemistry : international journal of experimental cellular physiology, biochemistry, and pharmacology* 2014, **34**:2256-2265.
287. Jacobi J, Lang E, Bissinger R, Frauenfeld L, Modicano P, Faggio C, Abed M, Lang F: **Stimulation of erythrocyte cell membrane scrambling by mitotane.** *Cellular physiology and*

- biochemistry : international journal of experimental cellular physiology, biochemistry, and pharmacology* 2014, **33**(5):1516-1526.
288. Bouguerra G, Aljanadi O, Bissinger R, Abbas S, Lang F: **Embelin-Induced Phosphatidylserine Translocation in the Erythrocyte Cell Membrane**. *Cellular physiology and biochemistry : international journal of experimental cellular physiology, biochemistry, and pharmacology* 2015, **37**(4):1629-1640.
289. Bouguerra G, Bissinger R, Abbas S, Lang F: **Stimulation of Eryptosis by Narasin**. *Cellular physiology and biochemistry : international journal of experimental cellular physiology, biochemistry, and pharmacology* 2015, **37**(5):1807-1816.
290. Bouguerra G, Bissinger R, Abbas S, Lang F: **Zopolrestat Induced Suicidal Death of Human Erythrocytes**. *Cellular physiology and biochemistry : international journal of experimental cellular physiology, biochemistry, and pharmacology* 2015, **37**(4):1537-1546.
291. Briglia M, Fazio A, Faggio C, Laufer S, Alzoubi K, Lang F: **Triggering of Suicidal Erythrocyte Death by Ruxolitinib**. *Cellular physiology and biochemistry : international journal of experimental cellular physiology, biochemistry, and pharmacology* 2015, **37**(2):768-778.
292. Briglia M, Fazio A, Signoretto E, Faggio C, Lang F: **Edelfosine Induced Suicidal Death of Human Erythrocytes**. *Cell Physiol Biochem* 2015, **37**(6):2221-2230.
293. Calabro S, Alzoubi K, Faggio C, Laufer S, Lang F: **Triggering of Suicidal Erythrocyte Death Following Boswellic Acid Exposure**. *Cellular physiology and biochemistry : international journal of experimental cellular physiology, biochemistry, and pharmacology* 2015, **37**(1):131-142.
294. Egler J, Lang F: **Licochalcone A Induced Suicidal Death of Human Erythrocytes**. *Cellular physiology and biochemistry : international journal of experimental cellular physiology, biochemistry, and pharmacology* 2015, **37**(5):2060-2070.
295. Faggio C, Alzoubi K, Calabro S, Lang F: **Stimulation of suicidal erythrocyte death by PRIMA-1**. *Cellular physiology and biochemistry : international journal of experimental cellular physiology, biochemistry, and pharmacology* 2015, **35**(2):529-540.
296. Fazio A, Briglia M, Faggio C, Alzoubi K, Lang F: **Stimulation of Suicidal Erythrocyte Death by Garcinol**. *Cellular physiology and biochemistry : international journal of experimental cellular physiology, biochemistry, and pharmacology* 2015, **37**(2):805-815.
297. Lang E, Jilani K, Bissinger R, Rexhepaj R, Zelenak C, Lupescu A, Lang F, Qadri SM: **Vitamin D-Rich Diet in Mice Modulates Erythrocyte Survival**. *Kidney & blood pressure research* 2015, **40**(4):403-412.

298. Lang E, Zelenak C, Eberhard M, Bissinger R, Rotte A, Ghashghaeinia M, Lupescu A, Lang F, Qadri SM: **Impact of Cyclin-Dependent Kinase CDK4 Inhibition on Eryptosis.** *Cellular physiology and biochemistry : international journal of experimental cellular physiology, biochemistry, and pharmacology* 2015, **37**(3):1178-1186.
299. Lupescu A, Bissinger R, Goebel T, Salker MS, Alzoubi K, Liu G, Chirigiu L, Mack AF, Qadri SM, Lang F: **Enhanced suicidal erythrocyte death contributing to anemia in the elderly.** *Cellular physiology and biochemistry : international journal of experimental cellular physiology, biochemistry, and pharmacology* 2015, **36**(2):773-783.
300. Lupescu A, Bissinger R, Herrmann T, Oswald G, Jilani K, Lang F: **Induction of suicidal erythrocyte death by novobiocin.** *Cellular physiology and biochemistry : international journal of experimental cellular physiology, biochemistry, and pharmacology* 2014, **33**(3):670-680.
301. Malik A, Bissinger R, Calabro S, Faggio C, Jilani K, Lang F: **Aristolochic Acid Induced Suicidal Erythrocyte Death.** *Kidney & blood pressure research* 2014, **39**(5):408-419.
302. Officioso A, Alzoubi K, Manna C, Lang F: **Clofazimine Induced Suicidal Death of Human Erythrocytes.** *Cellular physiology and biochemistry : international journal of experimental cellular physiology, biochemistry, and pharmacology* 2015, **37**(1):331-341.
303. Oswald G, Alzoubi K, Abed M, Lang F: **Stimulation of suicidal erythrocyte death by ribavirin.** *Basic & clinical pharmacology & toxicology* 2014, **114**(4):311-317.
304. Peter T, Bissinger R, Enkel S, Alzoubi K, Oswald G, Lang F: **Programmed erythrocyte death following in vitro Treosulfan treatment.** *Cellular physiology and biochemistry : international journal of experimental cellular physiology, biochemistry, and pharmacology* 2015, **35**(4):1372-1380.
305. Stockinger K, Bissinger R, Bouguerra G, Abbes S, Lang F: **Enhanced Eryptosis Following Exposure to Carnosic Acid.** *Cellular physiology and biochemistry : international journal of experimental cellular physiology, biochemistry, and pharmacology* 2015, **37**(5):1779-1791.
306. Tesoriere L, Attanzio A, Allegra M, Cilla A, Gentile C, Livrea MA: **Oxysterol mixture in hypercholesterolemia-relevant proportion causes oxidative stress-dependent eryptosis.** *Cellular physiology and biochemistry : international journal of experimental cellular physiology, biochemistry, and pharmacology* 2014, **34**(4):1075-1089.
307. Waibel S, Bissinger R, Bouguerra G, Abbes S, Lang F: **Saquinavir Induced Suicidal Death of Human Erythrocytes.** *Cellular physiology and biochemistry : international journal of experimental cellular physiology, biochemistry, and pharmacology* 2015, **37**(5):1973-1982.

308. Zierle J, Bissinger R, Egler J, Lang F: **Lapatinib Induced Suicidal Death of Human Erythrocytes**. *Cellular physiology and biochemistry : international journal of experimental cellular physiology, biochemistry, and pharmacology* 2015, **37**(6):2275-2287.
309. Carlson AM, Morris LS: **Coprescription of terfenadine and erythromycin or ketoconazole: an assessment of potential harm**. *J Am Pharm Assoc (Wash)* 1996, **NS36**(4):263-269.
310. Thompson D, Oster G: **Use of terfenadine and contraindicated drugs**. *JAMA* 1996, **275**(17):1339-1341.
311. Farrand L, Byun S, Kim JY, Im-Aram A, Lee J, Lim S, Lee KW, Suh JY, Lee HJ, Tsang BK: **Piceatannol enhances cisplatin sensitivity in ovarian cancer via modulation of p53, X-linked inhibitor of apoptosis protein (XIAP), and mitochondrial fission**. *The Journal of biological chemistry* 2013, **288**(33):23740-23750.
312. Kasiotis KM, Pratsinis H, Kletsas D, Haroutounian SA: **Resveratrol and related stilbenes: their anti-aging and anti-angiogenic properties**. *Food and chemical toxicology : an international journal published for the British Industrial Biological Research Association* 2013, **61**:112-120.
313. Liu B, Zhou Z, Zhou W, Liu J, Zhang Q, Xia J, Liu J, Chen N, Li M, Zhu R: **Resveratrol inhibits proliferation in human colorectal carcinoma cells by inducing G1/Sphase cell cycle arrest and apoptosis through caspase/cyclinCDK pathways**. *Molecular medicine reports* 2014, **10**(4):1697-1702.
314. Qadri SM, Foller M, Lang F: **Inhibition of suicidal erythrocyte death by resveratrol**. *Life Sci* 2009, **85**(1-2):33-38.
315. Kus G, Kabadere S, Uyar R, Kutlu HM: **Induction of apoptosis in prostate cancer cells by the novel ceramidase inhibitor ceranib-2**. *In Vitro Cell Dev Biol Anim* 2015, **51**(10):1056-1063.

17. FINAL CONCLUSION

The present study investigates several aspects of cellular iron homeostasis, including the importance of NRAMP transporters and eryptosis. Iron is an essential element in all living cells. Approximately, the adult human body contains 4 g of iron [115]. It has been shown that 75% of total body iron is associated with haemoglobin, which is involved in oxygen transport. Iron deficiency limits the synthesis of heme, a prosthetic group of haemoglobin that in turn limits the synthesis of haemoglobin and decreases the production of RBCs in the bone marrow, resulting in anaemia [115]. Since cellular energy metabolism is dependent on oxygen, anaemia has a broad range of clinical consequences. DMT1 is a key player in iron transport and absorption and is expressed in immature erythroid cells [23]. DMT1-deficiency negatively affects erythrocytes metabolism and reduces their capacity to cope with stress [114]. Mutations that impair its activity are associated with a severe defect in erythroid iron utilization and are correlated with hypochromic microcytic anemia both in human patients and rodent models (Belgrade rats) [6]. It has been shown that DMT1-mutant erythrocytes have shortened life span, accelerated glycolysis and increased oxidative stress [114]. The accelerated clearance of erythrocytes could be attributed to excessive hemolysis and/or induction of programmed cell death of erythrocytes, called eryptosis. This suicidal erythrocytes death is characterized by cell shrinkage, cell membrane blebbing and cell membrane phospholipid scrambling. Eryptosis can be triggered by oxidative stress, hyperosmotic shock and glucose depletion likely via activation of Ca^{2+} cation channels leading to an increase in the concentration of cytosolic Ca^{2+} [114]. Iron deficient erythrocytes, when exposed to stress conditions, have been demonstrated to activate Ca^{2+} -permeable cation channels allowing Ca^{2+} entry [96]. Ca^{2+} entry through these channels leads to activation of a scramblase with subsequent phosphatidylserine exposure and to activation of the Gardos channels leading to KCl loss and cell shrinkage [116]. DMT1 knockout animals (*Slc11a2^{-/-}*) die in the first week of life due to iron deficient erythropoiesis [114]. DMT1 deficiency leads to an impaired erythroid differentiation characterized by accumulation of immature forms of erythroblast, accelerated death of erythroid precursors and a decrease survival in the erythroid progenitors [114]. The accelerated clearance of RBCs during anemia could be attributed to an increase in membrane stiffness and a decrease in deformability. The decrease in deformability and increase in membrane stiffness of RBCs can be attributed to oxidative stress [115]. Iron deficiency may limit the synthesis of heme that in turn limits the synthesis of haemoglobin and decreases the production of RBCs in the bone marrow, resulting in anemia. Oxidative stress may increase haemoglobin autoxidation and subsequent generation of ROS could account for the shorter erythrocytes lifespan and other pathological changes associated with iron-deficiency anaemia [115]. Macrophages play an important role in

body iron homeostasis, as the main iron supply for erythropoiesis derives from the iron recycled by these cells after phagocytosis of senescent erythrocytes [38, 66]. This process is realized by macrophages of the spleen, bone marrow and in the Kupffer cells. Thus, senescent erythrocytes are cleared by macrophages, which can metabolize haemoglobin and haem, and can release iron into the blood flow [61]. Moreover, DMT1 (NRAMP2) is associated with erythrocyte-containing phagosomes [38]. Iron released from erythrocytes degradation is transported out of the phagosome by NRAMP2 [23]. Moreover, NRAMP1 is involved in metal export from phagosomes to the cytosol. Iron transported to the cytosol can be used for metabolic purposes, stored in ferritin or transported out of the cell by ferroportin [23]. It has been shown that NRAMP1 is involved in iron recycling during conditions of increased erythrophagocytosis [23, 38]. *D. discoideum* represents a model for the study of cellular iron homeostasis, showing subcellular localization of iron transporters resembling that of macrophages. Moreover, *Dictyostelium* cells resemble macrophages for their ability to engulf bacteria and death cell, to discriminate between self and non-self and to fight potential pathogens. The *Dictyostelium* genome shares with mammals many genes regulating iron homeostasis; in particular, *D. discoideum* expresses the ortholog of SLC11A1 transporter in phago-lysosomes and that of SLC11A2 in the contractile vacuole. To conclude, this thesis investigates aspects of both basic (first chapter: “Iron transporters NRAMP1 and NRAMP2 from *Dictyostelium discoideum* as a model of cellular iron homeostasis”) and applied physiology (second chapter: “Effects of xenobiotics on the suicidal death of erythrocytes”) in order to highlight the importance of cellular iron homeostasis.

18. ACKNOWLEDGMENTS

First and foremost, I would like to express my sincere gratitude to my tutor Dr. Michela Castagna for the continuous support of my PhD study. Her guidance helped me in all the time of research and writing of this thesis. I would like to thank my tutor also for encouraging my research and for allowing me to grow as a research scientist.

I am especially thankful to Prof. Florian Lang, who provided me an opportunity to work with his team, and who gave access to the laboratory and research facilities. He was always there to support me with his insightful suggestions and enormous encouragement. Without his precious support it would not be possible to conduct this research.

I would like also to express my gratitude to Prof. Salvatore Bozzaro (University of Turin) and Prof. Elena Bossi (University of Insubria) for their help in the conduction of this study.

I would like to extend my appreciation to my fellow labmates for their support, suggestions and encouragement.

Last but not the least, I would like to thank my parents for providing me with unfailing support and continuous encouragement throughout my years of study and through the process of researching and writing this thesis.

19. APPENDIX

Curriculum vitae

PERSONAL INFORMATIONS:

First name / Surname Elena Signoretto

Address Dante Alighieri 24, 21040 Venegono Inferiore (VA), Italy

E-mail elena.signoretto@unimi.it; ele.signoretto@gmail.com

Nationality Italian

Date of birth 04 May 1989

ACADEMIC PROFILE:

10/2011-10/2013: Master degree in Biology with honors. Faculty of Mathematical, Physical and Natural Sciences, University of Insubria, J.H. Dunant 03, 21100 Varese (VA), Italy.

Title of the thesis: "AgNPs and gene expression performed in *Rattus norvegicus*"

10/2008-09/2011: Bachelor degree in Biological Sciences. Faculty of Mathematical, Physical and Natural Sciences, University of Insubria, J.H. Dunant 03, 21100 Varese (VA), Italy.

Title of the thesis: "Genetic variability of *Austropotamobius italicus* of Toce using short tandem repeats"

List of Publications

1. Al Mamun Bhuyan A, Signoretto E, Lang F. Triggering of Suicidal Erythrocyte Death by Psammaplin A. *Cell Physiol Biochem*. 2016 Aug 9;39(3):908-918.
2. Al Mamun Bhuyan A, **Signoretto E**, Bissinger R, Lang F. Enhanced Eryptosis Following Exposure to Dolutegravir. *Cell Physiol Biochem*. 2016 Jul 21;39(2):639-650.
3. **Signoretto E**, Laufer SA, Lang F. Stimulating Effect of Sclareol on Suicidal Death of Human Erythrocytes. *Cell Physiol Biochem*. 2016 Jul 11;39(2):554-564.

4. Peter T, Bissinger R, **Signoretto E**, Mack AF, Lang F. Micafungin-Induced Suicidal Erythrocyte Death. *Cell Physiol Biochem*. 2016 Jul 11;39(2):584-595.
5. **Signoretto E**, Zierle J, Bhuyan AA, Castagna M, Lang F. Ceranib-2-induced suicidal erythrocyte death. *Cell Biochem Funct*. 2016 Jul;34(5):359-66.
6. **Signoretto E**, Castagna M, Lang F. Stimulation of Eryptosis, the Suicidal Erythrocyte Death by Piceatannol. *Cell Physiol Biochem*. 2016;38(6):2300-10.
7. **Signoretto E**, Castagna M, Al Mamun Bhuyan A, Lang F. Stimulating Effect of Terfenadine on Erythrocyte Cell Membrane Scrambling. *Cell Physiol Biochem*. 2016;38(4):1425-34.
8. Bissinger R, Bhuyan AA, **Signoretto E**, Lang F. Stimulating Effect of Elvitegravir on Suicidal Erythrocyte Death. *Cell Physiol Biochem*. 2016;38(3):1111-20.
9. **Signoretto E**, Bissinger R, Castagna M, Lang F. Stimulation of Eryptosis by Combretastatin A4 Phosphate Disodium (CA4P). *Cell Physiol Biochem*. 2016;38(3):969-81.
10. **Signoretto E**, Zierle J, Bissinger R, Castagna M, Bossi E, Lang F. Triggering of Suicidal Erythrocyte Death by Pazopanib. *Cell Physiol Biochem*. 2016;38(3):926-38.
11. **Signoretto E**, Honisch S, Briglia M, Faggio C, Castagna M, Lang F. Nocodazole Induced Suicidal Death of Human Erythrocytes. *Cell Physiol Biochem*. 2016;38(1):379-92.
12. Briglia M, Calabró S, **Signoretto E**, Alzoubi K, Laufer S, Faggio C, Lang F. Fucoxanthin Induced Suicidal Death of Human Erythrocytes. *Cell Physiol Biochem*. 2015;37(6):2464-75.
13. Briglia M, Fazio A, **Signoretto E**, Faggio C, Lang F. Edelfosine Induced Suicidal Death of Human Erythrocytes. *Cell Physiol Biochem*. 2015;37(6):2221-30.
14. Buracco S, Peracino B, Cinquetti R, **Signoretto E**, Vollero A, Imperiali F, Castagna M, Bossi E, Bozzaro S. *Dictyostelium* Nramp1, which is structurally and functionally similar to mammalian DMT1 transporter, mediates phagosomal iron efflux. *Journal of Cell Science*. 2015 Sep 1;128(17):3304-16.
15. Coccini T, Gornati R, Rossi F, **Signoretto E**, Vanetti I, Bernardini G & Manzo L. Gene Expression Changes in Rat Liver and Testes after Lung Instillation of a Low Dose of Silver Nanoparticles; *Journal of Nanomedicine and Nanotechnology*, 2014, Volume 5, Issue 5.

Congress communications

1. **Signoretto E**, Honisch S, Briglia M, Faggio C, Castagna M and Lang F (2016): "Nocodazole Induced Suicidal Death of Human Erythrocytes". 95th Annual Meeting of the German Physiological Society DPG, Lübeck (Germany), March 3-5; *poster*.

2. **Signoretto E**, Cinquetti R, Bossi E, Peracino B, Bozzaro S and Castagna M (2015): “Characterization of *Dictyostelium discoideum* Nramp1 and Nramp2 transporters expressed in *Xenopus* oocytes”. NextStep6, University of Milan (Milan), 2 July; *oral presentation*.
3. **Signoretto E**, Buracco S, Peracino B, Cinquetti R, Vollero A, Imperiali F, Castagna M, Bossi E and Bozzaro S (2015): “Characterization of *Dictyostelium discoideum* Nramp1 and Nramp2 transporters expressed in *Xenopus* oocytes”. SIF (“Young Research Meeting”), Florence (Italy), 7-9 May; *oral presentation*.
4. **Signoretto E**, Cinquetti R, Bossi E, Peracino B, Bozzaro S and Castagna M (2014): “Functional characterization of iron transporter from *Dictyostelium discoideum* as a model of cellular iron homeostasis”. SIF (“Young Research Meeting”), Florence (Italy), 28-31 May; *oral presentation*.

Visiting scientist

Visiting Ph.D. student (September 2015-March 2016) in the laboratory of Professor Florian Lang at the Department of Cardiology, Cardiovascular Medicine and Physiology, Eberhard-Karls-University of Tuebingen, Gmelinstraße 5, 72076 Tuebingen, Germany.

Teaching and tutoring activities

1. Taught one session of Physiology Laboratory for students of Pharmaceutical Biotechnologies at the School of Pharmacy, Università degli Studi di Milano.
2. Provided scientific tutoring for graduating student in Pharmaceutical Biotechnologies at the School of Pharmacy, Università degli Studi di Milano.
3. Assistant supervisor of Bachelor Degree thesis in Pharmaceutical Biotechnologies, Università degli Studi di Milano.

Referee experiences

Referee experience for scientific journals (*Cellular Physiology and Biochemistry*; *Kidney and Blood Pressure Research*).